Redox regulation of non-photosynthetic plant metabolism

Dissertation

Zur Erlangung des Doktorgrades der Naturwissenschaften

an der Fakultät für Biologie

der Ludwig-Maximilians-Universität München

vorgelegt von

Liang-Yu Hou

München, 2020

Diese Dissertation wurde angefertigt

unter der Leitung von Prof. Dr. Peter Geigenberger

an der Fakultät für Biologie

der Ludwig-Maximilians-Universität München

Erstgutachter: Prof. Dr. Peter Geigenberger

Zweitgutachter: Prof. Dr. Wolfgang Frank

Tag der Abgabe: 08.04.2020

Tag der mündlichen Prüfung: 29.06.2020

Summary

Reduction-oxidation (redox) regulation in metabolic pathways is governed by oxidoreductases. In autotrophic tissues, there are two major systems namely ferredoxin-thioredoxin (Fdx-TRX) system and NADPH-thioredoxin reductase-thioredoxin (NTR-TRX) system. Many reports have indicated the significance of both systems in regulating broad metabolic processes in chloroplast, while the redox regulation in non-photosynthetic plant metabolism remains unclear. In the present study, the impact of these thiol-redox systems on non-photosynthetic metabolism was investigated by analyzing (i) the role of mitochondrial TRX (TRXh2 and TRXo1) in Arabidopsis plants, and (ii) the role of plastidial NADPH-thioredoxin reductase C (NTRC) in heterotrophic tomato fruits.

To analyze the role of mitochondrial TRXs, two T-DNA insertion lines, *trxh2.1* and *trxo1.1*, and a cross double mutant, *trxh2.1trxo1.1*, were used for further assays. In the single and double mutants, the expression of corresponding genes decreased by over 95% compared to wild-type level. The mutant lines showed comparable growth phenotype to the wild type, even though there was a small decrease in leaf size depending on the light conditions. Nevertheless, the *trxh2.1trxo1.1* line tended to accumulate more soluble sugars and sugar phosphates at the end of day, suggestive of enhancement in photosynthetic processes, while the levels of several phosphate intermediates, such as phosphoenopyruvate (PEP) and adenine nucleotides (ATP and ADP), decreased in the *trxh2.1trxo1.1* line. This further implied that jointly decreasing the expression of *TRXh2* and *TRXo1* might affect energy metabolism. Metabolite profiling of mutants lines harvested at the end of night revealed an overall decrease in the metabolites of Gly decarboxylation and tricarboxylic acid cycle, while this change diminished in the samples from the end of day. This indicated that down regulating both mitochondrial TRXs affected metabolic processes in mitochondrion as well as peroxisome. Furthermore, the *trxh2.1trxo1.1* line showed a better photosynthetic performance compared to the wild type either in the condition of high CO_2 concentration or fluctuating light situation. This implied the potential of TRXh2 and TRXo1 in affecting extra-mitochondrial processes, such as photosynthesis.

In addition to its role in chloroplasts, NTRC is also present in non-photosynthetic plastids. To investigate the role of NTRC, a NTRC RNA interference (NTRC-RNAi) construct controlled by a fruit-specific promoter was introduced into tomato plants, which eventually led to a 60%-80% decrease in *NTRC* expression level in transgenic tomato fruits during their development. The NTRC-RNAi lines tended to generate smaller and lighter fruits with less accumulation of dry matters, compared to the wild type. At an early developmental stage, the accumulation of transient starch was greatly reduced in response to

I

NTRC down-regulation, which subsequently resulted in a significant decrease in ripe fruits. This mainly attributed to the inhibition on the redox-activation of two key enzymes in starch biosynthesis, namely ADP-Glc pyrophosphatase (AGPase) and soluble starch synthase. Furthermore, down-regulation of NTRC perturbed the redox poise of NAD(P)(H), which led to a large increase in the reductive states of NAD(H) and NADP(H). Through performing metabolomics, it was found that NTRC down-regulation led to a general decrease in the level of sugars, while the levels of amino acids and organic acids were mainly increased, implying the potential of NTRC in regulating osmotic balance. These changes in metabolite level are anticipated to influence the taste and flavor of tomato fruits. Overall, this indicates that NTRC serves as a central component in modulating carbon metabolism and redox balance, which ultimately affects fruit growth as well as quality.

In summary, these results indicate that in leaves mitochondrial TRXs are involved in interorganellar cross-talk, affecting photosynthetic processes in the chloroplast, while plastidial NTRC in important to regulate metabolism and redox-balance in heterotrophic fruits, affecting fruit size and quality.

Abbreviations

Metabolite	Abbreviation
3-PGA	3-phosphoglycerate
ADP-Glc	ADP-glucose
DHAP	dihydroxyacetine phosphate
F1,6BP	fructose 1,6-bisphosphate
F6P	fructose-6-phosphate
Fru	fructose
G1,6BP	glucose 1,6-bisphosphate
G1P	glucose-1-phosphate
G6P	glucose-6-phosphate
GAP	Glyceraldehyde 3-phosphate
Glc	glucose
PEP	phosphoenopyruvate
Suc	sucrose

Amino acid	Abbreviation
Cys	cystenine
GABA	4-aminobutanoic acid
Gln	glutamine
Glu	glutamate
His	histidine
Met	methionine
Trp	tryptophan

Protein	Abbreviation
2-Cys Prx	2-Cys peroxiredoxins
AGPase	ADP-glucose pyrophosphatase
APS1	AGPase small-subunit 1
BSA	bovine serum albumin
G6PDH	glucose-6-phosphate dehydrogenase
GAPDH	Glyceraldehyde 3-phosphate dehydrogenase
Lhcb2	Chlorophyll a-b binding protein 2
NTR	NADPH thioredoxin reductase
RbCL	ribulose 1,5-bisphosphate carboxylase/ oxygenase large subunit

Chemical	Abbreviation
DTT	dithiothreitol
EDTA	ethylenediaminetetraacetic acid
EGTA	egtazic acid
HEPES	4-(2-hydroxyethyl)-1-piperazineethanesulfonic acid
MTT	methylthiazolydiphenyl- tetrazolium bromide
PES	phenazine ethosulfate,
TBAHS	tetrebutylammonium hydrogen sulfate
TCA	trichloroacetic acid
TES	2-[[1,3-dihydroxy-2-(hydroxymethyl)propan-2-yl]amino]ethanesulfonic acid
Tris	tris(hydroxymethyl)aminomethane

1 Introduction

Reduction-oxidation (redox) regulation is determined to be important for many metabolic pathways in various subcellular compartments (Geigenberger and Fernie, 2014). There are many types of redox regulation in plants, including sulfuxidation, S-glurathioylation, S-nitrosylation and the formation of disulfide bond. These post-translation modifications are mediated by oxidoreductases called thioredoxins (TRXs) and glutaredoxins ([GRXs]; Michelet et al., 2013). In the following chapters, we will thoroughly introduce these redox systems.

1.1 Ferredoxin-thioredoxin system

In 1960s, it was found that a group of Calvin-Benson-Cycle (CBC) enzymes are light-activated (Michelet et al., 2013). This finding further led to the discovery of ferredoxin-thioredoxin (Fdx-TRX) system. As shown in the Fig. 1.1, the Fdx-TRX system serves as a central component in regulating the photosynthetic electron transport. Upon illumination, photosystem II (PSII) loses an electron. Then, chlorophyll in the reaction center is then strongly oxidized, and thus able to receive electrons from water. Oxygen and protons are generated in the lumen during this process. Those electrons are first transmitted to the plastoquinone pool (PQ), and further transferred to photosystem I (PSI) through cytochrome b6/f (Cyt b6/f) and plastocyanin (PC). Meanwhile, oxidized plastoquinone will release its protons into the lumen, resulting in an input of protons from stroma to lumen. When received electrons, chlorophyll in PSI reaction center is reduced, and then chlorophyll molecules donate electrons to Fdx. Fdx thus can reduce the stromal TRXs via ferredoxin-thioredoxin reductase (FTR), which further regulate CBC enzymes. Alternatively, Fdx can lead to a conversion of $NADP^+$ to NADPH through ferredoxin NADP reductase (FNR). NADPH can further be used in CBC. The processes of water photolysis and proton transport will establish a proton gradient, which empowers ATP synthase to produce ATP supporting the need of CBC.

The Fdx cooperates tightly with a group of TRXs. According to the primary structure, there are various groups of TRXs: the TRXf, h, m, o, x, y and z (Meyer et al., 2005; Meyer et al., 2008). The type-f, m, x, y and z TRXs are chloroplast-localized proteins, and of great importance for redox balance and chloroplast functions. The type-f TRX comprises two isoforms, TRXf1 and TRXf2. They are mainly responsible for the regulation of CBC enzymes and starch biosynthesis, and often cooperate with NTRC to facilitate photosynthetic processes (Michalska et al., 2009; Lepistö et al., 2013; Thormählen et al., 2013; Thormählen et al., 2015; Yoshida et al., 2015; Nikkanen et al., 2016). The type-m

TRX contains four isoforms, m1, m2, m3 and m4. They are involved in the regulation of malate valve to maintain redox balance (Okegawa and Motohashi, 2015; Thormählen et al., 2017) as well as the synthesis of ATP and chlorophyll (Luo et al., 2012; Carrillo et al., 2016; Yoshida and Hisabori, 2016). Furthermore, they modulate cyclic electron transport (Courteille et al., 2013) and the development of meristem (Benitez-Alfonso et al., 2009). The type-y TRX harbors two isoforms, which cooperate with type-x TRX to regulate antioxidant system (Lamkemeyer et al., 2006; Navrot et al., 2006; Bohrer et al., 2012). The type-z TRX is responsible for regulating the expression of plastid genes (Arsova et al., 2010).
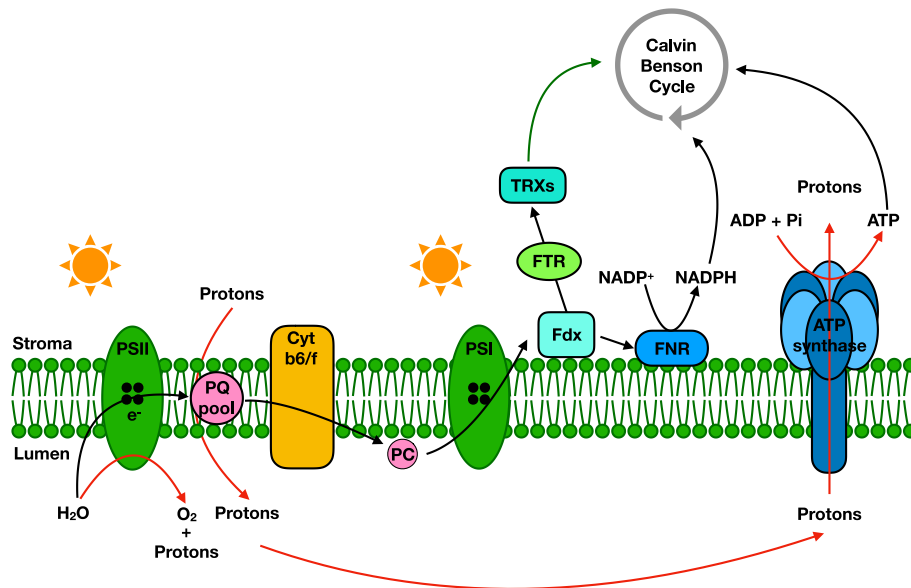
Figure 1.1 Photosynthetic electron transport via Fdx-TRX system (Michelet et al., 2013). PSII, photosystem II; PQ, plastoquinone; Cyt b6/f, cytochrome b6/f; PC, plastocyanin; PSI, photosystem I; Fdx, ferredoxin; FTR, ferredoxin-thioredoxin reductase; FNR, ferredoxin NADP reductase.

1.2 NADPH-thioredoxin reductase-thioredoxin (NTR-TRX) system

In addition to the Fdx-TRX system, the NTR-TRX system is another way to transduce redox signal in different cellular compartments. There are three types of NTR protein identified in plants, and all of them harbor disulfide reductase activity. NTRA is a cytosolic protein, and NTRB is localized in mitochondria (Serrato et al., 2004; Reichheld et al., 2005). Both NTRA and NTRC are able to use NADPH to reduce different types of TRXs. These two proteins share 82% sequence similarity and may function redundantly in redox regulation (Trotter and Grant, 2005; Reichheld et al., 2007). Several reports indicate the involvement of these two proteins for plants to tolerate against oxidative, drought and UV-light stresses (Reichheld et al., 2005; Bashandy et al., 2009; Cha et al., 2014). With the analysis on the *ntrantrb* double mutant, it is shown that these NTR proteins interplay with

glutathione pathways, and is able to facilitate enzyme activation in tricarboxylic acid cycle (Reichheld et al., 2007; Daloso et al., 2015).

NTRA and NTRB are responsible for the reduction of h and o-type TRX and further regulate downstream metabolic processes. The family of o-type TRX consists of two isoforms, TRXo1 and TRXo2. TRXo1 is mainly localized in mitochondrion, and, in some cases, this protein also appears in nucleus, while the localization of TRXo2 remains unclear (Laloi et al., 2001; Martí et al., 2009). TRXo1 harbors diverse functions. For example, TRXo1 has the potential to influence the growth of Arabidopsis plants and seed germination under salt stress (Ortiz-Espín et al., 2017; Calderón et al., 2018). Overexpressing pea (*Pisum sativum* L.) TRXo1 in a tobacco cell line leads to an alteration in the cell cycle progression(Calderón et al., 2017). More importantly, TRXo1 is determined to regulate many mitochondrial proteins, including tricarboxylic-acid-cycle enzymes (Daloso et al., 2015), alternative oxidase (AOX) of respiratory process (Laloi et al., 2001; Florez-Sarasa et al., 2019), while, there is commentary from Schwarzländer and Fuchs (2019) indicating that TRXo1 is not needed for AOX activation.

Type-h TRX belong to the largest TRX family, and most of them are identified as cytosolic proteins, while some are also reported to be localized in mitochondrion (Gelhaye et al., 2004; Meng et al., 2010), nucleus (Serrato and Cejudo, 2003), apoplast (Zhang et al., 2011), plasma membrane (Meng et al., 2010) or endomembrane reticulum (Traverso et al., 2013). The functions of type-h TRX are also very diverse, such as mobilization of storage protein during seed germination (Johnson et al., 1987; Kobrehel et al., 1992; Marx et al., 2003), involvement in self-incompatibility response (Cabrillac et al., 2001), and reactions against environmental challenges (Reichheld et al., 2002; Serrato and Cejudo, 2003; Laloi et al., 2004; Park et al., 2009). However, TRXh2 seems to be the only type-h TRX contributing plant metabolism. TRXh2 is an unusual protein concerning its subcellular localization. The localization of this protein can be in cytosol, mitochondrion as well as ER-Golgi complex (Meng et al., 2010; Traverso et al., 2013), raising a question whether TRXh2 is able to translocate to different subcellular compartment depending on the circumstances. The function of TRXh2 is also puzzled, since merely few reports describe its physiological function. With the use of recombinant TRXh2 protein, Daloso et al. (2015) first reported that TRXh2 has the potential to regulate tricarboxylic-acid-cycle enzymes with TRXo1.

The unique NTRC is identified as a chloroplast-localized protein. In a single polypeptide, NTRC harbors both NTR and TRX domain (Serrato et al., 2004). This allows NTRC to take advantage of NADPH to regulate various target proteins by facilitating the

formation of disulfide bond (Spínola et al., 2008; Geigenberger et al., 2017). Thus, NTRC is important for broad chloroplast functions as shown in the Fig. 1.2. For example, NTRC is able to reduce 2-Cys peroxiredoxin (2-Cys Prxs), which further regulates the removal of excess hydrogen peroxide generated during photosynthetic processes (Pérez-Ruiz et al., 2006; Kirchsteiger et al., 2009; Pérez-Ruiz and Cejudo, 2009). NTRC is also able to regulate ADP-Glc pyrophosphorylase (AGPase), and thus modulates the accumulation of starch (Michalska et al., 2009; Lepistö et al., 2013). Moreover, NTRC also has intimate crosstalk with Fdx-TRX system to enhance photosynthetic processes. For instance, this system can assist plants to get rid of excess light energy via non-photochemical quenching (NPQ), to regulate a group of CBC enzymes, and to be involved in the synthesis of chlorophyll, auxin and ATP (Richter et al., 2013; Pérez-Ruiz et al., 2014; Thormählen et al., 2015; Carrillo et al., 2016; Naranjo et al., 2016a; Nikkanen et al., 2016; Yoshida and Hisabori, 2016; Da et al., 2017; Thormählen et al., 2017). More importantly, the involvement of NTRC in Fdx-TRX system is beneficial for the maintenance of its reduction capacity by avoiding further reoxidation resulting from an interaction between oxidized 2-Cys Prxs and hydrogen peroxide (Pérez-Ruiz et al., 2017).
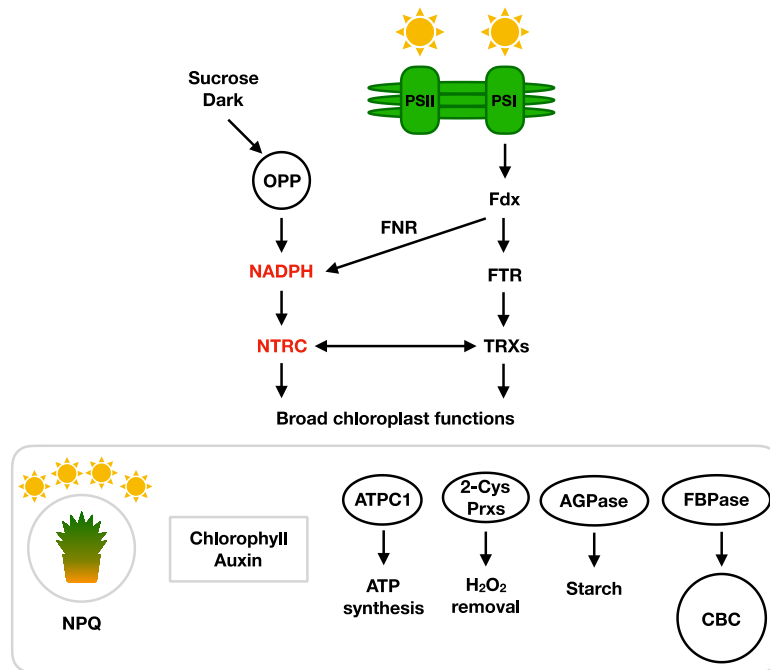
Figure 1.2 Summary of NTRC functions in photosynthetic processes. OPP: oxidative pentose phosphate pathway. NPQ, non-photochemical quenching; ATPC1, ATP synthase gamma chain 1; 2-Cys Prxs, 2-Cys perioxiredoxin; AGPase, ADP-Glc pyrophosphatase; FBPase, Fru 1,6-bisphosphatase; CBC, Calvin-Benson cycle.

In addition, NTRC is determined to be involved in the starch accumulation in Arabidopsis root (Michalska et al., 2009), but this seems to have no significance for plant growth. Expressing *NTRC* with leaf-specific promoter in *ntrc* mutant recovers the phenotype of growth retardation. However, when adopted a root-specific promoter, the phenotype of *ntrc* mutant is barely changed (Kirchsteiger et al., 2012). Thus, the results only point out the significance of NTRC in tissues with photosynthetic activity. NTRC functions in heterotrophic tissues still remain unclear.

1.3 Glutathione-glutaredoxin (GSH-GRX) system

Unlike NTR-TRX system, which obtains reducing power from NADPH, the reduction of GRX requires reduced glutathione (GSH). As shown in the Fig. 1.3, GRX mainly performs deglutathionylation on their target proteins, and GRX itself becomes glutathionylated. Then, GSH is used to reduce glutathionylated GRX, which eventually results in the release of oxidized glutathione (GSSG).

Figure 1.3 Deglutathionylation performed by glutaredoxin (GRX). GSH, reduced glutathione; GSSG, oxidized glutathione.

By analyzing the sequence similarity and the property of redox centers, plant GRX can be classified to five subgroups (Couturier et al., 2009). Among five subgroups, the subgroup III and IV are specifically belonged to vascular plants (Meyer et al., 2006). The functions of GRX are also very diverse (Meyer et al., 2012). In brief, genetic analyses unveil the significance of GRX on embryo development (Riondet et al., 2012), antioxidant mechanisms in chloroplast (Cheng et al., 2006), auxin-dependent development (Cheng et al., 2011), floral development (Xing et al., 2005; Li et al., 2009a; Murmu et al., 2010), responses to biotic stresses (Ndamukong et al., 2007; La Camera et al., 2011), protection in photooxidative stress (Laporte et al., 2012), and chloroplast movement (Whippo et al., 2011).

The crosstalk between TRX and GRX systems is well documented in *E. coli*. Compromising both systems at the same time results in lethality for cells (Toledano et al., 2007). In yeast (*S. cerevisiae*), similar results are described (Draculic et al., 2000; Trotter and Grant, 2002; Trotter and Grant, 2005), while several reports indicate that TRX and GRX systems are not necessarily functional redundant. In other word, the reduction of

TRX is independent from glutathione pathway (Trotter and Grant, 2003). In plants, the crosstalk between TRX and GRX systems is first proposed when investigated the multiple mutant of cytosolic TRXs. The phenotype of this mutant is comparable to wild-type plants when grown in a standard condition or challenged with stresses, suggestive of redundancy with other redox pathways (Meyer et al., 2012). This is further elucidated by analyzing the *ntrantrb* mutant and a triple mutant (*ntrantrbrml1*), in which GSH synthesis is defective (Vernoux et al., 2000). Furthermore, the reduction of TRXh5 also requires the assistance of GRX system (Sweat and Wolpert, 2007).

1.4 *Arabidopsis thaliana* and *Solanum lycopersicum*

Arabidopsis thaliana is a well-known model organism for investigations of plant physiology, genetics and evolution. There are several advantages when using Arabidopsis as a model plant. (i) Arabidopsis has a short life cycle, which allows researchers to perform experiments more efficiently. (ii) In comparison to other multicellular eukaryote, Arabidopsis harbors a small genome of around 135 megabase pairs. Furthermore, the whole genome sequencing was done in 2000. Approximate 27000 genes, which encode 35000 proteins, are identified in Arabidopsis (Kaul et al., 2000). The abundant information is advantageous for researchers to do functional characterization in genes of interest. (iii) It is relatively easier to establish transgenic mutant lines via *Agrobacterium tumefaciens*-mediated floral dipping (Clough and Bent, 1998) or treatment of chemical mutagens, such as ethylmethane sulfonate (Kim et al., 2006). Besides, there are ready-to-use mutant lines available in Nottingham Arabidopsis Stock Center (NASC). There are several commonly used wild-type lines, such as Columbia (Col), Landsberg erecta (L*er*) and Wassilewskija (Ws). The traits mentioned above make Arabidopsis a useful model plant for plant scientist, even though Arabidopsis is of minor significance for agriculture.

Tomato (*Solanum lycopersicum*) is one of the important horticultural crops, and also serves as a major component of human diet. Furthermore, tomato is an appropriate model plant for studying the physiology and development of fruit (Kanayama, 2017). Throughout the developmental processes of fruit, a series of changes, including color, firmness, taste and flavor take place. These changes are associated with shifts of metabolites. For example, the levels of carbohydrates, amino acids, organic acids and volatile substances dramatically changed during the ripening processes (Carrari and Fernie, 2006). The accumulation of carbohydrates is of importance for the yield and quality of tomato fruit (Kanayama, 2017). At the immature developmental stage, tomato fruits harbor strong sink activity. Large

amounts of carbon are first converted to Suc, and then imported into sink tissues from leaf tissues (Osorio and Fernie, 2014). In fruit tissues, the imported Suc is mobilized to Glc and Fru. With a series of enzyme reactions, the soluble sugars are subsequently converted to starch as an intermediate carbon source, which is able to improve the sink activity in immature tomato fruits (Osorio and Fernie, 2014). At the ripening stage, most starch is metabolized to soluble sugars. Fruit taste and quality are dependent on the accumulation of soluble sugars (Davies and Hobson, 1981; Gierson and Kader, 1986).

1.5 Applicative studies of redox systems in crops

Optimization of redox systems plays an important role in horticultural characteristics and applicative use of crops (Yano, 2014). In barley, increasing the expression of TRXh5 accelerates seed germination, which subsequently decreases production cost and enhances beer production (Cho et al., 1999; Wong et al., 2002). Furthermore, increasing the expression of TRXh5 in wheat results in higher gliadin solubility, which reduces the allergenicity of cereal (Li et al., 2009b). Down-regulation of TRXh9 in wheat is also found to increases its resistance to pre-harvest sprouting (Li et al., 2009b). In tobacco, overexpressing TRXf is able to increase the accumulation of starch and sugars. This feature makes transgenic tobacco an appropriate source for producing biofuel (Sanz-Barrio et al., 2013). In potato, transformants with decreased expression of TRXh1 shows a reduction in cold-induced accumulation of reducing sugars. Since excess accumulation of sugars promotes the formation of acrylamide when processed food, which is problematic for food industry, decreasing the sugar abundance further resolves this problem (He et al., 2012). In rice, the redox systems are involved in regulating the tolerance against abiotic and biotic stresses. For example, overexpressing a TRX peroxidase gene in rice enhances its resistance to oxidative stress (Kim et al., 2018). A type-m TRX is determined to be an antifungal protein in rice (Park et al., 2019). Moreover, rice NTRC is characterized as a high-efficient redox system against oxidative stress (Pérez-Ruiz et al., 2006). Taken together, redox regulation is an indispensible part for optimization of horticultural characteristics and industrial application in crops.

1.6 The connection between photosynthetic and non-photosynthetic metabolism

The photosynthetic metabolism mainly occurs in chloroplast, and this process is used to convert light energy into stable chemical substances. Photosynthetic metabolism contains two phases. The first one is the light-dependent reactions, and the second one is the carbon reactions (Buchanan et al., 2015). In the light reactions, the multiprotein

photosynthetic complexes (PSI and PSII) are responsible for absorbing light energy, and converting it into chemical energy. As described in Fig. 1.1, the photosystems are linked with other proteins, including cytochrome *b6f*, plastocyanin and plastoquinone, to form a photosynthetic electron transfer chain, which drives the production of O_2, ATP and NADPH. In the carbon reactions (Calvin-Benson cycle), the key enzyme ribulose-1,5-biphosphate carboxylase/oxygenase (Rubisco) is responsible for the assimilation of CO_2 from atmosphere. The enzyme uses the NADPH produced from the light reactions to generate three-carbon products, Through a series of enzyme reaction, the three-carbon sugars are metabolized to form sucrose and starch.

The non-photosynthetic metabolism mostly occurs outside chloroplast. This includes several reactions, such as photorespiration and dark respiration. Photorespiration refer to the reaction that Rubisco oxygenates ribulose-1,5-bisphosphate to generate 2-phosphoglycolate (2-PG) and 3-phosphoglycerate (PGA; Osmond et al., 1997; Igamberdiev et al., 2001). PGA re-enters Calvin-Benson cycle, since it is a carboxylation product. However, since 2-PG inhibits several enzymes of carbon assimilation, it needs to be detoxified immediately. With a series reactions in chloroplast, peroxisome and mitochondrion, 2-PG is converted into glycerate, and re-enters Calvin-Benson cycle (Fig. 1.4, upper and right). Respiration contains three phases – glycolysis, tricarboxylic acid cycle and electron transport/oxidative phosphorylation (Buchanan et al., 2015). Glycolysis refers to the reactions that metabolize sugars to pyruvate. Pyruvate is then metabolized to acetyl-CoA, which enters the tricarboxylic acid cycle. Enzyme reactions of tricarboxylic acid cycle drive the production of ATP and reduced cofactors (NADH and $FADH_2$). These reduced equivalents are further oxidized by mitochondrial electron transport chain to promote the production of ATP via oxidative phosphorylation.

Both photosynthetic and non-photosynthetic systems are required to coordinate intimately for optimization of plant growth and development. There are several aspects regarding to the crosstalk between the two systems. First of all, reducing equivalents excessively produced in chloroplast during photosynthesis can be dissipated to mitochondrion and other organelles via transport of various metabolites, including photorespiratory metabolites, malate, oxoglutarate or triose phosphates (Scheibe, 1991; Plaxton, 1996; Ocheretina et al., 2000; Gardeström et al., 2002; Padmasree et al., 2002). This mechanism can prevent over-reduction occurred in chloroplast, which leads to damage on thylakoid membranes (Niyogi, 1999; Niyogi, 2000). Furthermore, non-photosynthetic metabolism is beneficial for the optimization of photosynthesis. For example, triose phosphate exported from chloroplast can be converted to sucrose in cytosol,

which further increases the rate of carbon assimilation. ATP produced in mitochondrion can be transported to other subcellular compartments for the need of biosynthetic processes (Hoefnagel et al., 1998; Noctor and Foyer, 1998; Noctor and Foyer, 2000). The pathway of alternative oxidase (AOX) in mitochondrion is also important for the activation of several enzymes in chloroplast (Igamberdiev et al., 1998; Padmasree and Raghavendra, 2001). Thirdly, mitochondrion and peroxisome are able to help chloroplast to overcome photoinhibition via photorespiratory processes as mentioned above. Moreover, the photorespiratory reactions also maintain the provision of carbon, nitrogen and phosphorus (Osmond et al., 1997; Igamberdiev et al., 2001). To sum up, the exchange of metabolites and biochemical signals between various subcellular compartments form an intimate communication, which modulates photosynthesis, respiration and other metabolic processes (Fig. 1.4).
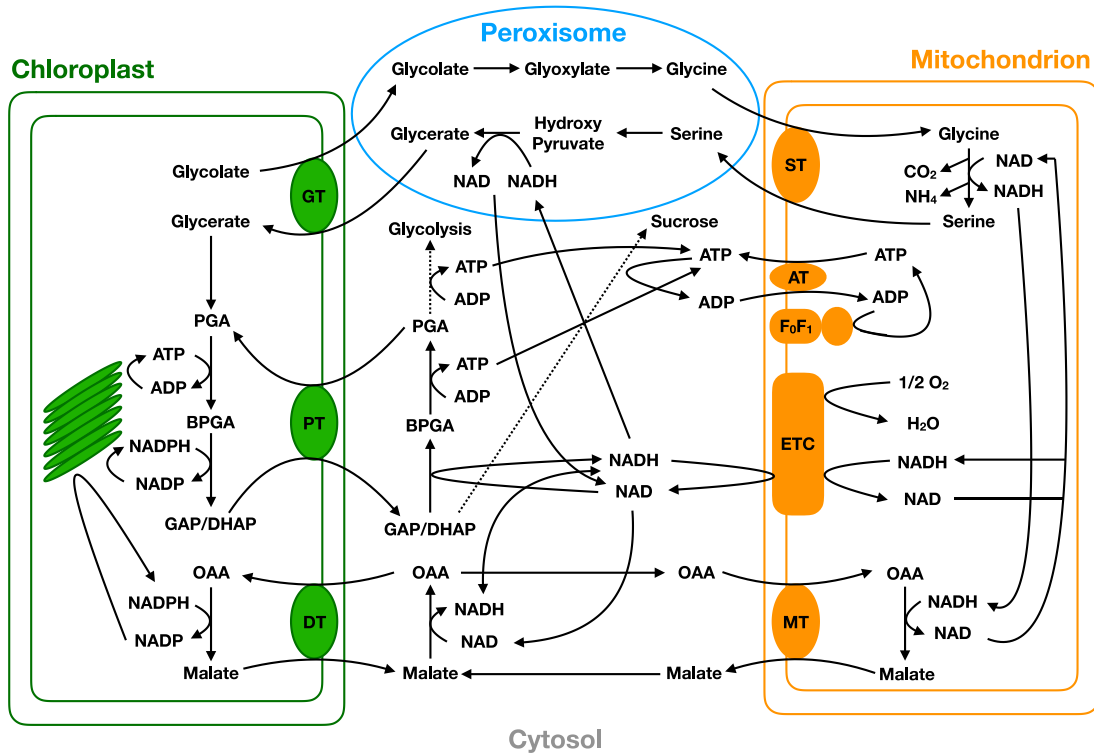
Figure 1.4 Communication between different subcellular compartments. This picture is adapted from a literature (Raghavendra and Padmasree, 2003). MT, malate translocator; ETC, electron transport chain; F0F1, ATPase complex; AT, adenylate translocator; ST, putative glycine-serine translocator; GT, glycolate-glycerate translocator; PT, phosphate translocator; DT, dicarboxylate translocatore BPGA, 1,3-bisphosphoglycerate; DHAP, dihydroxyacetone-3-phosphate; GAP, glyceraldehyde-3-phosphate; OAA, oxaloacetate; PGA, 3-phosphoglycerate.

1.7 Objectives of this study

Many reports have been addressed the redox regulation in photosynthetic plant metabolism. However, the redox regulation in non-photosynthetic plant metabolism is relatively less investigated. A major objective of this study is therefor to analyze the role of

NTR-TRX system in non-photosynthetic metabolism. Two approaches are used to address this topic.

The first aim is to characterize the function of mitochondrial TRXs, TRXh2 and TRXo1, in plant metabolism. In this project, two well-described T-DNA insertion mutants, *trxh2.1* and *trxo1.1*, and a cross double mutant, *trxh2.1trxo1.1*, were used for further investigations. With a series of analyses on phenotypes, metabolite, respiratory and photosynthetic parameters, it is proposed that TRXh2 and TRXo1 are involved in the regulation of metabolic processes inside mitochondrion, and also affect processes outside the mitochondrial boundaries, specifically when plants are subjected to a fluctuating environment (e.g. a day/night transition, and a change from medium to high light intensity).

The second aim is to investigate the role of plastidial NTRC in developing tomato fruits. A NTRC-RNAi construct controlled by the fruit-specific patatin B33 promoter was introduced into tomato plants to generate several transgenic lines, which NTRC level decreased by 60% to 80% compare to the wild type. A series of assays, including metabolite profiling and the redox state of NAD(H) and NADP(H) couples as well as the redox-activation state of AGPase and the activity of starch-metabolism enzymes, were performed in the transgenic tomato mutants. It is proposed that NTRC plays a significant role in carbon metabolism and redox balance in non-photosynthetic tissues.

2 Material and Methods

2.1 Plant material

2.1.1 *Solanum lycopersicum* cv Moneymaker (Tomato)

The tomato plants were grown in the greenhouse, where the light intensity was around 250 µmol m^{-2} s^{-1}, and the temperature was 22°C, under a long-day condition (16-h-light/8-h-dark). Tomato fruits were harvested at 35 day-after-flowering (DAF) as mature green stage, and 65 DAF as ripe stage. The complete pericarp was frozen in liquid nitrogen for latter use.

2.1.2 *Arabidopsis thaliana*

The Arabidopsis plants were grown in the growth chamber with a constant medium light condition (150 µmol m^{-2} s^{-1}) under a 16-h-light/8-h-dark regime for three weeks. The entire rosette leave were harvested at the end of night (EN) and end of day (ED), and frozen in liquid nitrogen for further analysis. For the treatment of fluctuating light, the Arabidopsis plants were grown in the climate chamber with 5 min low-light phase (50 µmol m^{-2} s^{-1}) and 1 min high-light phase (550 µmol m^{-2} s^{-1}) under a 12-h-light/12-h-dark regime for four weeks. The entire rosette leave were harvested at the middle of day, and frozen in liquid nitrogen for further analysis. The temperature of both chambers was maintained in 22°C.

2.2 Cloning and plant transformation

2.2.1 pEXB33-RNAi-NTRC

The primer pairs, attB1-RNAi-NTRC (5'-ggggacaagtttgtacaaaaaagcaggctcagat gtcaggaattttgatca-3') and attB2-RNAi-NTRC (5'-ggggaccactttgtacaagaaagctgggtcg cttgtcagatatctctccactgata-3'), were used to amplify the *NTRC* gene fragment from potato cDNA. This DNA fragment was then cloned into the pBINAR-RNAi vector containing a fruit-specific patatin B33 promoter (Rocha-Sosa et al., 1989; Frommer et al., 1994; Obiadalla-Ali et al., 2004) by using a GATEWAY cloning kit (Invitrogen).

2.2.2 Plant transformation

Tomato plants were transformed based on the *Agrobacterium tumefaciens*-mediated approach as detailed in the literature (Tauberger et al., 2000), and kanamycin served as the selection marker for the transformants.

Arabidopsis plants were transformed by using the floral dip method (Clough and Bent, 1998), and the potential transformants were selected using kanamycin.

2.3 Molecular characterization

2.3.1 Genomic DNA extraction and genotyping

Genomic DNA extraction was performed as described before with modifications (Doyle and Doyle, 1987). Approximate 50 mg of pulverized sample was suspended in 500 μL of DNA extraction buffer (100 mM Tris-HCl, pH 8.0, 1.4 M NaCl, 20 mM EDTA, 2% [w/v] cetyl-trimethyl-ammonium bromide, 0.2% [v/v] 2-mercaptoethanol) followed by the addition of 100 μL of chloroform. The mixture was vortexed vigorously and centrifuged for 10 min at 20,000g in 25°C for phase partition. The upper aqueous phase was transferred into a new microtube, and mixed with the equal volume of absolute isopropanol followed by centrifugation for 10 min at 20,000g in 25°C to precipitate DNA. The pellet was then washed with ethanol (70%, v/v) followed by centrifugation for 5 min at 20,000g in 25°C, and placed in the hood for the evaporation of remaining ethanol. The DNA pellet was re-suspended in 100 μL of nuclease-free water. For the genotyping, 0.5 μL of genomic DNA was mixed with 0.3 μL of forward primer (10 μM), 0.3 μL of reverse primer (10 μM), and 5 μL of double-strength MangoMix (Bioline), supplemented with nuclease-free water to make 10 μL in total volume. The PCR reaction was performed in a thermo cycler (C1000 Touch™ Thermo Cycler, Biorad) with the setting as below: initial denaturation at 95°C for 3 min, and 30 cycles, each containing denaturation at 95°C for 30 sec, annealing at 60°C for 30 sec, and elongation at 72°C for 30 sec. The final elongation step was at 72°C for 5 min. The product was analyzed with electrophoresis in 1% (w/v) agarose gel prepared in TAE buffer (40 mM Tris, 20 mM acetic acid, 1 mM EDTA). The primer sequences were listed below: Kana-F (5'-aactgttcgccaggctcaag-3'), Kana- R (5'-tcagaagaactcgtcaagaagg -3'), CAC-F (5'-cctccgttgtgatgtaactgg-3') and CAC-R (5'-attggtggaaagtaacatcatcg-3').

2.3.2 Total RNA extraction

Approximate 50 mg of pulverized material was suspended in 500 μl of RNAzol reagent (Sigma) followed by the addition of 100 μL of chloroform with vigorous vortex. The mixture was centrifuged for 10 min at 20,000g in 4°C. The upper aqueous phase was transferred into a new microtube, and mixed with the equal volume of isopropanol. The mixture was centrifuged for 10 min at 20,000g in 4°C to precipitate the total RNA. The RNA pellet was re-suspended in 200 μL of nuclease-free water, and then mixed with the equal volume of phenol/chloroform/isoamylalcohol reagent (v/v/v, 25:24:1). The mixture was centrifuged for 10 min at 20,000g in 4°C. The upper aqueous phase was transferred into a new microtube, and mixed with one-tenth volume of sodium acetate (3 M) and 2.5 times volume of absolute ethanol. The mixture was centrifuged for 10 min at 20,000g in 4°C to precipitate the total RNA. The RNA pellet was washed with ethanol (70%, v/v) and

air-dried in the hood. The pellet was re-suspended in 50 μL of nuclease-free water. The RNA concentration was quantified by using a spectrophotometer (NanoDrop™ 2000, ThermoFisher Scientific).

2.3.3 Reverse-transcription

Around 500 ng of total RNA was mixed with 2 μL of 5-fold reaction buffer and 0.5 μL of iScript reverse transcriptase (Biorad), and supplemented with nuclease-free water to make 10 μL in total volume. The sample was incubated in a thermo cycler (C1000 Touch™ Thermo Cycler, Biorad) with the setting as below: 25°C for 10 min, 42°C for 30 min, and 85°C for 5 min. The cDNA sample was diluted in 190 μL of nuclease-free water for latter use.

2.3.4 Real-time qPCR

Five microliter of cDNA was mixed with 10 μL of 2-fold SYBG reagent (Biorad), 0.5 μL of forward primer (10 μM), 0.5 μL of reverse primer (10 μM) and 4 μL of nuclease-free water. The reaction was performed in a thermo cycler (iQ5 Multicolor Real-Time PCR Detection System, Biorad) with the setting as following: initial denaturation at 95°C for 1 min, and 40 cycles, each containing denaturation at 95°C for 30 sec, annealing at 60°C for 30 sec, and elongation at 72°C for 30 sec. For generating melting curve, the temperature initiated at 55°C and then stepwise increased to 95°C in 0.5°C increments. The quantitative result was obtained by using the $2^{-\Delta\Delta Ct}$ method (Winer et al., 1999; Schmittgen et al., 2000). The primer sequences were listed below: NTRC-F (5'-aggtgtatttgcagctggagatg-3'), NTRC-R (5'-ttcttcagtagggggctggtggaa-3'), SAHH2-F (5'-gacgctcacagtggaacaacga-3'), SAHH2-R (5'-tcaactttccagcaaaatatcccc-3'), NOR-F (5'-agagaacgatgcatggaggtttgt-3'), NOR-R (5'-actggctcaggaaattggcaatgg-3'), TRXh2-F (5'-catgccatggctgataagttcaatg-3'), TRXh2-R (5'-tcaagttcgtccttttttggcacc-3'), TRXo1-F (5'-gcctggtgtggaccatgcag-3'), TRXo1-R (5'-cagtgttggcacagccgtgat-3'), EF1α-F (5'-tgagcacgctcttcttgctttca-3') and EF1α-R (5'-ggtggtggcatccatcttgttaca-3').

2.3.5 Protein extraction and immunoblotting

For tomato fruit tissues, total protein was extracted from 35 mg of material with 150 μL of double-strength Laemmli buffer (Laemmli, 1970) containing 10 mM DTT. For Arabidopsis leaf tissues, total protein was extracted from 25 mg of material with 250 μL of double-strength Laemmli buffer containing 10 mM DTT. The sample was incubated at 90°C for 5 min followed by centrifugation for 10 min at 20,000g in 4°C. Ten microliter of protein extract was applied into a 10 or 12% SDS-acrylamide gel for electrophoresis in 80 V for 20 min, and then 150 V for 1 hour. The gel was rinsed with double distill water several times to remove excess SDS, and the protein was transferred onto a 0.45-μm PVDF

membrane (Millipore) using a Wet/Tank Blotting System (Biorad) filled with the blotting buffer (25 mM Tris, 192 mM Gly, 10% [v/v] methanol) in 300 mA for 1 hour. The membrane was blocking with 5% (w/v) non-fat milk prepared in TBST buffer (10 mM Tris-HCl, pH 8.0, 150 mM NaCl, 0.1% [v/v] Tween-20) to avoid unspecific binding, and then incubated with the primary antibody prepared in 2% (w/v) BSA-TBST buffer at 4°C for 12 to 16 hours. The membrane was washed twice with sufficient TBST buffer, and then incubated with the secondary antibody conjugating horseradish peroxidase (Agrisera, 1:10000 dilution) at 25°C for 1 hour. Afterward, the membrane was washed twice with sufficient TBST buffer, and reacted with Prime ECL solution (GE Healthcare). The membrane was exposed to an X-ray film (Fuji) under dark to obtain protein signal. The protein signal was quantified using the software, Image-J. The information of primary antibodies was listed below: homemade NTRC antibody (1:1000 dilution), homemade APS1 antibody (1:3000 dilution), homemade 2-Cys Prx antibody (1:5000 dilution), Lhcb2 antibody (Agrisera, 1:5000 dilution), and RbCL antibody (Agrisera, 1:10000 dilution).

2.4 Respiration measurement

Before the measurement, the oxygen sensing system (OXY-4 mini, PreSens) was calibrated with 2-step approach. A small glass vial filled with TES-KOH buffer (50 mM, pH 6.5) served as the calibration of 100% oxygen (289 nmol O_2 mL^{-1}) in aqueous condition. Then, excess $Na_2S_2O_4$ was applied into the glass vial to consume out all oxygen. This served as the calibration of 0% oxygen in aqueous condition. Leaf discs were harvested from 3-week-old Arabidopsis plants, and placed into a small glass vial filled with TES buffer. A magnet bar was place into the vial with mild stirring to ensure the homogeneity of solution, and the glass vial was covered with blue tapes to avoid illumination. The oxygen consumption was detected via the Clark electrodes. The consumption rate was calculated within the range of 90%-to-80% oxygen content, and normalized with leaf fresh weight.

2.5 Carbon assimilation measurement

Carbon assimilation rate was measured using a gas-exchange system (GFS-3000, WALZ) equipped with a standard measuring head 3010-S. Before the measurement, the system was calibrated with an empty chamber, and the parameter was set as below: flow rate, 750 μmol min^{-1}, CO_2 concentration, 400 ppm, temperature, 25°C, and relative humidity, 70%. The setting of light intensity depended on the experimental design. Arabidopsis plants were grown on a roundish pot (diameter: 7 cm; height: 5 cm) for 18 to

20 days under a standard condition described above. The plant was placed into a chamber and sealed properly. For the response to different concentration of CO_2, the plant was first illuminated to photosynthetically active radiation of 1200 $\mu E\ m^{-2}\ s^{-1}$ under 400 ppm CO_2 for adaption, and then exposed to varied concentration of CO_2. The carbon assimilation was recorded every 30 sec.

2.6 Measurement of metabolites

2.6.1 Starch and soluble sugars

The determination of starch and soluble sugars was performed according to literatures with modifications (Shirokane et al., 2000; Hendriks et al., 2003). Around 20 mg of homogenized sample was suspended in 250 µL of ethanol (80%, v/v) followed by incubation at 90°C for 30 min. The sample was centrifuged for 10 min at 20,000g in 25°C, and the supernatant was transferred into a new microtube. The pellet was extracted again with 250 µL of ethanol (80%, v/v) and another 250 µL of ethanol (50%, v/v) by using the same procedure as above. Then, all supernatants were combined together for soluble sugar assay, and the insoluble pellet was used for starch assay.

For starch assay, the insoluble pellet was dried out using a vacuum, and then re-suspended in 400 µL of sodium hydroxide buffer (0.1 M) followed by incubation at 95°C for 1 hour with vigorous shaking. The sample was neutralized to pH 7.0 using HCl-acetate buffer (0.5 M HCl in 0.1 M acetate-NaOH buffer, pH 4.9) followed by centrifugation for 10 min at 20,000g in 25°C to remove residues. Forty microliter of the supernatant was mixed with 110 µL of starch degradation reagent (50 mM acetate-NaOH buffer, pH 4.9, 2.8 U mL^{-1} amyloglucosidase, 4 U mL^{-1} α-amylase), and incubated at 37°C for 12 to 16 hours. Afterward, 50 µL of digested sample was mixed with 160 µL of reaction buffer (100 mM HEPES-KOH, pH 7.0, 3 mM ATP, 1.3 mM NADP, 3 mM $MgCl_2$, 3.4 U mL^{-1} G6PDH). When the reaction reached to the stable state, 0.45 U hexokinase was applied into the sample. The amounts of NADPH produced in this reaction were equivalent to the amounts of starch. The signal was recorded using a spectrophotometer (FilterMax F5, Molecular Device) at 340 nm, and the calculation followed the Beer-Lamber law. Alternatively, for some samples containing low-abundant starch, the signal could also be detected using a florescence mode (excitation [Ex]: 340 nm, emission [Em]: 465 nm), and varied amounts of standard substances were used to build up the calibration curve.

For soluble sugar assay, the ethanol extract was first dried out using a vacuum, and then re-dissolved in the equal volume of double-distilled water. Twenty microliter of this extract was mixed with 200 µL of reaction buffer (50 mM HEPES-KOH, pH 7.0, 1.7 mM

ATP, 0.8 mM NADP, 5 mM $MgCl_2$, 0.7 U mL^{-1} G6PDH). When the reaction reached to the stable state, 0.5 U hexokinase, 0.2 U maltose phosphorylase, 1.2 U phosphoglucoisomerase, and 133 U invertase were applied into the sample for the detection of Glc, maltose, Fru and Suc, respectively. The detail of detection and calculation followed the same procedure as described above.

2.6.2 Hexose phosphates, triose phosphates and 3-PGA

This assay followed the method published previously (Häusler et al., 2000). The metabolites were extracted from 50 mg of homogenized samples with 500 μL of ice-cold $HClO_4$ solution (0.5 M). The sample was incubated on ice for 10 min followed by centrifugation for 10 min at 20,000g in 4ºC to remove residues. A potassium carbonate solution (2.5 M) was used to adjust the pH value of the extract to the range from 5.0 to 6.0. The formed precipitants were further removed by centrifuging for 10 min at 20,000g in 4ºC. The clear supernatant was exposed to 5 mg of active charcoal, and incubated on ice for 20 min to get rid of interfering substances. Charcoal was removed by centrifuging for 10 min at 20,000g in 4ºC, and the supernatant was used for the following measurements.

For detecting hexose phosphates, 20 to 50 μL of extract was mixed with 100 μL of reaction buffer (200 mM Tris-HCl, pH 8.1, 1.6 mM NADP, 10 mM $MgCl_2$, 2 μM G1,6BP), and supplemented with double-distilled water to make 200 μL in total volume. When this reaction reached to the stable state, 0.1 U G6PDH, 0.35 U phosphoglucoisomerase and 0.04 U phosphoglucomutase were applied into the sample for the detection of G6P, F6P and G1P, respectively, via NADPH production in this reaction using a florescence mode (Ex: 340 nm, Em: 465 nm) of the spectrophotometer (FilterMax F5, Molecular Device).

For detecting triose phosphates, 50 μL of extract was mixed with 100 μL of reaction buffer (100 mM HEPES-NaOH, pH 7.5, 1.2 mM NAD, 4 mM ADP, 2 mM $MgCl_2$, 4 mM NaH_2PO_4, 4.4 U mL^{-1} phosphoglucokinase), and supplemented with 50 μL of double-distilled water. When this reaction reached to the stable state, 0.08 U GAPDH, 1 U triose phosphate isomerase and 0.009 U Aldolase were applied into the sample for the detection of GAP, DHAP and F1,6BP, respectively, via NADH production in this reaction using a florescence mode (Ex: 340 nm, Em: 465 nm) of the spectrophotometer (FilterMax F5, Molecular Device).

For detecting 3-PGA, 20 to 50 μL of extract was mixed with 100 μL of reaction buffer (200 mM HEPES-NaOH, pH 7.0, 2 mM $MgCl_2$, 2 mM ATP, 8 μM NADH, 0.8 U mL^{-1} GAPDH), and supplemented with double-distilled water to make 200 μL in total volume. When this reaction reached to the stable state, 0.45 U phosphoglucokinase was applied into the sample for the detection of 3-PGA via NADH consumption in this reaction using a

florescence mode (Ex: 340 nm, Em: 465 nm) of the spectrophotometer (FilterMax F5, Molecular Device).

Varied amounts of NADPH and NADH were used to build up a calibration curve.

2.6.3 Pyruvate and PEP

The metabolite extraction followed the same procedure as described for sugar phosphates above (Häusler et al., 2000). Fifty microliter of the $HClO_4$ extract was mixed with 100 μL of reaction buffer (100 mM HEPES-NaOH, pH 7.5, 20 μM NADH, 2 mM ADP, 2 mM $MgCl_2$), and supplemented with 50 μL of double-distilled water. When this reaction reached to the stable state, 0.4 U lactate dehydrogenase and 2.2 U pyruvate kinase were applied into the sample for the detection of pyruvate and PEP, respectively, via NADH consumption in this reaction using a florescence mode (Ex: 340 nm, Em: 465 nm) of the spectrophotometer (FilterMax F5, Molecular Device). Varied amounts of NADH were used to build up a calibration curve.

2.6.4 Pyridine nucleotides

The assay of pyridine nucleotides was performed according to a literature (Lintala et al., 2014). Twenty-five milligram of homogenized sample was suspended in 250 μL of $HClO_4$ solution (0.1 M), and incubated on ice for 10 min followed by centrifugation for 10 min at 20,000g in 4°C to remove residues. The supernatant was first incubated at 95°C for 2 min to disrupt NADH and NADPH, and a KOH buffer (0.1 M) prepared in Tris-HCl solution (0.2 M, pH 8.4) was used to adjust the pH value of the supernatant to the range from 8.0 to 8.5. This extract was used for the detection of NAD^+ and $NADP^+$. Another 25 mg of homogenized sample was suspended in 250 μL of KOH solution (0.1 M), and incubated on ice for 10 min followed by centrifugation for 10 min at 20,000g in 4°C to remove residues. The supernatant was first incubated at 95°C for 2 min to disrupt NAD^+ and $NADP^+$, and a $HClO_4$ buffer (0.1 M) prepared in Tris-HCl solution (0.2 M, pH 8.4) was used to adjust the pH value of the supernatant to the range from 8.0 to 8.5. This extract was used for the detection of NADH and NADPH.

For the determination of NAD^+ and NADH, 50 μL of corresponding extract was first supplemented with 50 μL of double-distilled water, and mixed with 50 μL of reaction buffer (300 mM Tricine-KOH, pH 9.0, 12 mM EDTA, 1.5 M ethanol, 0.3 mM PES, 1.8 mM MTT, 18 U mL^{-1} alcohol dehydrogenase). For the determination of $NADP^+$ and NADPH, another 50 μL of corresponding extract was first supplemented with 50 μL of double-distilled water, and mixed with 50 μL of reaction buffer (300 mM Tricine-KOH, pH 9.0, 12 mM EDTA, 9 mM G6P, 0.3 mM PES, 1.8 mM MTT, 9 U mL^{-1} G6PDH). The signal was recorded every minute by using the spectrophotometer (FilterMax F5, Molecular

Device) at 540 nm. The slope generated from the linear region of reaction curve was used for calculation. Varied amounts of pyridine nucleotide standards were used to build up a calibration curve.

2.6.5 Adenine nucleotides

Adenine nucleotides were extracted as described previously (Jelitto et al., 1992). Approximate 50 mg of homogenized samples was suspended in 600 μL of TCA solution (16%, w/v) containing 5 mM EGTA followed by rigorously vortexed at 4°C for 1 hour, and the sample was centrifuged for 10 min at 20,000g in 4°C. Four milliliter of cold water-saturated diethylther was used to wash away excess TCA from the supernatant followed by centrifugation for 5 min at 1500g in 4°C, and the upper organic phase was discarded. This washing step was repeated again. Afterward, the lower aqueous phase was transferred into a new microtube, and, a neutralization buffer containing 5 M KOH and 1 M triethanoamine was used to adjust the pH value of the extract to the range from 6.0 to 7.0. The extract was placed in a hood to get rid of remaining diethyether. The determination of adenylate nucleotides was performed either by HPLC or spectrophotometer.

The HPLC-based method was described previously (Haink and Deussen, 2003). Briefly, 85 μL of TCA extract was mixed with 20 μL of citrate buffer (pH 5.2) containing 62 mM citric acid and 76 mM KH_2PO_4, and another 20 μL of chloroacetaldehyde (50%, v/v). The whole mixture was incubated at 80°C for 20 min for derivatization. Finally, 20 μL of the sample was injected into a HPLC system consisting of a NUCLEODUR 100-5 C_{18}ec column (MACHEREY-NAGEL) and a florescence detector (FINNIGAN SURVEYOR PDA Plus Detector, ThermoFisher Scientific), which the Ex was set to 280 nm, and Em was set to 410 nm. The sample was eluted by using the mixture of buffer A (10 mM KH_2PO_4 and 5.7 mM TBAHS) and buffer B (90% [v/v] acetonitile). The flow rate was set as 0.8 mL min^{-1}, and the gradient was set as below: 0 min (100% A/0% B), 18 min (86% A/14% B), 36 min (56% A/44% B), 38.4 min (17.5% A/82.5% B), 39.6 min (100% A/0% B), and 42 min (100% A/0% B).

The spectrophotometer-based method was performed according to a literature (Helenius et al., 2012). Five microliter of TCA extract first mixed with 78 μL of reaction buffer (32 mM Tricine, pH 7.8, 6.4 mM $MgSO_4$, 0.05 mM EDTA, 0.025 mM UTP) and 20 μL of ATP reagent SL (BioThema). The emission of light was measured immediately as the signal of ATP via the luminescence mode of the spectrophotometer (FilterMax F5, Molecular Device). When the reaction was stable, 2 μL of NDP kinase solution (1 μg μL^{-1})

was applied into the sample. The second emission of light was recorded immediately as the total signal of ATP and ADP.

Varied amounts of adenylate nucleotide standards were used to build up a calibration curve.

2.6.6 ADP-Glc

The extraction method followed a previous publication with modification (Lunn et al., 2006). ADP-Glc was extracted from 50 mg of homogenized sample with 375 µL of chloroform-methanol mixture (v/v, 3:7). The sample was vortex vigorously at 4°C for 10 min, and then 300 µL of double-distilled water was applied into the sample for phase separation followed by centrifugation for 10 min at 18,000g in 4°C. The upper aqueous phase was transferred into a new microtube, and dried out using a vacuum in ambient temperature. The pellet was then re-dissolved in 70 µL of double-distilled water, and 10 µL of the sample was injected into a LC-MS system for detecting ADP-Glc.

This LC-MS system consisted of a Dionex Ultimate 3000 UHPLC (ThermoFisher Scientific) and a timsTOF QTOF (Bruker Daltonik). The sample was first applied into a C18 column (Ultra AQ C18, 150 × 210 mm, 3 µm, Restek), and the flow rate was set as 300 µL min^{-1} and temperature was 22°C. The sample was eluted with LC-grade water (A) and acetonitrile (B), both containing formic acid (0.1%, v/v). The gradient was set as 1% B for the first minute, and then ramped to 25% B within 10 min. Then, the column was washed with 95% B for 4 min. Afterward, the gradient changed back to 1% B for 3 min to make equilibration. After elution, the analytes flowed through a diode array detector at 254 nm, and then entered the mass spectrometer. The negative mode of an electrospray ionization source was adopted at 5,000 V capillary voltage, and nitrogen served as dry gas with the flow rate, 8 L min^{-1}, at 200°C. The mass range of the timsTOF mass spectrometer was set from 50 to 1300 *m/z*. The specific mass (m/z), isotope pattern, and retention time were used to identify target compounds. Data was obtained using otofControl 4.0 (Bruker Daltonik), and evaluated using DataAnalysis 5.1 (Bruker Daltonik). Varied amounts of ADP-Glc were used to generate the calibration curve.

2.6.7 Total chlorophyll

Total chlorophyll was extract using acetone-based method (Porra et al., 1989). Approximate 35 mg of homogenized sample was suspended in 1 mL of ice-cold acetone (80%, v/v) followed by centrifugation for 10 min at 20,000g in 4°C to remove residues. Then, 250 µL of the supernatant was diluted four times using 80% acetone, and transferred into a quartz cuvette for detecting the optical density at 664 nm and 647 nm.

2.7 Metabolite profiling

Metabolite profiling was performed via gas chromatography coupled to time-of-flight mass spectrometry (GC-TOF-MS) as described before with modifications (Roessner et al., 2001; Lisec et al., 2006; Erban et al., 2007). The total metabolites were extracted from 50 mg of pulverized samples with 360 μL of cold methanol containing 10 μL of ribitol solution (0.2 mg mL^{-1}) and 10 μL of 13C-sorbitol solution (0.2 mg mL^{-1}) as internal control. The sample was incubated at 4°C for 30 min. Then, 200 μL of chloroform and 400 μL of water were applied into the sample, and the mixture was vortexed vigorously followed by centrifugation for 15 min at 25,000g in 4°C for phase partition. Fifty microliter of the upper polar phase was transferred into a glass vial, and dehydrated by a vacuum. For derivatization, the pellet was re-suspended in 10 μL of methoxyaminhydrochloride (20 mg mL^{-1}) prepared in pyridine, and incubated at 40°C for 90 min, and then mixed with 20 μL of N,O-Bis[trimethylsilyl]tri- fluoroacetamide containing 2.5 μL of linear alkanes (n-decane, n-dodecane, n-pentadecane, n-nonadecane, n-docosane, n-octacosane, n-dotriacontane) as retention time standard followed by incubation at 40°C for 45 min. One microliter of sample was applied into a GC-TOF-MS system (Pegasus HT, Leco). Helium served as carrier gas, and the flow rate was set as 1 mL min^{-1}. Gas chromatography was performed by using a VF-5ms column (30 m) conjugated with an EZ-Guard column (10 m) on an Agilent GC (7890A, Anilent). The split/splitless injector, the transfer line and the ion source were warmed up to 250°C. The oven temperature was increased from 70°C to 350 °C by 9°C min^{-1}. The solvent delay time was set as 340 sec to avoid contaminations. After compounds were ionized and fractionate at 70 eV, the signal from 35 to 800 *m/z* was scanned and recorded at 20 scans s^{-1} to obtain mass spectra. The results were analyzed by using ChromaTOF 4.5 and TagFinder 4.1 software (Luedemann et al., 2008).

2.8 Determination of protein redox state

The total protein was extracted by a TCA-based method to preserved protein redox state (Hendriks et al., 2003). Approximate 35 mg of pulverized material was suspended in 1 mL of ice-cold TCA solution (16%, w/v) prepared in water-saturated diethylether, and incubated at -20°C. In the beginning of incubation, the sample was vortex every 30 min, and this step repeated twice. Afterward, the sample was placed -20°C for 12 to 16 hours. The sample was centrifuged for 10 min at 20,000g in 4°C, and the supernatant was discarded. The protein pellet was washed twice with ice-cold pure acetone, and then placed in the hood to get rid of remaining acetone. The protein pellet was re-suspended in 150 to

250 µL of double-strength Laemmli buffer (Laemmli, 1970), and incubates at 90°C for 5 min with vigorous shaking. The protein extract was further centrifuged for 10 min at 20,000g in 4°C to remove debris, and 10 µL of the supernatant was applied into 10 or 12% SDS-acrylamide gel followed by immunoblotting performed as described previously.

2.9 Enzyme activity assay

2.9.1 AGPase

The AGPase activity was assayed by detecting the formation of ADP-Glc within a period of time according to a previous literature (Tiessen et al., 2002). Around 25 mg of homogenized sample was suspended in 150 µL of extraction buffer (50 mM HEPES-KOH, pH 7.5) followed by centrifugation for 10 min at 20,000g in 4°C to get rid of debris. The supernatant was passed through the Zeba desalting column (Thermo), which pre-equilibrated with 50 mM HEPES-KOH buffer (pH 7.5), to remove interfering substances. Then, 20 µL of the supernatant was mixed with 180 µL of reaction buffer (50 mM HEPES-KOH, pH 7.5, 7 mM $MgCl_2$, 1.5 mM ATP, 0.5 mM G1P, 0.25 to 10 mM 3-PGA), and incubated at 25°C for 30 min with mild shaking. One hundred microliter of chloroform was applied into the sample with vigorous shaking to terminate the reaction followed by centrifugation in 12,000 g at 25°C for 10 min for phase partition. Two microliter of the aqueous phase was applied into a LC-MS system for quantifying ADP-Glc as described previously.

2.9.2 Soluble starch synthase and granule-bound starch synthase

The starch synthase activity was assayed via detecting the generation of ADP within a period of time according to a previous literature with modifications (Kulichikhin et al., 2016). The total protein was extracted from 25 mg of homogenized sample with 150 µL of extraction buffer (100 mM HEPES-NaOH, pH 7.5, 8 mM $MgCl_2$, 2 mM EDTA, 12.5% [v/v] glycerol, 5% [w/v] PVP-10, one tablet protease inhibitor cocktail [Roche]). The sample was incubate on ice for 10 min, and the centrifuged for 10 min at 20,000g in 4°C. The supernatant was used for the assay of soluble starch synthase, and the insoluble pellet was used for the assay of granule-bound starch synthase.

For analyzing soluble starch synthase activity, the supernatant was first passed through a self-packed Sephadex G-25 column, which pre-equilibrated with 50 mM HEPES-NaOH buffer (pH 7.5) for the removal of excess salt and other interfering substances. Fifty microliter of the desalting protein extract was mixed with 50 µL of reaction buffer (100 mM HEPES-NaOH, pH 7.5, 2 mM ADP-Glc, 0.2% [w/v] amylopectin), and the incubated at 30°C for 30 min. Then, 30 µL of chloroform was

applied into the sample to stop the reaction followed by centrifugation in 12,000 g at 4°C for 10 min for phase separation. Ten microliter of the upper aqueous phase was applied into a LC-MS system for detecting ADP formation. ADP was assayed as described for detecting ADP-Glc. Varied amounts of ADP standard were used to build up the calibration curve.

For analyzing granule-bound starch synthase activity, the insoluble pellet was first rinsed with 1 mL of 50 mM HEPES-NaOH buffer (pH 7.5) twice to remove remaining SSS, and re-suspended by using 100 μL of reaction buffer containing 50 mM HEPES-NaOH (pH 7.5) and 1 mM ADP-Glc. The mixture was incubated at 30°C for 30 min with moderate shaking, and the following steps were processed as described above.

2.9.3 Starch phosphorylase

The starch phosphorylase activity was assayed by detecting the formation of G1P according to previous literatures (Zeeman et al., 1998; Häusler et al., 2000). The total protein was extracted from 25 mg of homogenized sample with 150 μL of extraction buffer containing 40 mM HEPES-NaOH (pH 7.5) and 1 mM EDTA, and incubated on ice for 10 min. The sample was centrifuged for 10 min at 20,000g in 4°C to remove residues. Then, 25 μL of the supernatant was mixed with 100 μL of reaction buffer (200 mM Tris-HCl, pH 8.1, 1.6 mM NADP, 10 mM $MgCl_2$, 2 μM G1,6BP, 20 mM sodium phosphate buffer, pH 6.9, 0.1% [w/v] amylopectin, 0.11 U G6PDH, 0.07 U phosphoglucomutase), and supplemented with 75 μL of double-distilled water. NADPH produced in this reaction was equivalent to the amounts of G1P. The NADPH signal was detected in the florescence mode of spectrophotometer (Ex: 340 nm, Em: 465 nm), and recorded every minute to build up a kinetic curve. The linear region of this kinetic curve was used for the calculation of enzyme activity.

2.9.4 Starch hydrolase

The starch hydrolase activity was assayed by detecting the release of reducing groups from starch using DNS reagent (Miller, 1959). The total protein was extracted from 25 mg of homogenized sample with 150 μL of extraction buffer containing 20 mM sodium phosphate buffer (pH 6.9) and 6 mM NaCl, and incubated on ice for 10 min. The sample was centrifuged for 10 min at 20,000g in 4°C to remove residues. To get rid of endogenous sugars, the supernatant was passed through a self-packed Sephadex G-25 column pre-equilibrated with the same extraction buffer. Fifty microliter of desalting protein extract was mixed with 50 μL of soluble starch (1%, w/v), and another 50 μL of protein extract was mixed with extraction buffer as the blank reaction. Both reactions were performed at 60°C for 30 min, and terminated by adding 100 μL of DNS reagent (1% [w/v]

3,5-dinitrosalicylic acid, 30% [w/v] sodium potassium tartrate tetrahydrate) followed by incubating at 95°C for 5 min. The signal was detected in the absorbance mode of spectrophotometer (540 nm). Varied amounts of maltose standard were used to build up the calibration curve.

2.9.5 Determination of protein concentration

The protein concentration was determined by using Pierce 660 nm protein reagent (Thermo) or Bradford reagent (Carl Roth). The detailed procedures were described in the manual.

2.10 Pulse-Amplitude-Modulation measurement

Foe non-acclimation condition, Arabidopsis plants were grown under constant medium light intensity (150 µmol m^{-2} s^{-1}) for three weeks. For acclimation condition, Arabidopsis plants were grown under fluctuating light intensities (50 µmol m^{-2} s^{-1} for 5 min; 550 µmol m^{-2} s^{-1} for 1 min) for four weeks. Before the measurement, plants were placed under dark for 30 min, and then shifted into a image-PAM instrument (MAXI version, WALZ). The plants were subjected to a short-term period of fluctuating light intensities as described above, and the signal was recorded every 30 sec. The calculation of the yield of photosystem II [Y(II)], non-photochemical quenching (NPQ) and the reduction of plastoquinone pool (1-qL) followed the equations: $Y(II) = (F_m' - F) / F_m'$; $NPQ = (F_m - F_m') / F_m'$; $qL = [(F_m' - F) F_o] / [(F_m' - F_o) F]$. F, fluorescence yield measured briefly before application of a saturation pulse; F_m, maximal fluorescence yield of dark-adapted sample with all PSII centers closed; F'_m, maximal fluorescence yield of illuminated sample with all PSII centers closed; F_o, minimal fluorescence yield of dark-adapted sample with all PSII centers open.

2.11 Statistical analysis

The software, Graphpad Prism 8.0, was used to generate all figures and perform statistical analyses. The difference between wild type and mutants was evaluated by ANOVA and Dunnett's post-hoc test unless otherwise stated.

2.12 Accession numbers

Sequence data is available in the GenBank/EMBL data libraries under accession numbers LOC101254347 (*SlNTRC*), Solyc09g092380 (*SlSAHH2*), Solyc10g006880 (*SlNOR*), and SGN- U314153 (*SlCAC*).

3 Results

3.1 Functional characterization of mitochondrial TRXs in Arabidopsis plants

To investigate the function of mitochondrial TRXs in Arabidopsis plants, T-DNA insertion mutant lines with decreased expression of *TRXh2* and *TRXo1* were used for further investigations.

3.1.1 Molecular characterization of T-DNA insertion Arabidopsis mutants

To investigate the function of mitochondrial thioredoxins, TRXh2 and TRXo1, Two T-DNA insertion mutants, *trxh2.1* and *trxo1.1* were selected for following assays. As shown in the Fig. 3.1.1A, the *trxh2.1* harbors a T-DNA fragment at the third exon of *TRXh2* genomic DNA, and the *trxo1.1* harbors a T-DNA fragment at the first intron of *TRXo1* genomic DNA. A double mutant, *trxh2.1trxo1.1*, was generated via crossing the *trxh2.1* and *trxo1.1*.
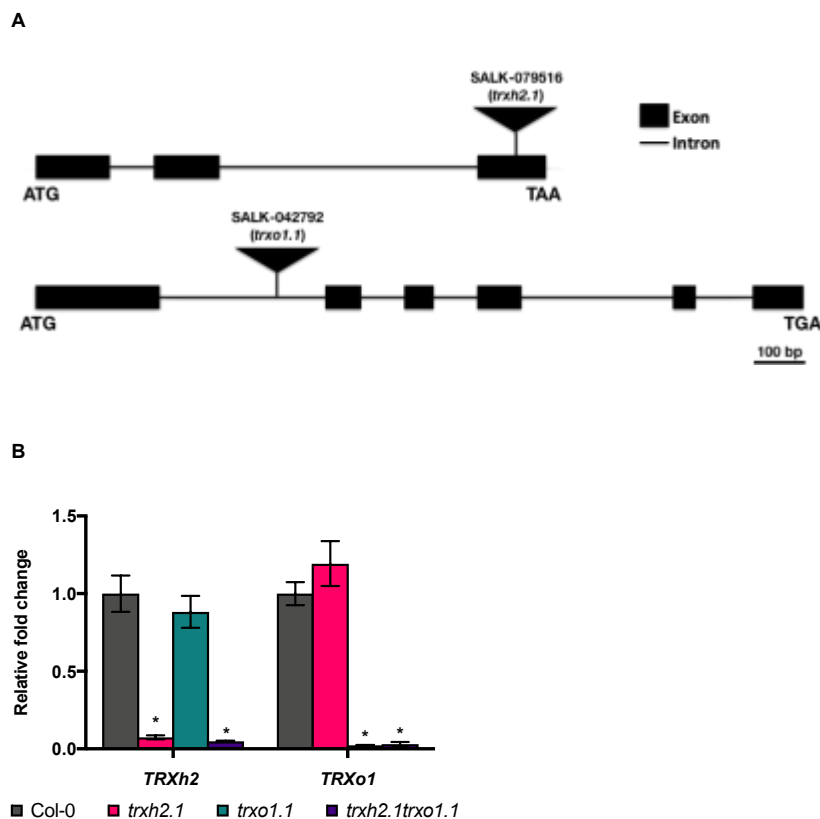
Figure 3.1.1 Molecular characterization of *trxh2.1*, *trxo1.1* and their double mutants, *trxh2.1trxo1.1*. A, The scheme of T-DNA insertion sites in t*rxh2.1* and *trxo1.1* mutants. B, The transcript levels of *TRXh2* and *TRXo1* in mutant lines compared to the wild type (Col-0). Mean values and standard errors derived from 6 biological replicates. The statistical analyses were performed by using ANOVA and the Dunnett's test (*$P<0.05$, in comparison to the wild type).

To examine the expression of *TRXh2* and *TRXo1* genes, a real-time quantitative PCR was performed in the mutant lines. In *trxh2.1*, the expression of *TRXh2* decreased by 95% in comparison to the wild type. In *trxo1.1*, the expression of *TRXo1* decreased by 95% in

comparison to the wild type (Fig. 3.1.1B). The expression levels of both *TRXh2* and *TRXo1* in the *trxh2.1trxo1.1* line also decreased by 95% when compared to wild-type level. Thus, the three mutant lines were appropriate for the following applications.

3.1.2 The effects of down-regulating *TRXh2* and *TRXo1* on the growth of Arabidopsis plants

To understand whether down-regulating the two mitochondrial TRXs affects the growth of Arabidopsis plants, several growth parameters of adult Arabidopsis plants grown under different light conditions were analyzed.
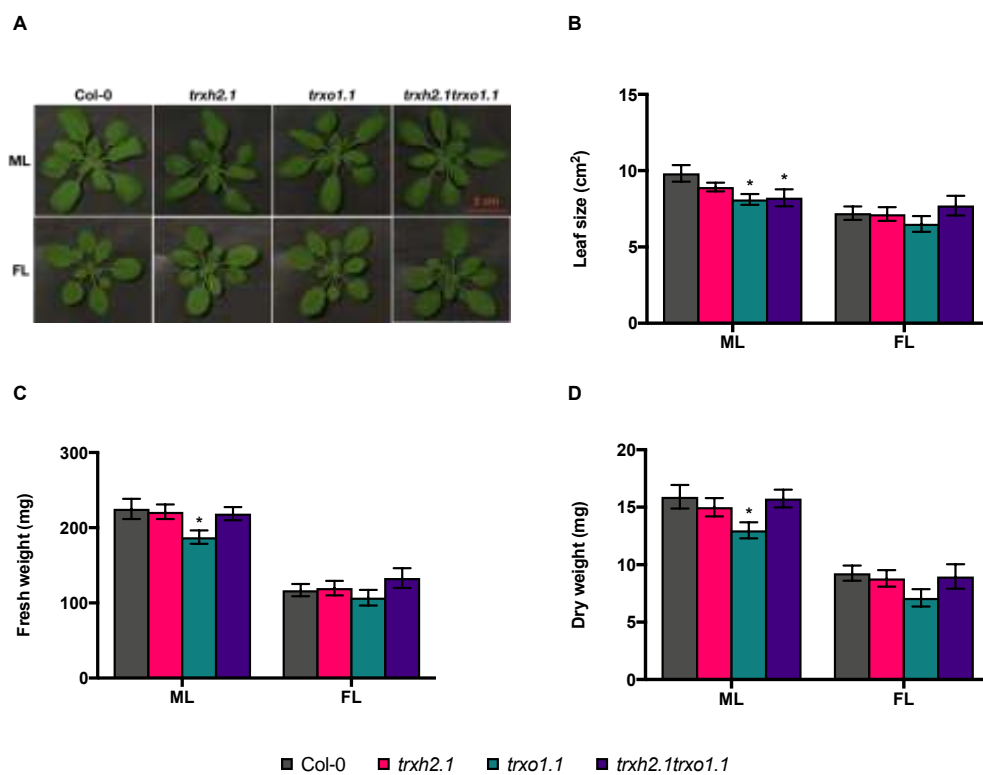
Figure 3.1.2 Phenotypic analysis of the wild type (Col-0) and mutant lines (*trxh2.1*, *trxo1.1* and *trxh2.1trxo1.1*) grown under medium light (ML) or fluctuating light (FL) condition. A, Visible phenotype of rosette leaves. B, Leaf size. C, Leaf fresh weight. D, Leaf dry weight. Mean values and standard errors derived from 10 to 14 plants. The statistical analyses were performed by using ANOVA and the Dunnett's test (*$P<0.05$, in comparison to the wild type). Scale bar = 2 cm.

The light intensity of medium condition (ML) was maintained at 150 μmol m^{-2} s^{-1}. The light intensity of fluctuation condition (FL) was set at 50 μmol m^{-2} s^{-1} for 5 min as a low-light phase and then changed to 550 μmol m^{-2} s^{-1} for 1 min as a high-light phase. In both light condition, all mutant lines shared similar morphology as the wild type (Fig. 3.1.2A). The entire leaf size and weight were further analyzed. In the medium light condition, the leaf size of *trxo1.1* and *trxh2.1trxo1.1* lines was smaller than the wild type (Fig. 3.1.2B). Interestingly, only *trxo1.1* showed a significant decrease in fresh and dry

weight compared to the wild type (Fig. 3.1.2, C and D). In fluctuating light condition, plant size and weight of mutant lines were not significant changed compared to the wild type (Fig. 3.1.2, B, C and D).

3.1.3 The effects of down-regulating *TRXh2* and *TRXo1* on the accumulation of starch and soluble sugars

To study whether down-regulation of mitochondrial TRXs is able to affect the carbon metabolism, the accumulation of starch and soluble sugars was measured in the wild type and mutant lines at the end of night (EN) and the end of day (ED).
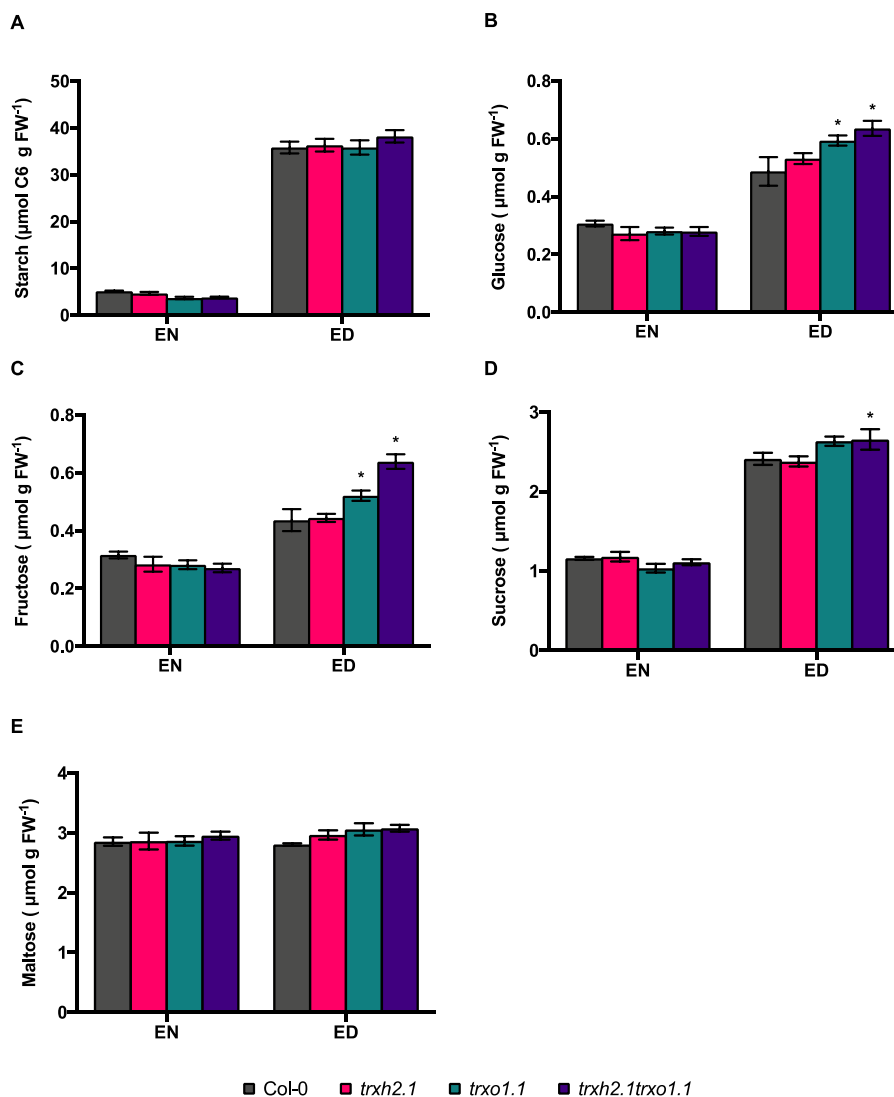
Figure 3.1.3 The accumulation of starch and soluble sugars in the wild type (Col-0) and the mutant lines (*trxh2.1*, *trxo1.1* and *trxh2.1trxo1.1*). Arabidopsis rosette leaves were harvested at the end of night (EN) and the end of day (ED). A, The starch level. B, The Glc level. C, The Fru level. D, The Suc level. E, The maltose level. Mean values and standard errors derived from 6 biological replicates. The statistical analyses were performed by using ANOVA and the Dunnett's test (*$P < 0.05$, in comparison to the wild type).

Independent of the genotypes, there were diurnal changes in carbohydrate levels, showing an increase in the levels of starch, Glc, Fru and Suc at the ED. Either at the EN or ED, the level of starch was not changed in *trxh2.1*, *trxo1.1* and *trxh2.1trxo1.1* compared to Col-0 (Fig. 3.1.3A). At the EN, the levels of soluble sugars were not significantly changed between the genotypes (Fig. 3.1.3, B, C and D). Interestingly, at the ED, the Glc level significantly increased by 10% in *trxo1.1* and 20% in *trxh2.1trxo1.1* when compared to wild-type level (Fig. 3.1.3, B). The Fru level also increased by 25% in *trxo1.1* and 50% in *trxh2.1trxo1.1* in comparison to wild-type level (Fig. 3.1.3, C). The level of Suc marginally - but significantly - increased by 10% in *trxh2.1trxo1.1* compared to wild-type level (Fig. 3.1.3D). The level of maltose was not significantly changed between genotypes (Fig. 3.1.3E), even though the mutant lines showed a small tendency to higher level compared to the wild type.

3.1.4 The effects of down-regulating *TRXh2* and *TRXo1* on the accumulation of phosphorylated intermediates and adenine nucleotides

To test whether TRXh2 and TRXo1 are involved in cellular energy metabolism, several metabolites involved in pathways of cellular energy provision, such as glycolysis and respiration, were further analyzed.

In the wild type, there were higher levels of G6P, F6P, G1P, DHAP and F1,6BP at the ED compared to the EN, while the level of 3-PGA showed an opposite behavior. In the *trxh2.1trxo1.1* double mutant, the levels of G6P and G1P were more strongly increased at the ED compared to Col-0 (Fig. 3.1.4, A and C). Surprisingly, the level of F6P was not changed in *trxh2.1trxo1.1* line, but significantly decreased in *trxh2.1* and *trxo1.1* (Fig. 3.1.4B). Nevertheless, at the EN and ED, the levels of 3-PGA and triose phosphates were not substantially changed in mutant lines compared to the wild type (Fig. 3.1.4, D, E and F).
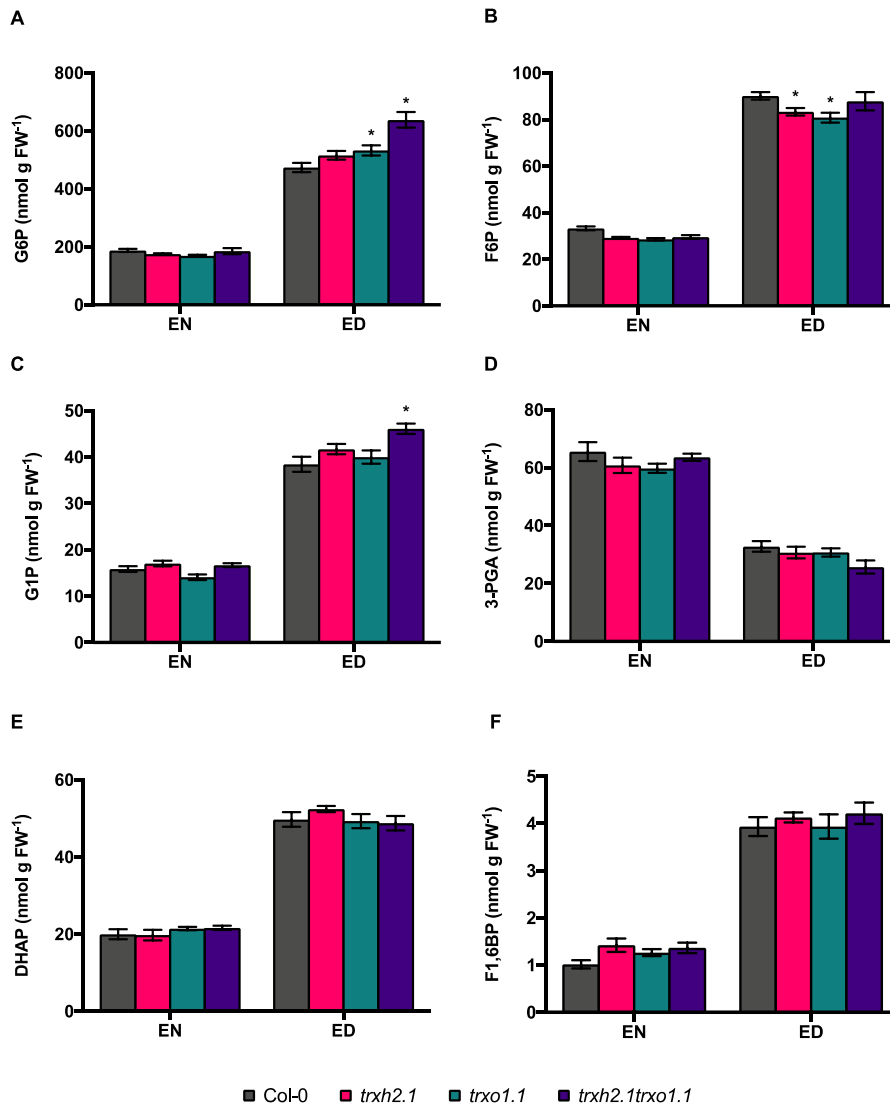
Figure 3.1.4 The accumulation of hexose phosphate, 3-PGA and triode phosphate in the wild type (Col-0) and the mutant lines (*trxh2.1*, *trxo1.1* and *trxh2.1trxo1.1*). Arabidopsis rosette leaves were harvested at the end of night (EN) and the end of day (ED). A, The G6P level. B, The F6P level. C, The G1P level. D, The 3-PGA level. E, The DHAP level. F, The F1,6BP level. Mean values and standard errors derived from 6 biological replicates. The statistical analyses were performed by using ANOVA and the Dunnett's test (*$P<0.05$, in comparison to the wild type).

Furthermore, to understand whether the glycolytic processes are affected in the mutant lines, the levels of pyruvate, PEP and adenine nucleotides were further analyzed. In the wild type, there were higher levels of ATP and ADP at the ED compare to the EN, while the levels of pyruvate and PEP were not substantially changed between two time points. The level of pyruvate was not changed between genotypes (Fig. 3.1.5A), but *trxh2.1*, *trxo1.1* and *trxh2.1trxo1.1* showed a 25% decrease of PEP level at the EN and a 30%-to-40% decrease of PEP level at the ED compared to the wild type (Fig. 3.1.5B). The ATP level was not significantly changed in mutant lines, while *trxo1.1* and the DoMu line showed a clearly decreased pattern in the ADP level especially at the EN (Fig. 3.1.5, C and D). This is indicative of a higher ATP-to-ADP ratio in *trxh2.1trxo1.1* at the EN (Fig.

3.1.5E). To sum up, decreasing the expression of TRXh2 and TRXo1 affects glycolytic metabolism and adenylate energy state.
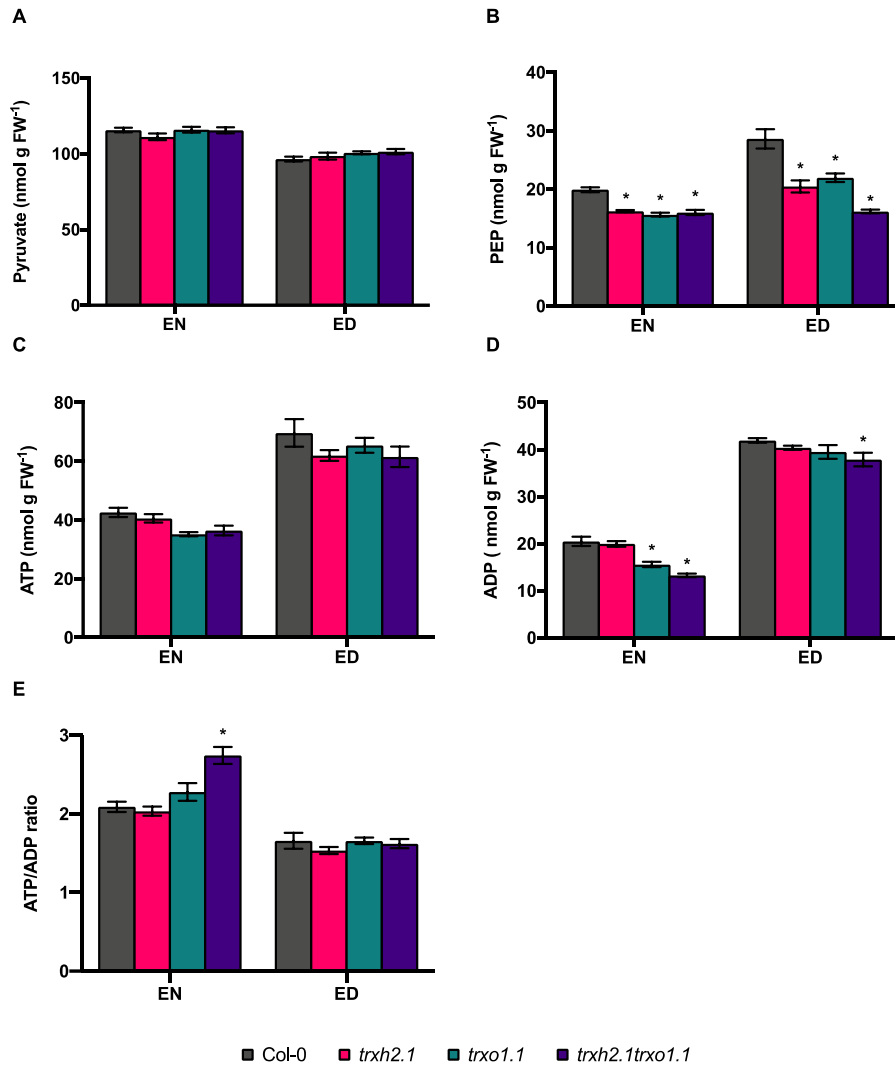
Figure 3.1.5 The accumulation of glycolytic intermediates and adenylate nucleotides in the wild type (Col-0) and the mutant lines (*trxh2.1*, *trxo1.1* and *trxh2.1trxo1.1*). Arabidopsis rosette leaves were harvested at the end of night (EN) and the end of day (ED). A, The pyruvate level. B, The PEP level. C, The ATP level. D, The ADP level. E, The ATP-to-ADP ratio. Mean values and standard errors derived from 6 biological replicates. The statistical analyses were performed by using ANOVA and the Dunnett's test (*$P<0.05$, in comparison to the wild type).

3.1.5 The effects of down-regulating *TRXh2* and *TRXo1* on the global levels of metabolites

To obtain in-depth understanding in the global changes of metabolite levels in the mutants of mitochondrial TRXs compared to the wild type, a metabolite profile via GC-TOF-MS was performed.
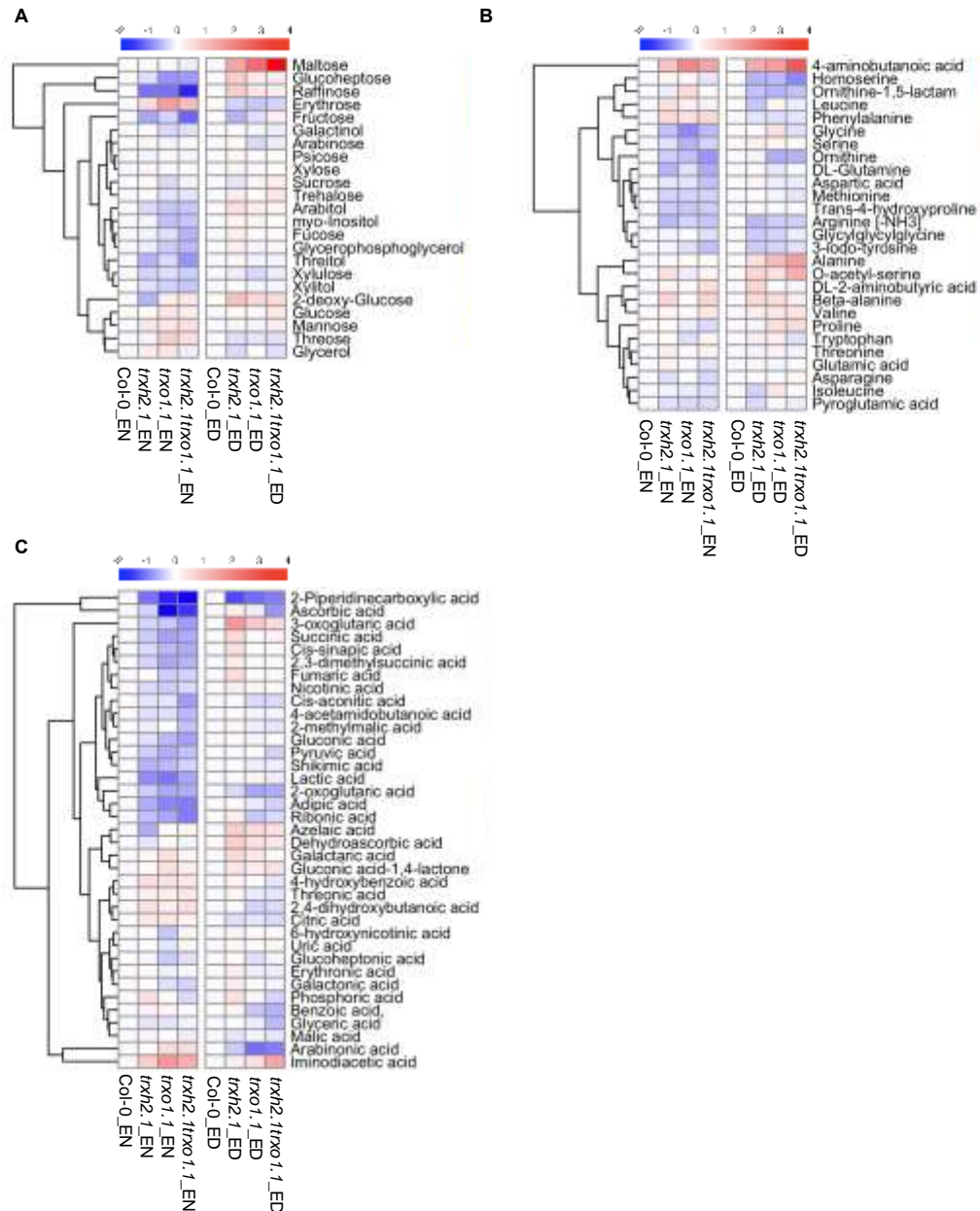
Figure 3.1.6 Metabolite profile of the wild type (Col-0) and the mutant lines (*trxh2.1*, *trxo1.1* and *trxh2.1trxo1.1*). The metabolite profile was measured in Arabidopsis leaves harvested at the end of night (EN, left panel) and the end of day (ED, right panel) by using GC-TOF-MS. A, Sugars and sugar alcohols. B, Amino acids. C, Organic acids and tricaboxylic acid cycle intermediates. Results are normalized to Col-0 with $\log_2$ transformation and visualized as a heatmap with hierarchical clustering done by R software. The original data and statistic analysis are in Supplemental Table S2.

The levels of several sugars were decreased in *trxh2.1*, *trxo1.1* and *trxh2.1trxo1.1* compared to the wild type at the EN, which was the case for erythrose, glucoheptose, raffinose and Fru. Other sugars and sugar alcohols were moderately altered in *trxh2.1*, *trxo1.1* and *trxh2.1trxo1.1* when compared to Col-0 (Fig. 3.1.6A, left; Suppl. Table S1). Interestingly, at the ED, the *trxh2.1* and *trxo1.1* lines showed two-to-four times higher level of maltose than wild-type level. The double mutant even showed fourteen times higher maltose level when compared to wild-type level (Fig. 3.1.6A, right; Suppl. Table

S1). However, this result was not consistent to the results from spectrophotometric assay (Fig. 3.1.3E). This might be due to the difference of extraction methods between GC-TOF-MS and spectrophotometric assay. The levels of several amino acids showed a decreased tendency, such as Met, Gly and Ser, in *trxh2.1*, *trxo1.1* and *trxh2.1trxo1.1* compared to the wild type at the EN (Fig. 3.1.6B, left; Suppl. Table S1). Unlike the samples from the EN, the levels of most amino acid were not significantly changed between genotypes at the ED (Fig. 3.1.6B, right; Suppl. Table S1). Notably, either at the EN or ED, the level of 4-aminobutanoic acid (GABA) in *trxh2.1*, *trxo1.1* and *trxh2.1trxo1.1* was clearly increased to two-to-five times wild-type level. In addition to amino acids, the levels of many organic acids were also decreased in *trxh2.1*, *trxo1.1* and *trxh2.1trxo1.1* at the EN compared to the wild type, including those of 2-piperidinecarboxylic acid, adipic acid, gluconic acid and lactic acid (Fig. 3.1.6C, left; Suppl. Table S1), while the changes between genotypes were nearly diminished at the ED (Fig. 3.2.6C, right; Suppl. Table S1). The intermediates of tricarboxylic acid cycle, including aconitic acid, fumaric acid, 2-oxoglutaric acid, and succinic acid, were moderately decreased in *trxh2.1*, *trxo1.1* and *trxh2.1trxo1.1* at the EN compared to the wild type, but the changes between genotypes was disappeared at the ED (Fig. 3.1.6C; Suppl. Table S1). Although the level of pyruvic acid was decreased in *trxh2.1*, *trxo1.1* and *trxh2.1trxo1.1* at the EN in comparison to the wild type (Fig. 3.1.6C, left; Suppl. Table S1), the result was not matched to the results of spectrophotometric assay (Fig. 3.1.5A). This might attribute to the differences between analyzing approaches. Taken together, these results indicated that perturbing the expression of TRXh2 and TRXo1 affects the metabolisms of sugars, amino acids and organic acids, especially during night.

3.1.6 The performance of respiratory and photosynthetic parameters in the mutants of TRXh2 and TRXo1

To unveil the physiological phenotype of the mutant lines, the oxygen consumption rate was measured by using leaf discs in dark. As shown in Fig. 3.1.7A, *trxh2.1* and *trxo1.1* showed comparable dark respiration rate to the wild type, and the dark respiration rate of *trxh2.1trxo1.1* line was slightly decreased compared to the wild type. We then measured CO_2 assimilation rate of levels in saturating light conditions. When the *trxh2.1trxo1.1* line was exposed to elevated CO_2 concentration, the carbon assimilation rate of the double mutant was higher than the wild type (Fig. 3.1.7B).
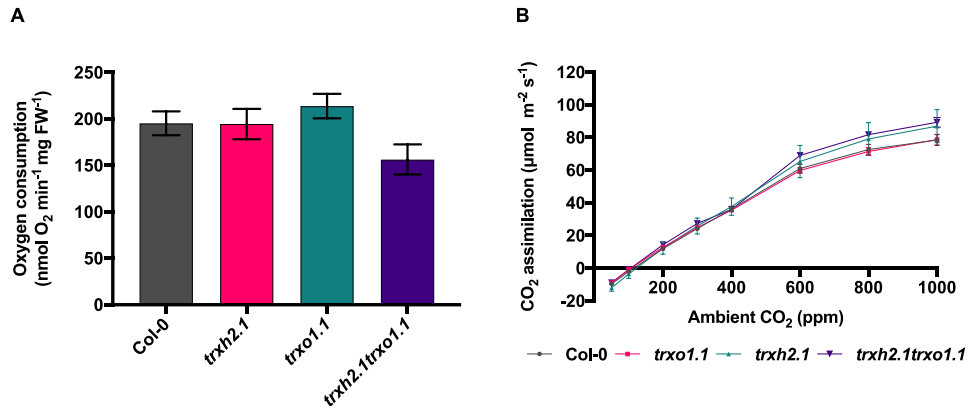
Figure 3.1.7 The performance of dark respiration and carbon assimilation in the leaves of wild type (Col-0) and the mutant lines (*trxh2.1*, *trxo1.1* and *trxh2.1trxo1.1*). A, The changes of respiration rate in dark. B, The changes of carbon assimilation rate in response to different CO_2 concentration under saturated light condition. Mean values and standard errors derived from 6 biological replicates.
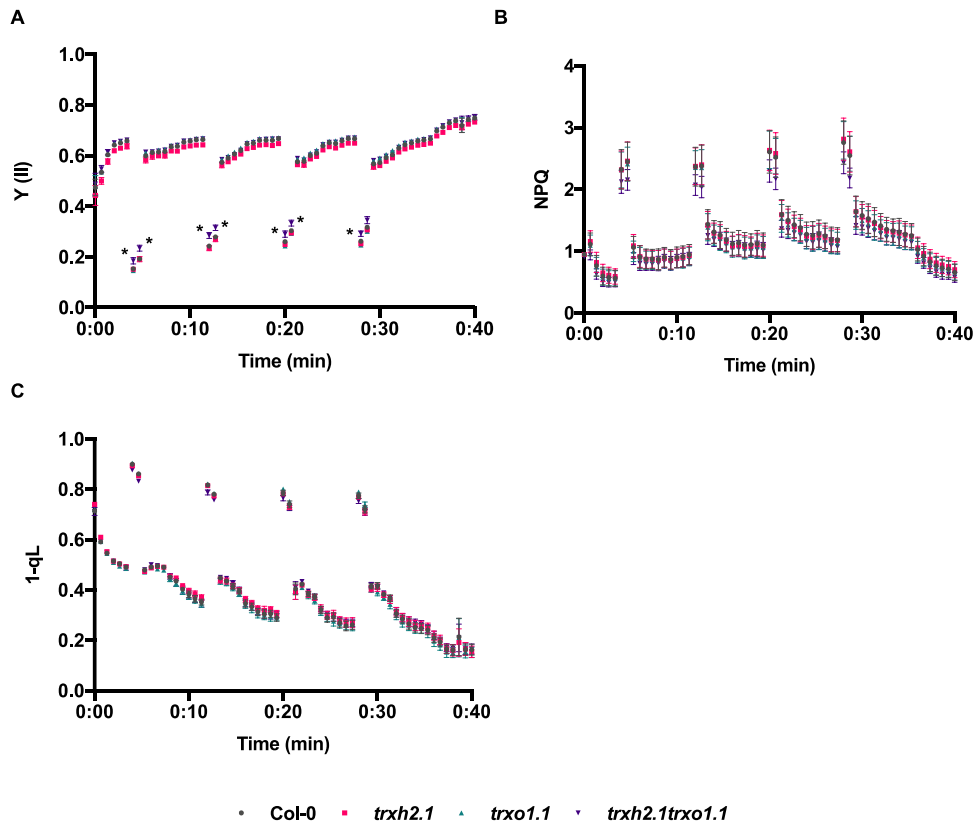
Figure 3.1.8 Photosynthetic performance and changes in photosynthetic parameters between the wild type (Col-0) and the mutant lines (*trxh2.1*, *trxo1.1* and *trxh2.1trxo1.1*). The plants were grown under constant medium light (150 μmol m^{-2} s^{-1}) for three weeks and then subjected to fluctuating light intensities (50 μmol m^{-2} s^{-1} for 5 min; 550 μmol m^{-2} s^{-1} for 1 min). A, B and C, The changes in the quantum yield of photosystem II (A), non-photochemical quenching (NPQ) (B) and the reduction of plastoquinone pool (1-qL) (C) under the condition of fluctuating light. Mean values and standard errors derived from 6 biological replicates. The statistical analyses were performed by using ANOVA and the Dunnett's test (*$P<0.05$, in comparison to the wild type).

Furthermore, we exposed the mutant lines grown under constant medium light (150 μmol m^{-2} s^{-1}) to a short-term period of fluctuating light condition (50 μmol m^{-2} s^{-1} for 5 min; 550 μmol m^{-2} s^{-1} for 1 min). As shown in the Fig. 3.1.8, the single mutants, *trxh2.1*

and *trxo1.1*, behaved like the wild type, which was the case for the quantum yield of photosystem II (Y[II]), non-photochemical quenching (NPQ) and the reduction of plastoquinone pool (1-qL). However, the *trxh2.1trxo1.1* line showed higher Y(II) and lower NPQ in the high-light phase when compared to the wild type (Fig. 3.1.8, A and B). To further test whether pre-acclimated plants show better photosynthetic performance than non-acclimated plants, the Arabidopsis plants were grown under fluctuating light condition for four weeks, and then exposed to a short-term period of fluctuating light condition. The levels of Y(II), NPQ and 1-qL in *trxo1.1* were comparable to wild-type level (Fig. 3.1.9, A, B and C), while *trxh2.1* showed a decrease in the level of Y(II) at the beginning of low-light phase and at the end when light was off. Nevertheless, the *trxh2.1trxo1.1* showed a significant increase in Y(II) and decrease in NPQ during the high-light phase when compared to the wild type (Fig. 3.1.9, A, B). Taken together, the results indicated that joint deficiencies of mitochondrial TRXh2 and TRXo1 lead to an improved photosynthetic performance in fluctuating light environments.
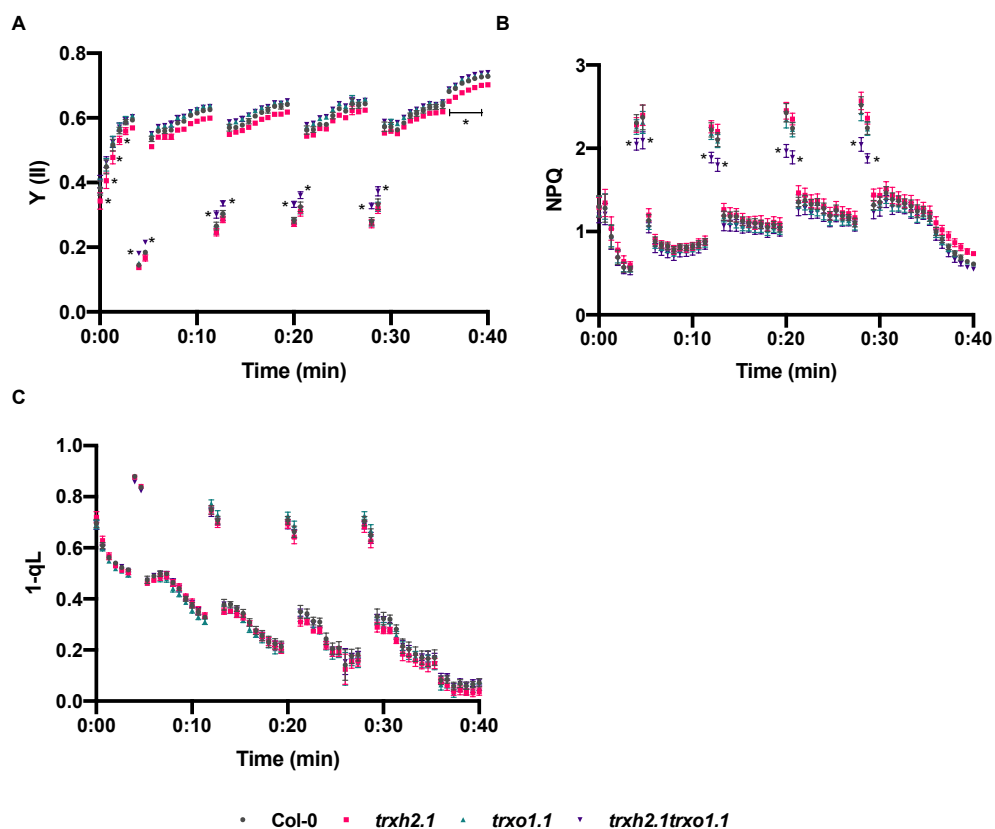
Figure 3.1.9 Photosynthetic performance and changes in photosynthetic parameters between the wild type (Col-0) and the mutant lines (*trxh2.1*, *trxo1.1* and *trxh2.1trxo1.1*). The plants were grown under fluctuating light (50 μmol m^{-2} s^{-1} for 5 min; 550 μmol m^{-2} s^{-1} for 1 min) for four weeks and then subjected to a short-term period of fluctuating light intensities. A, B and C, The changes in the quantum yield of photosystem II (A), non-photochemical quenching (NPQ) (B) and the reduction of plastoquinone pool (1-qL) (C) under the condition of fluctuating light. Mean values and standard errors derived from 6 biological replicates. The statistical analyses were performed by using ANOVA and the Dunnett's test (*$P<0.05$, in comparison to the wild type).

3.2 Functional characterization of NTRC in developing tomato fruits

To investigate the role of NTRC in heterotrophic tissues of crop plants, transgenic tomato plants with decreased NTRC expression under control of a fruit-specific promoter were analyzed.

3.2.1 Molecular characterization of transgenic tomato plants under control of a fruit-specific promoter

To obtain the transgenic tomato plants with decreased *NTRC* expression in fruit tissues, a fruit-specific promoter, patatin B33, was adopted to generate a RNA interference (RNAi) construct (Rocha-Sosa et al., 1989; Frommer et al., 1994; Obiadalla-Ali et al., 2004).
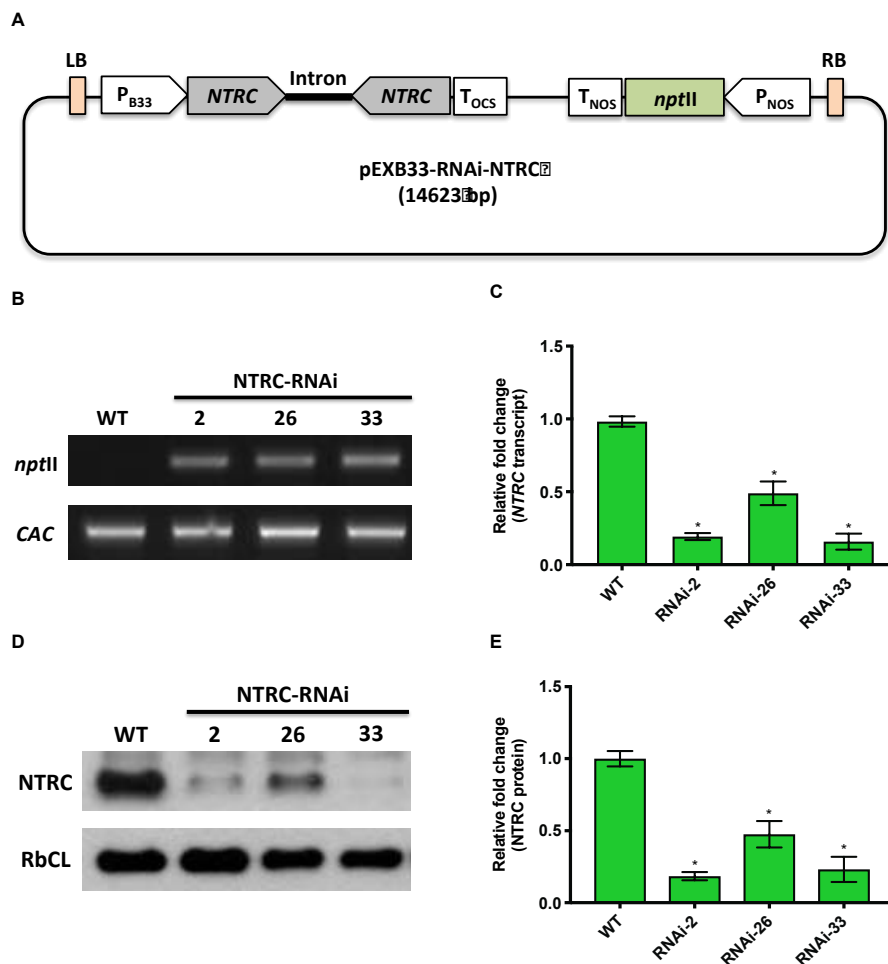
Figure 3.2.1 Molecular characterization of the wild type and NTRC-RNAi lines in 35-DAF tomato fruits. A, The scheme of NTRC-RNAi construct. B, Genotyping to detect the *npt*II gene fragment in NTRC-RNAi lines. C, The transcript level of *NTRC* gene in NTRC-RNAi lines compared to the wild type (WT). D, The protein level of NTRC detected by immunoblot analysis. E, Quantification of NTRC protein level. Clathrin adaptor complexes (CAC) and ribulose 1,5-bisphosphate carboxylase/oxygenase large subunit (RbcL) served as control. Mean values and standard errors derived from 6 biological replicates. The statistical analyses were performed by using ANOVA and the Dunnett's test (*$P<0.05$, in comparison to the wild type).

This construct harbored a neomycin phosphotransferase II (*npt*II) gene fragment, which conferred the resistance of kanamycin. The RNAi cassette contained two *NTRC* gene fragments with opposite orientations, and an intro was incorporated between two fragments (Fig. 3.2.1A). This construct was transformed into tomato plants using an *Agrobacterium tumefaciens*-mediated approach. The 35 day-after-flowering (DAF) fruits were harvested for genotyping. The *npt*II gene fragment was detected in NTRC-RNAi lines 2, 26 and 33 (Fig. 3.2.1B). Furthermore, the transcript and protein levels of NTRC were analyzed in the three RNAi lines. In the NTRC-RNAi lines, the expression of *NTRC* gene significantly decreased by 60% to 80% compared to the wild type (Fig. 3.2.1C), and the NTRC protein level also greatly decreased by 50% to 80% in comparison to the wild type (Fig. 3.2.1, D and E).
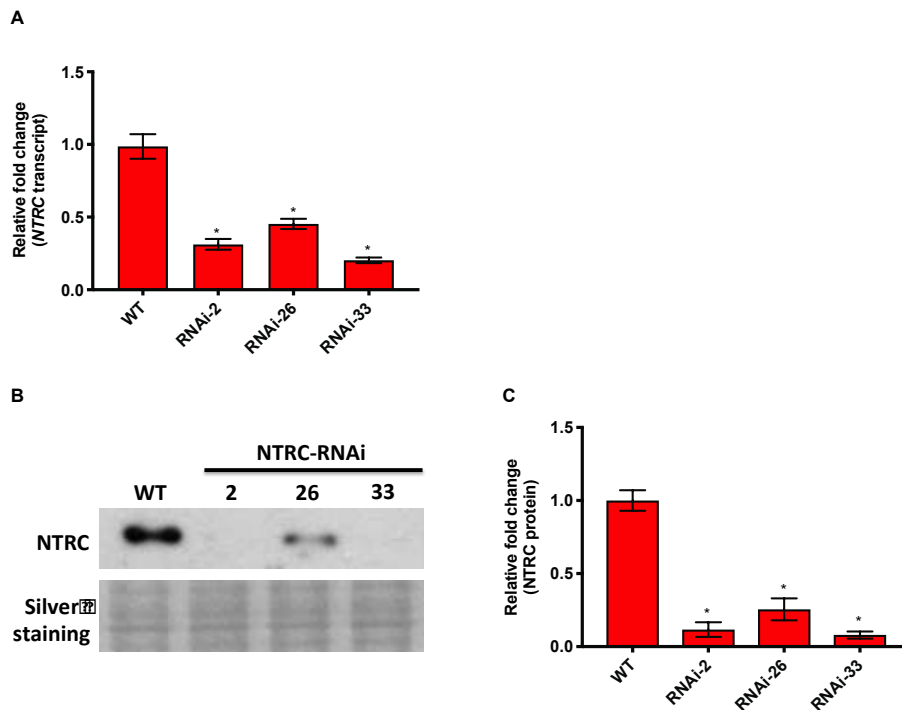
Figure 3.2.2 Molecular characterization of the wild type and NTRC-RNAi lines in 65-DAF tomato fruits. A, The transcript level of *NTRC* gene in NTRC-RNAi lines compared to the wild type (WT). B, The protein level of NTRC detected by immunoblot analysis. C, Quantification of NTRC protein level. The gel stained with silve nitrate served as control. Mean values and standard errors derived from 6 biological replicates. The statistical analyses were performed by using ANOVA and the Dunnett's test (*$P<0.05$, in comparison to the wild type).

The 65 DAF fruit samples were also analyzed. In the NTRC-RNAi lines, both transcript and protein level of NTRC significantly decreased when compared to the wild type (Fig. 3.2.2, A, B and C). Conclusively, the three NTRC-RNAi lines were suitable for investigating the role of NTRC in tomato fruits.

3.2.2 The effects of fruit-specific NTRC down-regulation on the development of tomato fruits

To obtain the insight into whether reducing NTRC expression affects the development of tomato fruits, several factors associated to pigmentation and ripening were evaluated, including the content of chlorophyll, the protein abundance of light-harvesting complex II (Lhcb2) and the expression of genes related to the pathway of ethylene production and fruit ripening.
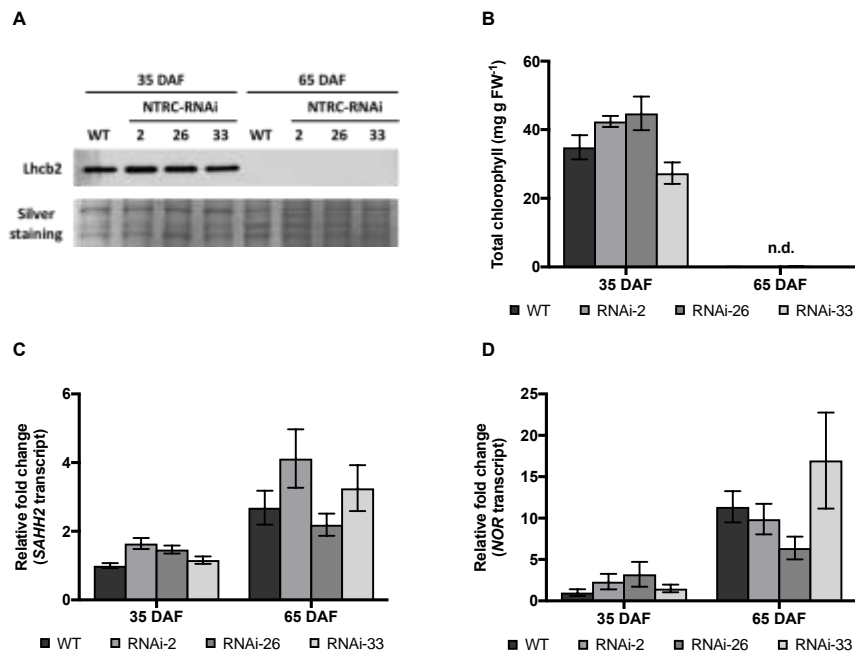
Figure 3.2.3 Characterization of factors associated to fruit development in 35 and 65-DAF tomato fruits. A, The protein level of Lhcb2 in NTRC-RNAi lines in comparison to the wild type (WT). B, The accumulation of total chlorophyll in NTRC-RNAi lines in comparison to the WT. C and D, The gene expression of ethylene production factor (*SAHH2*) and ripening factor (*NOR*) in NTRC-RNAi lines in comparison to the WT. Mean values and standard errors derived from 6 biological replicates. The statistical analyses were performed by using ANOVA and the Dunnett's test (*$P<0.05$, in comparison to the wild type).

In 35-DAF tomato fruits, reducing NTRC expression did not change the accumulation of Lhcb2 protein and chlorophyll in comparison to the wild type. But, either parameter was too low to be detectable in 65-DAF tomato fruits (Fig. 3.2.3, A and B). For the expression of ethylene production factor (S-adenosylhomo-Cys hydrolase [SAHH2]; Yang et al., 2017) and ripening factor (NON-RIPENING [NOR], Ma et al., 2019), there was a general increase in the transcript level of both genes when fruits became ripe. However, the changes between the wild type and NTRC-RNAi lines were not significant (Fig. 3.2.3, C and D). To sum up, reducing NTRC expression specifically in fruit tissues resulted in no substantial change in the developmental processes of tomato fruits.

3.2.3 The effects of fruit-specific NTRC down-regulation on the growth of tomato fruits

To understand the effect of reducing NTRC expression on the growth of tomato fruits, the size and weight of 65-DAF tomato fruits were measured.
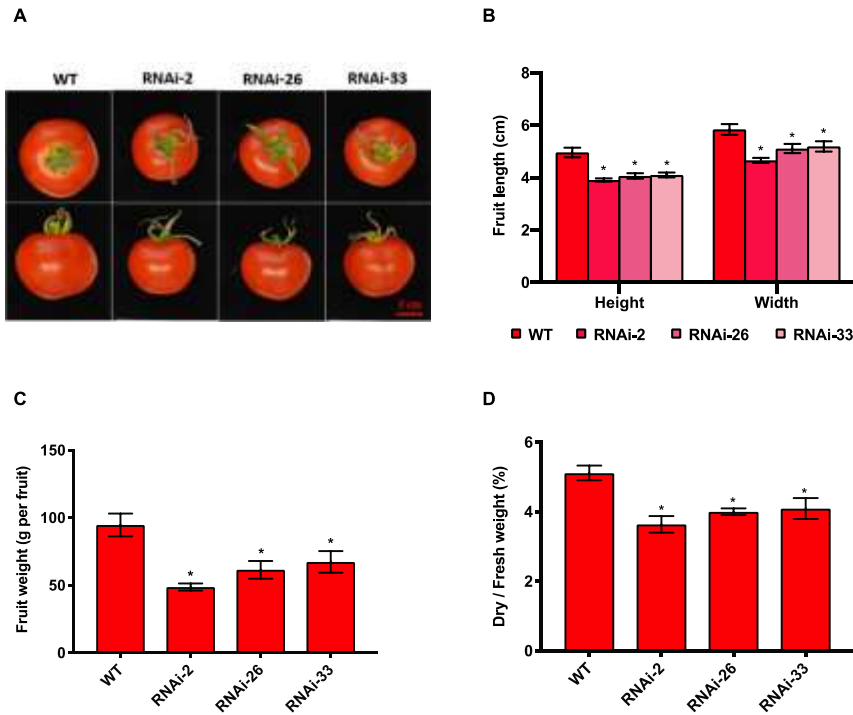
Figure 3.2.4 Analysis of phenotype in 65-DAF tomato fruits. A, The appearance of tomato fruits. Scale bar = 2 cm. B, The comparison of fruit height and width between the wild type (WT) and NTRC-RNAi lines. C, The comparison of fruit weight between the wild type (WT) and NTRC-RNAi lines. D The comparison of dry-to-fresh-weight ratio between the wild type (WT) and NTRC-RNAi lines. Mean values and standard errors derived from 6 biological replicates. The statistical analyses were performed by using ANOVA and the Dunnett's test (*$P<0.05$, in comparison to the wild type).

Both wild-type and NTRC-RNAi fruits ripened normally (Fig. 3.2.4A), but the NTRC-RNAi fruits was smaller than the wild type. To obtain more precise information, the height and width of tomato fruits were measured. In the NTRC-RNAi lines, the fruit height decreased by 20%, and the fruit width decreased by 15% in comparison to the wild type (Fig. 3.2.4B). As expected, the fresh weight of NTRC-RNAi fruits also decreased by 40% compared to the wild type (Fig. 3.2.4C). By calculating the dry-to-fresh-weight ratio, it was found that there were less dry matters and more water in the NTRC-RNAi fruits compared to the wild-type fruits (Fig. 3.2.4D).
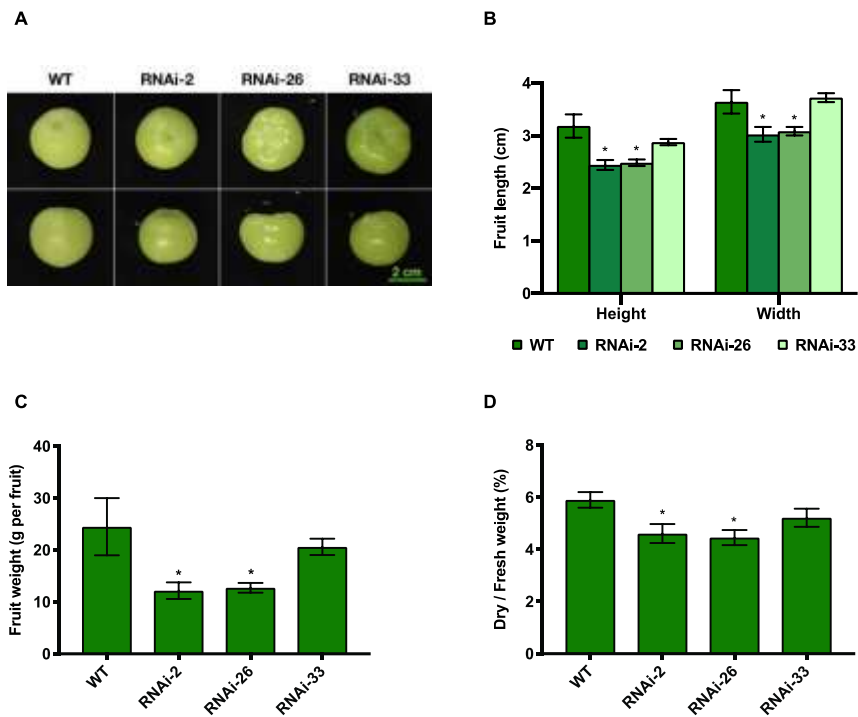
Figure 3.2.5 Analysis of phenotype in 35-DAF tomato fruits. A, The appearance of tomato fruits. Scale bar = 2 cm. B, The comparison of fruit height and width between the wild type (WT) and NTRC-RNAi lines. C, The comparison of fruit weight between the wild type (WT) and NTRC-RNAi lines. D The comparison of dry-to-fresh-weight ratio between the wild type (WT) and NTRC-RNAi lines. Mean values and standard errors derived from 6 biological replicates. The statistical analyses were performed by using ANOVA and the Dunnett's test (*$P<0.05$, in comparison to the wild type).

The phenotype of 35-DAF tomato fruits was also analyzed. In this stage, the size and weight of NTRC-RNAi fruits were also decreased in comparison to the wild-type fruits (Fig. 3.2.5). This finding indicated that the effects of NTRC down-regulation on fruit growth were not due to the developmental effects. To sum up, reducing NTRC expression in fruit tissues eventually led to the production of smaller and lighter fruits containing less dry matter in tomato plants.

3.2.4 The effects of fruit-specific NTRC down-regulation on the accumulation of starch and soluble sugars

Starch is an important transient carbon provision for tomato fruits. When fruits become mature, starch is mobilized to soluble sugars, specifically Glc, which eventually affects the growth of tomato fruits (Schaffer et al., 2000).
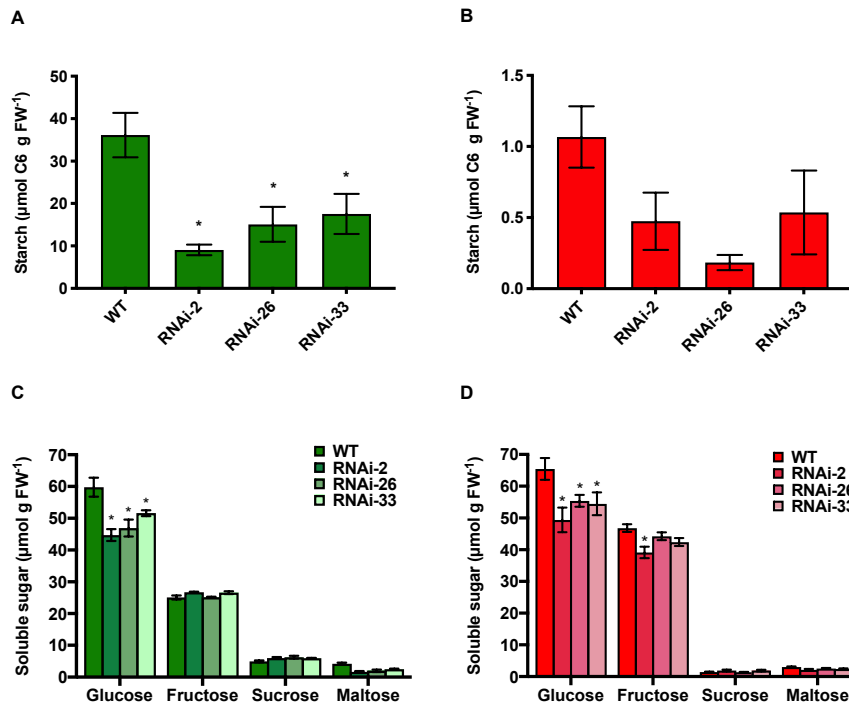
Figure 3.2.6 Assay of starch and soluble sugar content in the wild type (WT) and NTRC-RNAi lines. A and B, The accumulation of starch in 35 (A) and 65-DAF (B) tomato fruits. C and D, The accumulation of soluble sugars in 35 (C) and 65-DAF (D) tomato fruits. Mean values and standard errors derived from 6 biological replicates. The results normalized to fruit fresh weight (FW). The statistical analyses were performed by using ANOVA and the Dunnett's test (*$P<0.05$, in comparison to the wild type).

To study whether fruit-specific silencing of NTRC is able to change carbon provisions, the accumulation of starch and soluble sugars was measured. The starch level of NTRC-RNAi lines was decreased by 50% to 75% in comparison to the wild type (Fig. 3.2.6A) in 35-DAF tomato fruits. In 65-DAF tomato fruits, starch had been mobilized as soluble sugars. Although the starch content was generally low in all genotypes, the NTRC-RNAi lines still showed a decreased pattern in starch level compared to the wild type (Fig. 3.2.6B). Compromising starch accumulation often leads to a great change in the levels of soluble sugars. As expected, the Glc level was significantly decreased in NTRC-RNAi lines in comparison to the wild type at both developing stages, while other sugar levels such as Fru, Suc and maltose were slightly changed (Fig. 3.2.6, C and D). The total protein level was also analyzed, but there was no substantial difference between the wild type and NTRC-RNAi line at both developmental stages (Fig. 3.2.7).
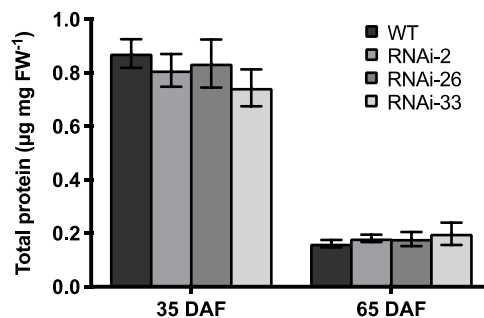
Figure 3.2.7 Total protein content of NTRC-RNAi lines compared to the wild type (WT) in 35 and 65-DAF tomato fruits. Mean values and standard errors derived from 6 biological replicates. The results normalized to fruit fresh weight (FW). The statistical analyses were performed by using ANOVA and the Dunnett's test (*P<0.05, in comparison to the wild type).

Taken together, reducing NTRC expression in tomato fruits led to a great decrease in starch accumulation, which subsequently affected the accumulation of soluble sugars during fruit development. However, the total protein levels of NTRC-RNAi lines were comparable to the wild type.

3.2.5 The effects of fruit-specific NTRC down-regulation on the accumulation of phosphorylated metabolites and adenine nucleotides

Since the NTRC-RNAi lines showed a large decrease in the level of starch and soluble sugars, it was proposed that this decrease might be related to the metabolism of sugars and energy. Thus, the content of sugar phosphates and adenine nucleotides was measured.

Table 3.2.1 The level of sugar phosphates and adenine nucleotides in the wild type (WT) and NTRC-RNAi lines. The results normalized to fruit fresh weight (FW). The statistical analyses were performed by using ANOVA and the Dunnett's test (*P<0.05, in comparison to the wild type).

Metabolite	Genotype	35 DAF	65 DAF
G6P	WT	262±18.9	173.7±11.3
(nmol g FW^{-1})	RNAi-2	165.2±17*	149.2±6.8*
	RNAi-26	194.6±15.1*	164±14.2*
	RNAi-33	239.8±10.1	152.8±8.6
F6P	WT	77.2±6.1	55±5
(nmol g FW^{-1})	RNAi-2	44.2±3.8	39.4±2.6
	RNAi-26	57.9±6.2	43.4±5.2
	RNAi-33	73.7±2.4	43.1±3.3
G1P	WT	69.5±5.4	94.8±3.8
(nmol g FW^{-1})	RNAi-2	46.7±5.4	100.5±2.8*
	RNAi-26	53±1.5	96.4±4.9
	RNAi-33	72.1±2.2	89.3±4.8
3-PGA	WT	69.5±1.2	78.1±4
(nmol g FW^{-1})	RNAi-2	70±1.4	87.4±2.6
	RNAi-26	67.2±1.6	100.6±2.9*
	RNAi-33	70.3±2.4	92.2±3.6*
ATP	WT	548.2±129.8	319±87.5
(nmol g FW^{-1})	RNAi-2	423±88.6	454.3±46.7
	RNAi-26	372.9±52.1	389.9±44.2
	RNAi-33	455.1±43.6	451.8±52.8
ADP	WT	141.6±34.6	116.6±21.5
(nmol g FW^{-1})	RNAi-2	105.4±23.6	136.2±19.6
	RNAi-26	121.1±27.3	133.9±15.6
	RNAi-33	114.7±17.7	135.2±9.9
ATP/ADP ratio	WT	4.1±0.5	2.7±0.5
	RNAi-2	4.3±0.5	3.5±0.4
	RNAi-26	3.6±0.5	3±0.4
	RNAi-33	4.2±0.5	3.5±0.5

As shown in the Table 3.2.1, the levels of G6P and F6P was decreased in NTRC-RNAi lines in comparison to the wild type, while the level of G1P remained unchanged. The level of 3-PGA in NTRC-RNAi lines was comparable to wild-type level at the mature-green developmental stage (35 DAF), while the NTRC-RNAi lines accumulated high level of 3-PGA at the ripe developmental stage (65 DAF). Nevertheless, the changes were not consistent to the data from metabolite profile (Supplemental Table S1), in which the levels of phosphorylated metabolites were generally increased in NTRC-RNAi lines in comparison to the wild type. The level of triose phosphates was also assayed, but the level was too low to be detectable, which was the character of glycolytic processes in heterotrophic tissues (Hatzfeld and Stitt, 1990). In NTRC-RNAi lines, the levels of adenine nucleotides (ATP and ADP) and the ATP-to-ADP ratio were comparable to the wild type (Table 3.2.1). Taken together, the glycolytic metabolism and adenylate energy status were not perturbed when NTRC was down-regulated in developing fruits.

3.2.6 The effects of fruit-specific NTRC down-regulation on the levels of holistic metabolites

To study the global changes of metabolite levels resulted from NTRC down-regulation in tomato fruits, a metabolite profiling was performed via GC-TOF-MS. The NTRC-RNAi lines showed a large decrease in the levels of major sugars compared to the wild type at both developmental stages: the Glc level decreased by 20% to 45%; the Fru level decreased by 15% to 35%; the Suc level decreased by 45% to 60% (Fig. 3.2.8A; Suppl. Table S2). Moreover, the levels of several sugars, such as gentiobiose, maltose and ribose, were strongly decreased in NTRC-RNAi lines compared to the wild type at the ripe developmental stage (Fig. 3.2.8A, right; Suppl. Table S2). Thus, the sugar levels of NTRC-RNAi lines were generally lower than the wild type. For the sugar alcohols, there was a decrease in the level of myo-inositol in NTRC-RNAi lines compared to the wild type at the both developmental stages, but the levels of other sugar alcohols remained unchanged (Fig. 3.2.8A; Suppl. Table S2).

NTRC-RNAi lines showed an increased pattern in the levels of several organic acids, such as 2-imindazolidone-4-carboxylic acid, transaconitic acid, transcaffeic acid, and quinic acid, while the levels of others, such as 1-pyroline-2-carboxylate, gulonic acid, were decreased in the NTRC-RNAi lines compared to the wild type (Fig. 3.2.8B; Suppl. Table S2). For the metabolites of tricarboxylic acid cycle, the levels of citric acid and 2-oxo-glutaric acid in NTRC-RNAi lines were increased to two-to-four times wild-type level at both developmental stages. But, the levels of malic acid, fumaric acid, and succinic

acid in NTRC-RNAi lines remained comparable to wild-type level (Fig. 3.2.8C; Suppl. Table S2). Intriguingly, the level of pyruvic acid in NTRC-RNAi lines was only increased at the mature-green developmental stage (35 DAF) compared to the wild type (Fig. 3.2.8C, left; Suppl. Table S2).
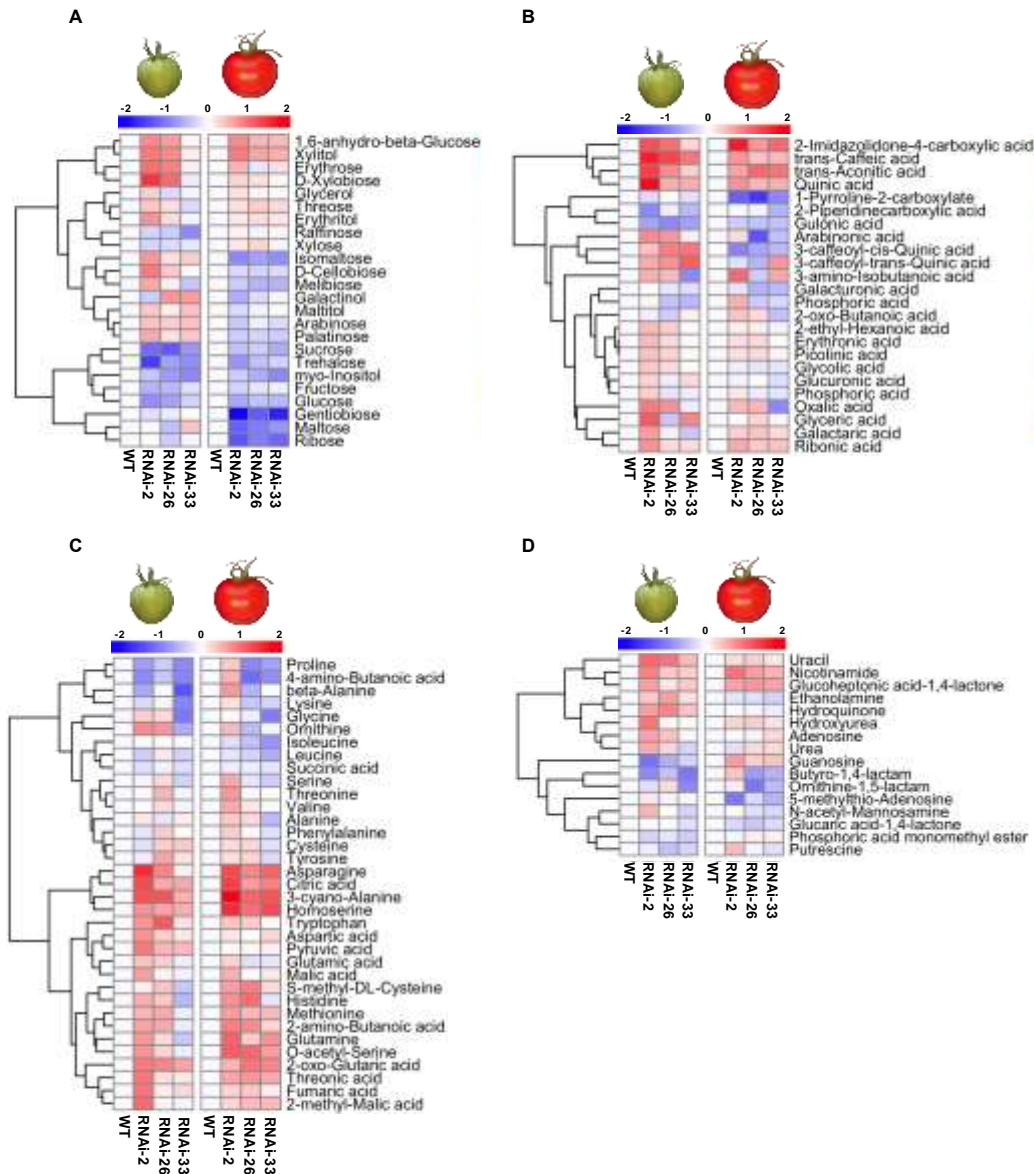
Figure 3.2.8 Metabolite profile of the wild type (WT) and NTRC-RNAi lines. The left part of each figure represents the results of 35-DAF fruits, and the right part represents the results of 65-DAF fruits. A, The levels of sugars and sugar alcohols. B, The levels of organic acids. C, The levels of amino acids and tricarboxylic-acid-cycle metabolites. D, Miscellaneous. Results are normalized to the wild type with base-2 logarithm transformation. The R software is used to visualize the outcome as a heatmap and perform the hierarchical clustering. Data is derived from Supplemental Table S1.

NTRC-RNAi lines showed an increased pattern in the levels of amino acids compared to the wild type. The levels of Asn, 3-cyano-Ala and homo-Ser in NTRC-RNAi lines were increased to around two times wild-type level at the mature-green developmental stage

(Fig. 3.2.8C, left; Suppl. Table S2), and this tendency became more clear as fruits ripened (Fig. 3.2.8C, right; Suppl. Table S2). The levels of other amino acids, such as Trp, His, Gln and Met, were moderately increased in NTRC-RNAi lines compared to wild-type level. The levels of urea, amines, nucleosides, and their derivatives in NTRC-RNAi lines remained comparable to wild-type level at the both developmental stages (Fig. 3.2.8D; Suppl. Table S2). Taken together, fruit-specific NTRC down-regulation reprogramed the metabolisms between sugars, organic acids and amino acids during the process of fruit development.

3.2.7 The effects of fruit-specific NTRC down-regulation on the redox state of pyridine nucleotides

The redox couples of NAD(H) and NADP(H) serve as important cofactors for different metabolic processes in distinct subcellular compartments (Berger et al., 2004; Geigenberger and Fernie, 2014). Besides, NADPH is also crucial for NTRC since it provides reducing power for NTRC to reduce plastidial proteins (Pérez-Ruiz and Cejudo, 2009). Thus, the levels of pyridine nucleotides in developing tomato fruits were further assayed.
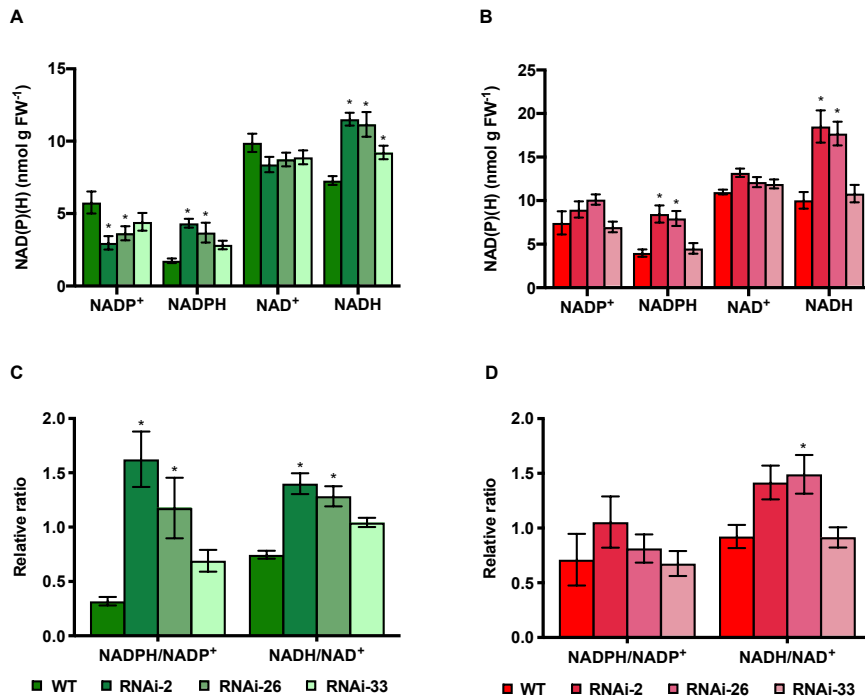
Figure 3.2.9 The levels of pyridine nucleotides in the wild type (WT) and NTRC-RNAi lines. A and B, The levels of $NADP^+$, NADPH, NAD^+, and NADH in 35 (A) and 65-DAF (B) tomato fruits. C and D, The ratio of NADPH to $NADP^+$ and NADH to NAD^+ in 35 (C) and 65-DAF (D) tomato fruits. Mean values and standard errors derived from 6 biological replicates. The results normalized to fruit fresh weight (FW). The statistical analyses were performed by using ANOVA and the Dunnett's test (*$P<0.05$, in comparison to the wild type).

At the mature-green developmental stage (35 DAF), the levels of reduced form, NADPH and NADH, in NTRC-RNAi lines were significantly elevated, while the levels of oxidized form, $NADP^+$ and NAD^+, were decreased when compared to the wild type (Fig. 3.2.9A). Thus, in NTRC-RNAi lines, the ratio of NADPH to $NADP^+$ was increased to two-to-five times wild-type level, and the ratio of NADH to NAD^+ was increased to around two times wild-type level (Fig. 3.2.9C).

At the ripe developmental stage (65 DAF), the levels of NADPH and NADH in NTRC-RNAi lines were still increased compared to the wild type, but the levels of $NADP^+$ and NAD^+ remained unchanged (Fig. 3.2.9B). This eventually led to a subtle change in the reduced-to-oxidized ratio of pyridine nucleotides (Fig. 3.2.9D). To sum up, fruit-specific NTRC down-regulation altered the redox state of pyridine nucleotides, which the NAD(H) and NADP(H) redox couples tended to attenuate in reductive state. However, this change was alleviated as fruits ripened.

3.2.8 The effects of fruit-specific NTRC down-regulation on the redox-activation state of AGPase

To understand how NTRC regulate starch accumulation in developing tomato fruits, the activities of enzymes involved in starch metabolism were analyzed. We first focused on AGPase, which is the first committed step of starch synthesis. Furthermore, the activity of AGPase is determined to be redox-regulated via the systems of Trx and NTRC in the plastid (Geigenberger and Fernie, 2014; Geigenberger et al., 2017).

Since AGPase activity is regulated by the reduction of intermolecular disulfide bond between the two small subunits (AGPase small-subunit 1 [APS1]) of the heterotetrameric holoenzyme (Ballicora et al., 2000; Tiessen et al., 2002; Hendriks et al., 2003), we analyzed the monomerization pattern of APS1 in NTRC-RNAi lines to determine the changes of APS1 redox status. In 35-DAF tomato fruits, the monomerization ratio of APS1 in NTRC-RNAi lines decreased by 20% to 30% (Fig. 3.2.10A). This indicated that the oxidation of APS1 increased due to NTRC down-regulation.

AGPase activity is also regulated by the allosteric activator, 3-PGA, and the inhibitor, Pi, and the regulation is associated with the redox state of APS1. Oxidation of APS1 decreases the sensitivity of AGPase to allosteric activation (Tiessen et al., 2002; Hendriks et al., 2003). To test whether NTRC down-regulation changes the kinetic properties of AGPase, we thus assayed AGPase activity with or without the allosteric activator, 3-PGA. In the non-activation condition, the NTRC-RNAi lines showed comparable AGPase activity to the wild type. However, with the addition of 10 mM 3-PGA, AGPase activity in

NTRC-RNAi lines decreased by 30% compared to the wild type (Fig. 3.2.10B). To investigate the changes in AGPase kinetics in response to 3-PGA, we further performed AGPase activity assays with the addition of different concentrations of 3-PGA from 0.025 to 10 mM. When incubated with 0.25 to 10 mM 3-PGA, the sensitivity to 3-PGA activation in NTRC-RNAi lines was largely reduced, resulting in a 30%-to-50% decrease of AGPase activity compared to the wild-type level (Fig. 3.2.10C). Furthermore, the level of endogenous ADP-Glc was also assayed, since ADP-Glc is the direct product of AGPase reaction. As shown in the Fig. 3.2.10D, the ADP-Glc level in NTRC-RNAi lines decreased by 25% to 50% compared to the wild type. Taken together, the results confirmed that NTRC down-regulation results in a suppression of AGPase activity in vivo.
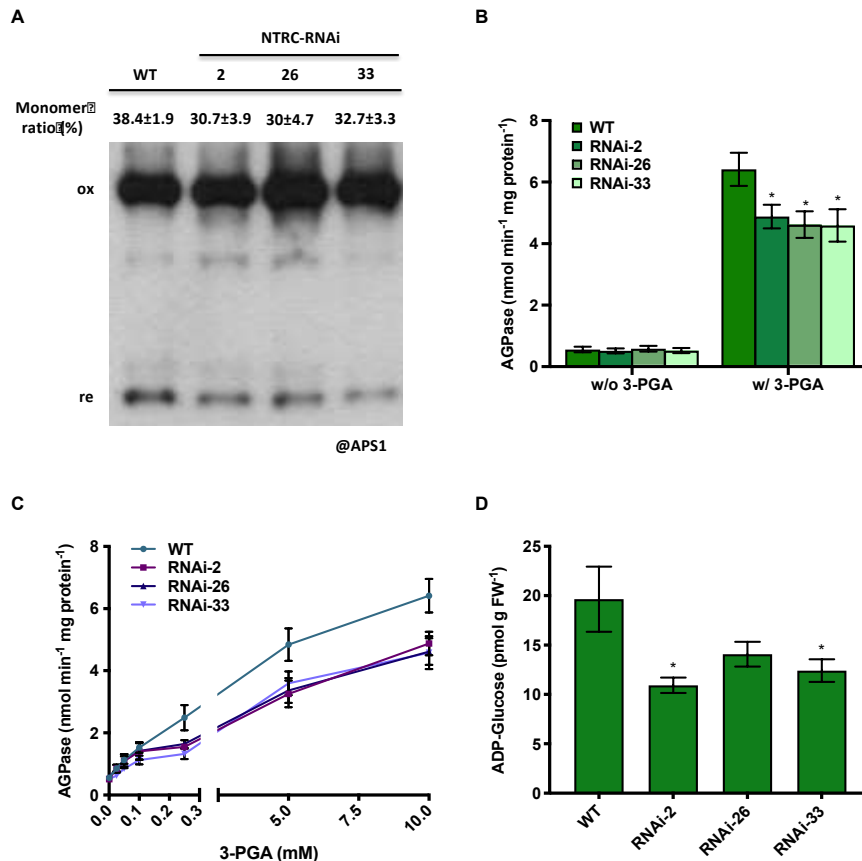
Figure 3.2.10 The redox and allosteric state of AGPase and the accumulation of ADP-Glc in 35-DAF tomato fruits of the wild type (WT) and NTRC-RNAi lines. A. The monomerization ratio of APS1. B, The AGPase activity in the absence or presence of 3-PGA (10 mM). C, The enzyme kinetic curve of AGPase in response to different concentrations of 3-PGA. D, The level of endogenous ADP-Glc. Mean values and standard errors derived from 5 to 6 biological replicates. The results of enzyme activity normalized to total protein, and the ADP-Glc level normalized to fruit fresh weight (FW). The statistical analyses were performed by using ANOVA and the Dunnett's test (*$P<0.05$, in comparison to the wild type).

The redox and allosteric properties of AGPase in 65-DAF tomato fruits were also assayed. The monomerization ratio of APS1 in NTRC-RNAi lines was comparable to the

wild type (Fig. 3.2.11A). Besides, the AGPase activity was generally lower in ripe fruits than in immature fruits. With or without the activation of 3-PGA, the AGPase activity in NTRC-RNAi lines was not substantially changed in comparison to the wild type (Fig. 3.2.11B).
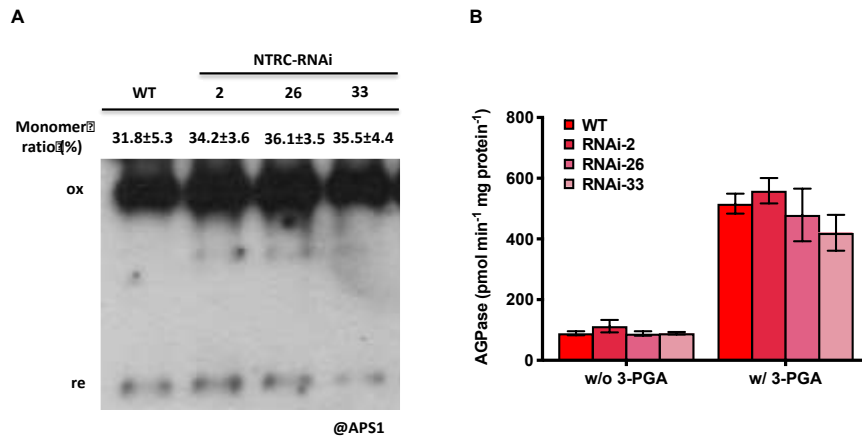
Figure 3.2.11 The redox and allosteric state of AGPase in 65-DAF tomato fruits of the wild type (WT) and NTRC-RNAi lines. A. The monomerization ratio of APS1. B, The AGPase activity in the absence or presence of 3-PGA (10 mM). Mean values and standard errors derived from 5 to 6 biological replicates. The results of enzyme activity normalized to total protein.

3.2.9 The effects of fruit-specific NTRC down-regulation on the enzymes involved in starch metabolism

To obtain in-depth understandings on the role of NTRC in starch metabolism, we further performed activity assays for other enzymes involved in starch metabolism, As shown in the Table 3.2.2, the activity of soluble starch synthase in NTRC-RNAi lines decreased by 60% to 75% in comparison to the wild type, while the activity of granule-bound starch synthase in NTRC-RNAi lines was marginally decreased. On the other hand, the activities of starch phosphorylases and starch hydrolyses in NTRC-RNAi lines were comparable to the wild type (Table 3.2.2). This indicated that NTRC down-regulation had no significant effects on starch degradation. To sum up, NTRC down-regulation significantly compromised the activities of AGPase and soluble starch synthase, and thus led to a decrease in starch accumulation.

Table 3.2.2 The activity of starch-metabolism enzymes in 35-DAF tomato fruits of the wild type (WT) and NTRC-RNAi lines. Mean values and standard errors derived from 6 biological replicates. The results of enzyme activity normalized to total protein. The statistical analyses were performed by using ANOVA and the Dunnett's test (*$P<0.05$, in comparison to the wild type).

Enzymes	WT	RNAi-2	RNAi-26	RNAi-33
Soluble starch synthase (nmol min^{-1} mg protein^{-1})	44.8±4.2	16.8±2.6*	11.4±3.3*	18.6±6.2*
Granule-bound starch synthase (pmol min^{-1} mg FW^{-1})	2.9±0.2	2.0±0.1*	2.0±0.1*	2.4±0.2
Starch phosphorylase (nmol min^{-1} mg protein^{-1})	49.6±10.9	76.5±18.3	30.7±4.2	40.0±11.3
Starch hydrolases (μmol min^{-1} mg protein^{-1})	2.4±0.4	2.3±0.7	1.1±0.2	1.0±0.4

3.2.10 The effects of fruit-specific NTRC down-regulation on the redox property of 2-Cys Prxs

2-Cys Prxs serve as a scavenger of hydrogen peroxide during photosynthesis, and also well-known targets of NTRC in Arabidopsis leaves (Cejudo et al., 2012). The activation of 2-Cys Prxs is regulated by the reduction of intermolecular disulfide bond between the two subunits of the homodimer (Pérez-Ruiz et al., 2006; Pérez-Ruiz et al., 2017).

A

NTRC-RNAi
WT | 2 | 26 | 33
Monomer ratio (%) 30.3±5.2 | 27.4±5.5 | 22.5±3.4 | 20.5±3.4
ox
re
@2-Cys-Prx

B

NTRC-RNAi
WT | 2 | 26 | 33
Monomer ratio (%) 25.7±6.4 | 26.5±5.4 | 21.6±4.3 | 13.3±3.5
ox
re
@2-Cys-Prx
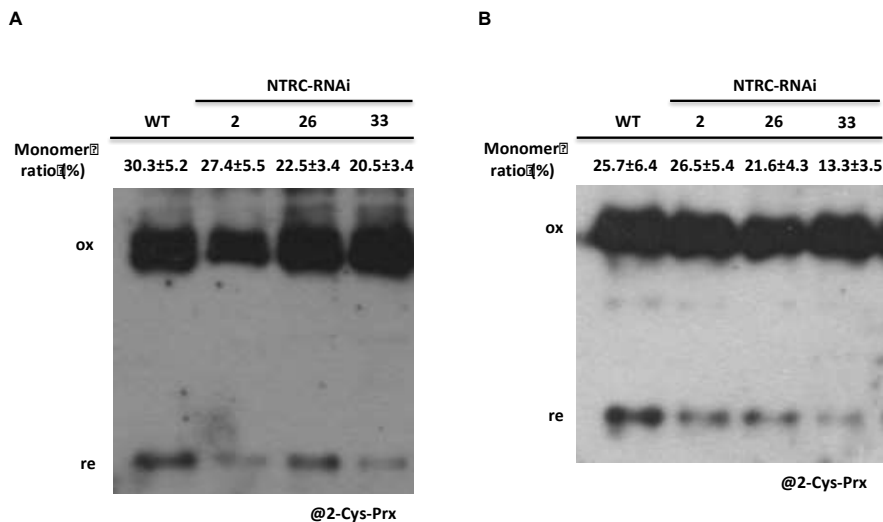
Figure 3.2.12 The redox state of 2-Cys Prx in the wild type (WT) and NTRC-RNAi lines. A, The monomerization ratio in 35-DAF tomato fruits. B, The monomerization ratio in 65-DAF tomato fruits. Mean values and standard errors derived from 6 biological replicates

To understand whether NTRC down-regulation affects the reduction of 2-Cys Prxs in tomato fruits, we thus analyzed the changes in the redox state of 2-Cys Prxs in NTRC-RNAi lines. Either in 35 or 65-DAF tomato fruits, the monomerization ratio of

2-Cys Prxs in NTRC-RNAi lines was not substantially changed in comparison to the wild type (Fig. 3.2.12). Unlike in Arabidopsis leaves, NTRC may be of minor importance for regulating the redox state of 2-Cys Prxs in tomato fruits.

4   Discussion

Despite the regulation based on TRXs is believed to ensure light-responsive control of metabolic functions in chloroplasts, little is known on the role of TRX system in non-photosynthetic metabolism. In the present study, the impact of thiol-redox systems on non-photosynthetic metabolism was investigated by two different approaches. First, the role of mitochondrial TRXs (TRXh2 and TRXo1) was analyzed in Arabidopsis plants. Secondly, the role of the plastidial NADPH-thioredoxin reductase C (NTRC) was analyzed in heterotrophic tomato fruits. The results showed that mitochondrial TRXs are important to regulate metabolic processes inside mitochondrion, affecting processes outside the mitochondrial boundaries, while plastidial NTRC is important to regulate carbon metabolism and redox balance in heterotrophic tomato fruits, affecting final fruit size and quality.

4.1 The function of mitochondrial thioredoxins in Arabidopsis plants

Deficiencies in the mitochondrial TRXs (TRXh2 and TRXo1) leads to changes in Arabidopsis plant growth and metabolic processes inside mitochondrion, which subsequently affects photosynthetic performance in response to fluctuating environments.

4.1.1 The impact of perturbing mitochondrial TRX system on growth phenotype

The *trxo1.1* and *trxh2.1trxo1.1* lines showed a 10%-to-15% decrease in plant size, while the *trxh2.1* grew similarly to the wild type. Surprisingly, despite the *trxh2.1trxo1.1* line was smaller than the wild type, its biomass was comparable to Col-0 (Fig. 3.1.2). Opinions regarding to phenotypes of *trxh* and *trxo* mutants were varied. Meyer et al. (2012) mentioned that a mutant, in which five h-type TRXs were inactivated, showed no growth defect in standard and stress conditions. Calderón et al. (2018) also proposed that *trxo1* mutants grew normally as the wild type in a standard condition, while da Fonseca-Pereira et al. (2020) showed that there was a slight increase in growth of *trxh2* mutants compared to wild type in a long-day condition. Several reports indicated a possible role of TRXh2 and TRXo1 in the regulation of photorespiration (Reinholdt et al., 2019b; da Fonseca-Pereira et al., 2020). Timm and Bauwe (2013) suggested that photorespiratory mutants showed growth retardation when grown under a standard condition, but the phenotype was restored via supply of high CO_2 concentration. This might partly explain why the leaf size of *trxo1.1* and *trxh2.1trxo1.1* lines was smaller than the wild type. Besides, since the *trxh2.1trxo1.1* line showed higher carbon assimilation rate than the wild

type when subjected to high CO_2 concentration (Fig. 3.1.7B), it is possible that the *trxh2.1trxo1.1* line may grow better under a condition of high CO_2 concentration.

4.1.2 The impact of perturbing mitochondrial TRX system on metabolic processes

There was a general increase in the levels of major sugars, including Glc, Fru, and Suc, in *trxo1* mutant at the ED and this tendency became clearer in the double mutant line (Fig. 3.1.3, B, C and D), while the starch level remained unaltered (Fig. 3.1.3A). This is partly in agreement with previous findings in *trxh2* and *trxo1* mutants (Daloso et al., 2015; da Fonseca-Pereira et al., 2020). Furthermore, the levels of G6P and G1P were significantly elevated in the *trxh2.1trxo1.1* line at the ED (Fig. 3.1.4, A and C), but not in the single mutants. Due to the significance of sugar phosphates in energy transfer, this implies the potential of TRXh2 and TRXo1 in regulating energy metabolism. Thus, other phosphate intermediates were further analyzed in all mutant lines. Interestingly, the PEP level was greatly reduced in the single mutants and the *trxh2.1trxo1.1* line at both EN and ED (Fig. 3.1.5B). The *trxh2.1trxo1.1* line further showed a decrease in the levels of ATP and ADP (Fig. 3.1.5, C and D), which led to a higher ATP-to-ADP ratio (Fig. 3.1.5E). Taken together, this indicates that jointly decreasing the expression of TRXh2 and TRXo1 affects the balance of cellular energy metabolism.

Apart from energy metabolism, it is proposed that TRXh2 and TRXo1 both are involved in other metabolic processes of mitochondrion and peroxisome. Clear decreased patterns in the levels of Gly and Ser were found in both single and double mutants at the EN (Fig. 3.1.6B, left), which was in line with previous finding in a *trxo1* mutant (Daloso et al., 2015), but contradicted to the finding in *trxh2* mutants (da Fonseca-Pereira et al., 2020). The results indicated an overall perturbation in Gly cleavage system, including Gly decarboxylation, Ser hydroxymethyltransferase (SHMT) reaction, and other coupled enzyme reactions in these mitochondrial TRX mutants. While this point to a role of these TRXs in photorespiration, the following findings argue against it. The changes in the levels of Gly and Ser were diminished upon illumination (Fig. 3.1.6B, right). Furthermore, an important photorespiratory intermediate, glycerate, remained unaltered between genotypes at both EN and ED (Fig. 3.1.6C). Intriguingly, this joint decrease in Gly and Ser levels was also found in a mitochondrial mutant defect in a uncoupling protein (ucp1; Sweetlove et al., 2006; Florian et al., 2013). Since UCP1 catalyzes the conductance of protons through mitochondrial membrane, this protein may be a potential target of mitochondrial TRXs.

In addition to photorespiratory metabolites, several metabolites of tricarboxylic acid cycle, such as aconitic acid, fumaric acid, 2-oxoglutaric acid, and succinic acid were

decreased in all mutant lines at the EN (Fig. 3.1.6C; Suppl. Table S1). This implies that jointly decreasing the expression of TRXh2 and TRXo1 possibly perturbs enzyme activation in tricarboxylic acid cycle. This is in line with the finding, which characterize TRXh2 and TRXo1 as proteins in regulating enzymes of tricarboxylic acid cycle (Daloso et al., 2015). Alongside the changes in metabolites of tricarboxylic acid cycle, the level of 4-aminobutanoic acid (GABA) was increased in all mutant lines at both EN and ED, while the level of its precursor, Glu, was barely changed (Fig. 3.1.6B; Suppl. Table S1). Thus, the accumulation of GABA in mutant lines is possibly due to the degradation of polyamine, such as putrescine or spermidine (Fait et al., 2008; Shelp et al., 2012). Furthermore, all mutant lines showed a significant decrease in the level of putrescine at the EN (Supple. Table S1), which might partly indicate the stimulation of polyamine degradation resulted from the down-regulation of TRXh2 and TRXo1. The additionally produced GABA may also re-enter tricarboxylic acid cycle via a series of enzyme reactions (Michaeli and Fromm, 2015). Taken together, jointly down-regulating the expression of TRXh2 and TRXo1 leads to an overall perturbation in mitochondrial and peroxisomal metabolic processes.

4.1.3 The mitochondrial TRX system affects photosynthetic processes depending on the light conditions

In nature, environments are dynamic, such as the change of light intensity. Plants often encounter such challenges, and thus require complicated mechanisms to overcome these fluctuations. Many reports have comprehensively discussed how plants adapt to fluctuate environments via the optimization of photosynthetic processes (Müller et al., 2001; Carrillo et al., 2016; Naranjo et al., 2016b; Thormählen et al., 2017; Saroussi et al., 2019). Alternatively, in response to high light situation, plants are also able to transfer excess reducing equivalents produced in chloroplast to other subcellular compartments via the OAA/malate shuttle (Scheibe, 1987; Backhausen et al., 2000; Maurino and Engqvist, 2015). The export of reducing equivalents from chloroplast is contributory to mitochondrial metabolism (Raghavendra and Padmasree, 2003). There was an interesting enhancement of photosynthetic performance in the *trxh2.1trxo1.1* line when exposed to a situation of elevate CO_2 concentration (Fig. 3.1.7B) or a high light phase of fluctuating light intensities (Fig. 3.1.8A; Fig. 3.1.9A). Excess light promotes photosynthetic activity leading to the production of abundant reducing equivalent. Therefore, the improvement of photosynthetic performance in the *trxh2.1trxo1.1* line may attribute to an efficient transport of reducing power to other organelles, which avoid the occurrence of over-reduction in

chloroplast. If it is this case, our findings then indicate the potential of TRXh2 and TRXo1 in regulating the OAA/malate shuttle. On the other hand, as we proposed above, jointly decreasing TRXh2 and TRXo1 may compromise mitochondrial and peroxisomal metabolisms, which further restricts the production of NADH in these organelles. In this scenario, the *trxh2.1trxo1.1* line is supposed to harbor greater capacity to metabolize reducing equivalents exported from chloroplast.

4.1.4 Outlook with respect to the role of mitochondrial TRX system in acclimation to environmental changes

From the results above, it is likely that mitochondrial TRX system play a role in response to environmental fluctuations. Nevertheless, direct evidences regarding to this hypothesis are still in short so further investigations are required. At first, it is still unresolved whether joint down-regulation of TRXh2 and TRXo1 also affect plant metabolism in different conditions, such as different light intensities or various CO_2 concentrations. To address this question, a series of different light conditions need to be applied onto the *trxh2.1trxo1.1* line, and then again comprehensive analyses including metabolomics, gas-exchange measurement and PAM measurement are necessary. In addition, a report indicates the role of TRXo1 in short-term light/dark transitions (Reinholdt et al., 2019a). Thus, it is also interesting to test the response of *trxh2.1trxo1.1* line in such condition.

4.2 The role of NTRC in developing tomato fruits

Decreasing NTRC expression in tomato fruits leads to strong changes in carbon metabolism and redox balance in developing tomato fruits. The changes subsequently affect the yield and quality of tomato fruits.

4.2.1 The role of NTRC in the optimization of fruit size and quality

Tomato is an important crop for horticulture and human diet (Kanayama, 2017). There are many reports showing considerable interest in the optimization of yield and quality of tomato fruits via genetic strategies (Giovannoni, 2004; Carrari and Fernie, 2006), while studies about the role of redox regulation remains restricted. To analyze the role of NTRC in tomato fruits, NTRC-RNAi tomato lines controlled by fruit-specific promoter were generated. The NTRC-RNAi lines showed a 60%-to-80% decrease in NTRC expression (Fig. 3.2.1 and 3.2.2) in fruit tissues when compared to the wild type. The tomato fruits of NTRC-RNAi lines showed wild-type behavior with respect to the process of their

development and ripening (Fig. 3.2.3). However, at the ripe stage, fruits of NTRC-RNAi lines were significantly smaller and lighter than wild-type fruits, and also contain less dry matter and more water (Fig. 3.2.4). Furthermore, NTRC-RNAi lines showed a decrease in soluble sugar levels (Fig. 3.2.6D and 3.2.8A; Suppl. Table S2) and an increase in the levels of amino acids, organic acids and phenolic compounds (Fig. 3.2.8, B, C and D; Suppl. Table S2). Domesticated tomatoes preferably accumulate abundant amounts of Glc and Fru, so its sweet taste largely depends on the accumulation of Glc, Fru, and additional minor sugars. Furthermore, the ratio of acid to sugar largely affects the sour taste of fruits (Davies and Hobson, 1981; Gierson and Kader, 1986). Taken together, the metabolic changes resulted from NTRC down-regulation are very likely to affect the sweetness and sourness of tomato fruits.

The significance of NTRC in growth and development of Arabidopsis plants via regulating broad photosynthetic processes is well described (Pérez-Ruiz et al., 2006; Lepisto et al., 2009; Thormählen et al., 2015), while the understanding on the role of NTRC in heterotrophic tissues is relatively poor. Here, we directly show that NTRC is important to promote the growth of heterotrophic storage organs, affecting final fruit size and quality. It has to be noted that the effects of NTRC down-regulation on fruit growth is unlikely due to the involvement of NTRC in photosynthetic processes even though immature fruits still harbor restricted photosynthetic activity (Fig. 3.2.3). Indeed, a previous article suggests that compromising a chlorophyll-synthesis gene barely has effects on fruit growth and development (Lytovchenko et al., 2011).

4.2.2 The role of NTRC in the regulation of transient starch accumulation in developing tomato fruits

Transient starch accumulation at the immature stage is of importance for tomato fruit growth, since starch serves as a carbon source for the accumulation of soluble sugars at the ripe stage (Schaffer et al., 2000). In our study, NTRC down-regulation led to a great decrease in the levels of starch and soluble sugars during maturation (Fig. 3.2.6, A, C and D; Fig. 3.2.8A), and eventually resulted in the generation of smaller fruits (Fig. 3.2.4). The decrease in transient starch level was accompanied by a decrease in redox-activation state of AGPase (Fig. 3.2.10), which was the key enzyme for starch synthesis (Schaffer et al., 2000; Geigenberger et al., 2004; Vigeolas et al., 2004; Neuhaus and Stitt, 2006; Faix et al., 2012) as well as a target protein of NTRC (Geigenberger et al., 2017). In NTRC-RNAi line, a decrease in the reduction state of APS1 also led to a decrease in the sensitivity of AGPase to its allosteric activator 3-PGA (Fig. 3.2.10, B and C). According to previous studies, the

subcellular concentration of 3-PGA is around 0.3 to 0.5 mM (Farré et al., 2001; Tiessen et al., 2002; Tiessen et al., 2012). As shown in the Fig. 3.2.10B, the AGPase activity of NTRC-RNAi lines in developing fruits decreased by 30% to 50% under in vivo situation. ADP-Glc is a direct product of AGPase reaction. As shown in the Fig. 3.2.10D, the level of ADP-Glc in NTRC-RNAi lines decreased by 25% to 50% compared to the wild type. Taken together, the results provide direct evidence that NTRC down-regulation leads to a strong restriction on AGPase activity in developing tomato fruits. Our results are also in line with the findings in near-isogenic tomato lines, in which increased AGPase activity resulted in an elevation in the levels of starch and soluble sugars, and eventually the generation of larger tomato fruits (Petreikov et al., 2009). Furthermore, modulating the redox state of NAD(P)(H) led to an increase in the redox activation state of AGPase, which subsequently enhanced starch synthesis and increased the level of soluble sugars in ripe tomato fruits (Centeno et al., 2011).

Intriguingly, our results also indicate that decreasing NTRC expression strongly compromised the activity of soluble starch synthase, while other enzymes been involved in starch degradation were not affected (Table 3.2.2). Soluble starch synthase catalyzes the polymerization step of starch biosynthesis. According to several in vitro studies, its activity is regulated in a redox-based manner, and it is a potential target of NTRC and TRXf1 (Skryhan et al., 2015; Skryhan et al., 2018). Now, in combination with our findings, the relationship between NTRC and soluble starch synthase in respect to starch accumulation can then be extended to an in vivo circumstance. Moreover, our results also shed light on the ability of NTRC in regulating redox-activation of both AGPase and soluble starch synthase, and this regulation eventually contributes to starch accumulation and growth of tomato fruits.

The significance of NTRC in regulating the accumulation of transient starch in Arabidopsis leaf tissues is well described (Lepistö et al., 2013; Thormählen et al., 2015). In leaf tissues, NTRC relies on NADPH generated from photosynthetic light reactions, and takes part in the regulation of Calvin-Benson cycle. In this context, the supply of substrates and allosteric activators required for AGPase is indirectly modulated by NTRC, which eventually affect the regulation of starch synthesis (Thormählen et al., 2015). Nevertheless, unlike the situation in photosynthetic tissues, the redox-activation of AGPase and the accumulation of starch are mainly governed by the transient provision of sugars through the phloem in heterotrophic tissues (Tiessen et al., 2002; Michalska et al., 2009). Alteration in the availability of sugars is likely to affect the activity of oxidative pentose phosphate pathway (OPPP; Geigenberger and Fernie, 2014), resulting in changes in the redox poise

of NAD(P)H and hence in NTRC activity. Furthermore, Kolbe et al. (2005) performed a Glc feeding experiment in potato tuber tissues. Their results indicate that Glc feeding is able to increase the ratio of NADPH to $NADP^+$. Taken together, this indicates that in developing fruits, NTRC facilitates starch accumulation by redox regulating AGPase and soluble starch synthase in response to sugar availability eventually results in changes in NADPH through affecting OPPP. This mechanism is of importance to adjust fruit sink activity to Suc supply form leaves, and thus optimize fruit growth.

4.2.3 The role of NTRC in the regulation of NAD(P)H redox homeostasis in developing tomato fruits

The redox balance is dependent on NADPH in heterotrophic plastids. Since NTRC requires NADPH to reduce its downstream targets, it is very likely that NTRC serves an important role in the maintenance of plastidial redox homeostasis. We found that decreasing the expression of NTRC strongly affects the redox state of NAD(H) and NADP(H) in developing fruits (Fig. 3.2.9), suggestive of the importance of NTRC in regulating cellular redox poise in heterotrophic tissues. However, the regulatory mechanism remains unclear. NTRC requires NADPH as a substrate, so NTRC may directly affect the ratio of NADPH to $NADP^+$. In addition, NTRC may also affect the NADPH-to-NADP+ ratio via regulating NADPH-dependent plastidial pathways, such as OPPP. Another possibility is that NTRC influences the shuttle of redox equivalents between different subcellular compartments, which further alter the redox regulation between various organelles. Since the NAD(P)H systems between plastid and mitochondrion are connected via malate/oxaloacetate shuttle, also known as malate valve (Centeno et al., 2011), it is possible that an increase in the redox state of NADPH resulted from NTRC down-regulation in plastids is transferred to mitochondria, and the redox state of NADH is subsequently increased. Similar changes in the redox state of NADP(H) and NAD(H) are found in the NTRC knockout mutant of Arabidopsis, while this change is likely due to NTRC regulating the balance between the light reaction, Calvin-Benson cycle and NADPH transport mediated by the malate valve. Hence, these results indicate the central role of NTRC in controlling the redox balance in heterotrophic and photosynthetic tissues.

NTRC also serves as a key component in the removal of hydrogen peroxide by supplying reducing equivalents to 2-Cys Prx. In photosynthetic leaf tissues, NTRC deficiency strongly compromises the reduction of 2-Cys-Prx (Pérez-Ruiz et al., 2006; Pérez-Ruiz et al., 2017). In comparison to the situation of photosynthetic tissues, we found

that decreasing NTRC expression in fruit tissues merely leads to slight changes in the reduction of 2-Cys Prxs (Fig. 3.2.12). Nevertheless, it has to be mentioned that leaf tissues harbor strong photosynthetic activity, which increase the generation of hydrogen peroxide. Accordingly, the antioxidant activity mediated by NTRC-2-Cys Prxs system has to work more efficiently. In combination of these results, it is proposed that the role of NTRC on antioxidant function is of minor importance in non-photosynthetic tissues.

4.2.4 The role of NTRC in the regulation of carbon-nitrogen balance in developing tomato fruits

Our results indicate that decreasing NTRC expression results in a decrease in the level of soluble sugars, but an opposite pattern in the level of amino acids in developing fruits (Fig. 3.2.8; Suppl. Table S2). Since the level of total protein is not changed (Fig. 3.2.7), it is unlikely that the increase in amino acid level is due to protein degradation. Instead, it is proposed that NTRC down-regulation stimulates synthesis of amino acids. The biosynthesis of amino acids needs reducing equivalents as substrates. Thus, an increase in the ratio of NAD(P)H to NAD(P)$^+$ resulting from NTRC down-regulation may promote amino acid synthesis. An increase in amino acid level accompanied by a decrease in soluble sugar level is also found in NTRC knockout mutant of Arabidopsis (Lepisto et al., 2009; Thormählen et al., 2015), suggestive of a similar effect of NTRC on the synthesis of amino acid in photosynthetic and heterotrophic tissues. An opposite relationship between sugars and amino acids is also reported in other studies to be important for osmotic balance (Trethewey et al., 1998; Fernie et al., 2003; Roessner-Tunali et al., 2003; Faix et al., 2012). To sum up, our results point out the significance of NTRC on maintenance of sugar-amino acid homeostasis to regulate osmotic balance in developing fruits.

5   Appendix

Supplemental Table S1. Fold changes in metabolite profiles in Arabidopsis leaves of the wild type (Col-0) and thioredoxin mutant lines (*trxh2.1*, *trxo1.1* and *trxh2.1trxo1.1*). Arabidopsis rosette leaves were harvested at the end of night (EN) and the end of day (ED). Mean values and standard errors derived from 6 biological replicates. The statistical analyses were performed by using ANOVA and the Dunnett's test (*$P<0.05$, in comparison to the wild type).

Time point	Arabidopsis leaves (EN)						
Genotype	Col-0	*trxh2.1*		*trxo1.1*		*trxh2.1trxo1.1*	
Metabolite	Fold change	Fold change	p-value	Fold change	p-value	Fold change	p-value
Soluble sugars							
Arabinose	1.00±0.02	1.10±0.03	0.7130	0.97±0.07	0.9820	1.03±0.14	0.9880
Erythrose	1.00±0.11	1.39±0.14	0.6458	2.39±0.35	**0.0058**	1.84±0.39	0.1142
Fructose	1.00±0.30	0.69±0.17	0.5090	0.84±0.11	0.8740	0.51±0.03	0.1680
Fucose	1.00±0.08	0.95±0.08	0.9372	0.88±0.08	0.5190	0.73±0.06	0.0517
Glucoheptose	1.00±0.06	0.88±0.06	0.2250	0.64±0.03	**0.0010**	0.65±0.04	**0.0010**
Glucose	1.00±0.06	1.02±0.08	0.9930	1.19±0.12	0.2450	1.14±0.05	0.4990
2-deoxy-glucose	1.00±0.07	0.72±0.11	0.3070	1.16±0.12	0.6950	1.23±0.19	0.4590
Maltose	1.00±0.04	1.05±0.06	0.8270	1.04±0.04	0.9180	0.94±0.06	0.7430
Mannose	1.00±0.13	1.22±0.10	0.4540	1.22±0.13	0.4500	1.28±0.12	0.2650
Psicose	1.00±0.19	0.97±0.08	0.9970	1.01±0.06	1.0000	0.97±0.09	0.9950
Raffinose	1.00±0.19	0.54±0.11	**0.0231**	0.54±0.06	**0.0218**	0.37±0.03	**0.0020**
Sucrose	1.00±0.05	1.02±0.07	0.9760	0.87±0.03	0.1640	0.95±0.04	0.8480
Threose	1.00±0.08	0.96±0.05	0.9937	1.51±0.19	0.0733	1.29±0.22	0.4211
Trehalose	1.00±0.08	1.04±0.02	0.8950	0.90±0.05	0.4920	0.90±0.05	0.4580

Xylose	1.00±0.04	1.08±0.06	0.6510	0.98±0.05	0.9870	1.02±0.07	0.9930
Xylulose	1.00±0.07	0.83±0.04	0.3510	0.87±0.06	0.5700	0.81±0.12	0.2740
Sugar alcohols						
Arabitol	1.00±0.11	0.86±0.13	0.6350	0.80±0.05	0.3590	0.79±0.10	0.3380
Galactinol	1.00±0.09	0.98±0.02	0.9850	0.86±0.04	0.2090	0.89±0.05	0.3920
Glycerol	1.00±0.02	1.15±0.10	0.5680	1.20±0.13	0.3290	0.93±0.10	0.9150
Glycerophosphoglycerol	1.00±0.11	0.93±0.04	0.8159	0.81±0.03	0.1483	0.75±0.05	**0.0406**
myo-Inosito	1.00±0.10	0.97±0.06	0.9789	0.77±0.05	0.0654	0.78±0.06	0.0895
Threitol	1.00±0.08	0.73±0.11	0.1104	0.85±0.09	0.4991	0.63±0.07	**0.0192**
Xylitol	1.00±0.08	0.87±0.11	0.7020	0.84±0.07	0.5680	0.79±0.14	0.3350
Organic acids						
2-piperidinecarboxylic acid	1.00±0.24	0.54±0.09	0.0531	0.36±0.04	**0.0068**	0.30±0.04	**0.0031**
Adipic acid	1.00±0.16	0.71±0.07	0.1550	0.57±0.09	**0.0268**	0.56±0.08	**0.0215**
Arabinonic acid	1.00±0.15	1.05±0.11	0.9970	1.38±0.28	0.5750	1.39±0.37	0.5680
Ascorbic acid	1.00±0.14	0.83±0.02	0.2580	0.29±0.04	**0.0010**	0.39±0.02	**0.0010**
Azelaic Acid	1.00±0.08	0.71±0.11	0.2020	1.03±0.10	0.9950	1.09±0.14	0.9040
Benzoic acid	1.00±0.05	1.13±0.07	0.6260	1.10±0.11	0.7620	0.98±0.11	0.9970
4-hydroxybenzoic acid	1.00±0.20	1.25±0.18	0.5480	1.31±0.14	0.3900	1.23±0.10	0.6230
2,4-dihydroxybutanoic acid	1.00±0.11	1.30±0.15	0.3630	1.17±0.16	0.7570	1.28±0.15	0.4140
4-acetamidobutanoic acid	1.00±0.04	0.88±0.07	0.4485	0.88±0.08	0.4759	0.74±0.08	**0.0362**
Dehydroascorbic acid	1.00±0.16	0.90±0.06	0.8400	1.05±0.07	0.9710	0.97±0.12	0.9960
Erythronic acid	1.00±0.12	1.02±0.14	0.9990	0.93±0.10	0.9570	0.97±0.13	0.9980

Galactaric acid	1.00±0.10	1.08±0.07	0.9120	1.29±0.08	0.1280	1.07±0.14	0.9370
Galactonic acid	1.00±0.08	1.01±0.05	1.0000	0.88±0.01	0.4000	0.84±0.08	0.2000
Glucoheptonic acid	1.00±0.07	0.96±0.09	0.9670	0.82±0.04	0.2070	0.88±0.07	0.5130
Gluconic acid	1.00±0.03	0.88±0.03	0.1769	0.75±0.02	**0.0022**	0.68±0.08	**0.0010**
Gluconic acid-1,4-lactone	1.00±0.03	1.05±0.10	0.9780	1.30±0.16	0.1390	1.18±0.09	0.5050
3-oxoglutaric acid	1.00±0.12	0.83±0.08	0.4244	0.78±0.05	0.2285	0.65±0.09	**0.0305**
Glyceric acid	1.00±0.09	0.90±0.13	0.9210	0.90±0.14	0.9100	0.96±0.17	0.9920
Iminodiacetic acid	1.00±0.09	1.54±0.18	0.2294	2.61±0.34	**0.0010**	2.03±0.20	**0.0098**
Lactic acid	1.00±0.08	0.61±0.05	**0.0010**	0.55±0.03	**0.0010**	0.69±0.06	**0.0023**
Nicotinic acid	1.00±0.08	0.86±0.06	0.4590	0.80±0.06	0.2200	0.87±0.10	0.5100
6-hydroxynicotinic acid	1.00±0.12	0.97±0.10	0.9960	0.78±0.11	0.3560	1.08±0.08	0.9180
Phosphoric acid	1.00±0.07	1.26±0.11	0.1540	1.03±0.11	0.9900	0.86±0.08	0.6090
Ribonic acid	1.00±0.12	0.76±0.10	0.2001	0.69±0.07	0.0771	0.57±0.07	**0.0105**
Shikimic acid	1.00±0.10	0.72±0.10	0.0862	0.76±0.08	0.1527	0.84±0.07	0.4506
Cis-sinapic acid	1.00±0.06	0.85±0.04	0.3288	0.75±0.08	0.0575	0.71±0.09	**0.0258**
Threonic acid	1.00±0.11	1.12±0.09	0.8120	1.18±0.13	0.5810	1.23±0.14	0.3850
Uric acid	1.00±0.05	1.01±0.08	0.9980	0.91±0.11	0.7670	1.08±0.06	0.7830
1-pyrroline-2-carboxylate	1.00±0.11	1.24±0.20	0.7360	1.25±0.28	0.6950	0.66±0.14	0.4890
Amino acids							
3-iodotyrosine	1.00±0.07	0.97±0.06	0.9700	0.88±0.04	0.3520	0.78±0.06	**0.0350**
4-aminobutanoic acid	1.00±0.10	1.70±0.20	0.1688	2.93±0.39	**0.0010**	2.24±0.27	**0.0084**
Alanine	1.00±0.05	1.00±0.06	1.0000	1.01±0.05	0.9900	1.01±0.09	0.9900

Arginine [-NH3]	1.00±0.08	0.76±0.11	0.2400	0.84±0.10	0.5450	0.79±0.10	0.3600
Asparagine	1.00±0.06	0.89±0.04	0.6740	1.00±0.10	1.0000	0.85±0.11	0.4480
Aspartic acid	1.00±0.05	0.90±0.06	0.6380	0.90±0.08	0.5893	0.76±0.08	0.0678
Beta- alanine	1.00±0.07	1.40±0.15	0.1680	1.01±0.13	1.0000	1.42±0.22	0.1460
DL-2-aminobutyric acid	1.00±0.05	1.10±0.07	0.8520	1.01±0.13	1.0000	1.28±0.16	0.2020
DL-glutamine	1.00±0.12	0.73±0.06	0.0838	0.88±0.06	0.6089	0.71±0.08	0.0610
Glutamic acid	1.00±0.09	1.08±0.07	0.7160	0.98±0.05	0.9950	0.91±0.05	0.6660
Glycine	1.00±0.06	0.78±0.08	0.2034	0.61±0.07	**0.0123**	0.75±0.12	0.1339
Glycylglycylglycine	1.00±0.10	0.96±0.05	0.9450	1.02±0.05	0.9960	0.87±0.07	0.4520
Homoserine	1.00±0.09	1.06±0.07	0.9660	1.11±0.11	0.8290	0.92±0.17	0.9160
Isoleucine	1.00±0.07	0.97±0.08	0.9930	0.93±0.12	0.9310	0.89±0.13	0.7920
Leucine	1.00±0.07	1.27±0.10	0.1750	1.13±0.13	0.7000	0.96±0.10	0.9850
Methionine	1.00±0.14	0.83±0.11	0.5650	0.83±0.09	0.5670	0.84±0.10	0.6110
O-acetylserine	1.00±0.08	1.27±0.18	0.3490	0.93±0.11	0.9670	1.06±0.15	0.9750
Ornithine	1.00±0.11	0.80±0.09	0.2740	0.76±0.07	0.1480	0.63±0.07	**0.0170**
Ornithine-1,5-lactam	1.00±0.15	0.92±0.09	0.9730	1.40±0.13	0.1940	1.01±0.23	1.0000
Phenylalanine	1.00±0.10	1.40±0.12	**0.0394**	1.31±0.09	0.1229	1.36±0.11	0.0701
Proline	1.00±0.05	1.02±0.07	0.9970	0.93±0.12	0.9300	0.87±0.14	0.6640
Pyroglutamic acid	1.00±0.07	0.88±0.06	0.5960	0.85±0.09	0.4640	0.86±0.11	0.5180
Serine	1.00±0.14	0.89±0.11	0.8230	0.73±0.07	0.2390	0.84±0.12	0.6120
Threonine	1.00±0.08	1.14±0.11	0.6360	1.02±0.09	0.9970	1.06±0.12	0.9560
Trans-4-hydroxyproline	1.00±0.11	0.81±0.10	0.4100	0.79±0.09	0.3260	0.80±0.10	0.3690

Tryptophan	1.00±0.11	1.04±0.09	0.9810	0.88±0.07	0.7200	1.08±0.13	0.8980
Valine	1.00±0.06	1.08±0.10	0.9230	1.04±0.10	0.9820	1.21±0.15	0.3840
TCA cycle intermediates							
Cis-aconitic acid	1.00±0.08	0.92±0.08	0.8586	0.90±0.12	0.7614	0.64±0.08	**0.0301**
Citric acid	1.00±0.05	1.21±0.10	0.1580	1.20±0.09	0.1640	1.11±0.04	0.5850
Fumaric acid	1.00±0.11	1.01±0.18	1.0000	0.80±0.03	0.4400	0.84±0.04	0.6000
2-oxoglutaric acid	1.00±0.04	0.82±0.11	0.3097	0.69±0.10	**0.0345**	0.71±0.05	0.0519
Malic acid	1.00±0.12	1.08±0.21	0.9440	1.03±0.06	0.9960	0.93±0.05	0.9530
Pyruvic acid	1.00±0.03	0.82±0.06	0.0700	0.71±0.04	**0.0031**	0.78±0.07	**0.0213**
Succinic acid	1.00±0.08	0.81±0.10	0.3388	0.67±0.08	0.0555	0.72±0.11	0.1033
2-methylmalic acid	1.00±0.12	0.92±0.19	0.9610	1.01±0.09	1.0000	0.76±0.13	0.4850
2,3-dimethylsuccinic acid	1.00±0.14	0.84±0.08	0.6070	0.70±0.10	0.1480	0.74±0.10	0.2300
Phosphate intermediates							
Fructose-6-phosphate	1.00±0.07	0.67±0.08	**0.0064**	0.82±0.05	0.1613	0.74±0.05	**0.0312**
Glucose-6-phosphate	1.00±0.08	0.98±0.07	0.9860	0.85±0.04	0.2460	0.83±0.05	0.1520
2-amino-2-deoxyglucose-6-phosphate	1.00±0.15	1.02±0.07	0.9980	0.69±0.06	0.0853	0.75±0.08	0.1932
Glycerol-3-phosphate	1.00±0.11	0.87±0.06	0.5420	0.74±0.08	0.0868	0.59±0.07	**0.0064**
Miscellaneous							
5-methylthioadenosine	1.00±0.08	1.04±0.04	0.9600	0.99±0.02	0.9990	1.13±0.08	0.3670
Butylamine	1.00±0.09	0.83±0.04	0.1756	0.90±0.04	0.5833	0.75±0.07	**0.0313**
Putrescine	1.00±0.09	0.73±0.06	**0.0302**	0.64±0.06	**0.0045**	0.62±0.06	**0.0030**
2,3-dihydroxypyridine	1.00±0.06	0.68±0.09	**0.0189**	0.47±0.05	**0.0010**	0.54±0.09	**0.0010**

	Col-0	trxh2.1		trxo1.1		trxh2.1trxo1.1	
Spermidine	1.00±0.10	1.16±0.13	0.6770	0.98±0.08	0.9990	1.23±0.15	0.3870
Sphingosine	1.00±0.08	0.87±0.08	0.3920	0.86±0.04	0.3360	0.82±0.05	0.1850
Ethanolamine	1.00±0.10	1.60±0.13	0.1237	2.16±0.29	**0.0018**	1.80±0.24	**0.0310**
1,2,4-triolbenzene	1.00±0.31	0.89±0.16	0.9600	0.71±0.07	0.6180	0.84±0.18	0.8950
Nicotinamide	1.00±0.08	0.81±0.12	0.4072	0.81±0.09	0.4077	0.69±0.09	0.0848
Uracil	1.00±0.07	0.88±0.11	0.6850	0.76±0.07	0.1880	0.83±0.11	0.4130
Urea	1.00±0.08	0.84±0.07	0.3350	0.75±0.06	0.0740	0.82±0.09	0.2360
3-indoleacetonitrile	1.00±0.05	1.11±0.10	0.6450	0.97±0.09	0.9840	0.99±0.08	0.9990
Time point	**Arabidopsis leaves (ED)**						
Genotype	**Col-0**	*trxh2.1*		*trxo1.1*		*trxh2.1trxo1.1*	
Metabolite	**Fold change**	**Fold change**	**p-value**	**Fold change**	**p-value**	**Fold change**	**p-value**
Soluble sugars							
Arabinose	1.00±0.07	1.02±0.11	0.9980	0.87±0.06	0.5400	0.95±0.08	0.9370
Erythrose	1.00±0.12	0.83±0.17	0.7110	0.79±0.10	0.5780	0.83±0.13	0.7150
Fructose	1.00±0.25	0.73±0.05	0.4000	0.89±0.05	0.9040	1.12±0.07	0.8710
Fucose	1.00±0.09	1.18±0.12	0.3660	1.01±0.07	1.0000	1.01±0.07	1.0000
Glucoheptose	1.00±0.07	1.50±0.18	**0.0167**	1.17±0.08	0.5908	1.18±0.10	0.5487
Glucose	1.00±0.24	1.03±0.10	0.9980	1.06±0.08	0.9850	1.22±0.08	0.5680
2-deoxy-glucose	1.00±0.29	1.69±0.48	0.3560	1.36±0.25	0.7950	1.40±0.28	0.7340
Maltose	1.00±0.36	2.28±0.28	0.5682	3.91±0.76	0.0554	13.77±1.40	**0.0010**
Mannose	1.00±0.08	1.09±0.09	0.7570	0.97±0.06	0.9800	1.12±0.08	0.5740
Psicose	1.00±0.08	1.08±0.07	0.7900	1.00±0.09	1.0000	1.01±0.07	0.9990

Raffinose	1.00±0.23	1.55±0.21	0.0778	1.21±0.08	0.7197	1.13±0.08	0.9048
Sucrose	1.00±0.09	0.90±0.02	0.5910	1.06±0.05	0.8390	1.15±0.08	0.2430
Threose	1.00±0.08	0.88±0.13	0.7010	0.90±0.07	0.8140	0.88±0.09	0.7280
Trehalose	1.00±0.10	1.13±0.15	0.6810	1.05±0.06	0.9660	1.25±0.06	0.2110
Xylose	1.00±0.07	1.11±0.10	0.6390	1.00±0.06	1.0000	1.01±0.06	1.0000
Xylulose	1.00±0.09	0.94±0.11	0.9320	0.85±0.08	0.5600	0.94±0.10	0.9460
Sugar alcohols							
Arabitol	1.00±0.11	1.29±0.18	0.2750	1.14±0.10	0.7800	1.09±0.11	0.9150
Galactinol	1.00±0.08	1.03±0.13	0.9890	0.97±0.06	0.9870	0.94±0.06	0.9400
Glycerol	1.00±0.12	0.86±0.15	0.7930	1.01±0.16	1.0000	0.89±0.07	0.8690
Glycerophosphoglycerol	1.00±0.08	1.14±0.12	0.4950	0.96±0.06	0.9680	1.07±0.06	0.8710
myo-Inosito	1.00±0.08	1.08±0.09	0.7980	1.11±0.07	0.6000	1.05±0.05	0.9500
Threitol	1.00±0.09	1.09±0.12	0.8540	0.96±0.08	0.9790	0.96±0.08	0.9820
Xylitol	1.00±0.05	1.01±0.11	0.9990	0.97±0.07	0.9870	0.97±0.08	0.9860
Organic acids							
2-piperidinecarboxylic acid	1.00±0.41	0.44±0.09	0.1900	0.52±0.08	0.2870	0.56±0.07	0.3590
Adipic acid	1.00±0.09	1.04±0.13	0.9860	0.93±0.08	0.9120	0.85±0.07	0.5320
Arabinonic acid	1.00±0.24	0.82±0.27	0.8760	0.53±0.14	0.3000	0.57±0.18	0.3750
Ascorbic acid	1.00±0.16	1.17±0.11	0.7490	0.94±0.16	0.9800	0.64±0.15	0.2190
Azelaic Acid	1.00±0.18	1.52±0.36	0.3600	1.34±0.22	0.6610	1.30±0.21	0.7360
Benzoic acid	1.00±0.23	1.08±0.21	0.9770	0.79±0.10	0.7130	0.73±0.07	0.5440
4-hydroxybenzoic acid	1.00±0.15	1.12±0.23	0.9480	1.00±0.21	1.0000	0.91±0.14	0.9740

2,4-dihydroxybutanoic acid	1.00±0.14	0.98±0.15	0.9980	0.85±0.08	0.7180	0.85±0.11	0.7490
4-acetamidobutanoic acid	1.00±0.10	1.05±0.16	0.9820	0.96±0.12	0.9880	0.95±0.06	0.9810
Dehydroascorbic acid	1.00±0.12	1.49±0.30	0.2430	1.27±0.20	0.6860	1.24±0.15	0.7540
Erythronic acid	1.00±0.09	1.16±0.10	0.4150	0.94±0.07	0.9080	0.95±0.07	0.9410
Galactaric acid	1.00±0.08	1.34±0.28	0.3650	1.19±0.14	0.7680	1.01±0.08	1.0000
Galactonic acid	1.00±0.09	1.13±0.16	0.6820	1.05±0.08	0.9710	0.95±0.06	0.9710
Glucoheptonic acid	1.00±0.07	1.02±0.08	0.9960	0.89±0.06	0.4950	0.97±0.05	0.9720
Gluconic acid	1.00±0.09	0.98±0.08	0.9940	0.97±0.08	0.9860	1.00±0.09	1.0000
Gluconic acid-1,4-lactone	1.00±0.12	1.20±0.07	0.4990	1.18±0.13	0.5570	1.31±0.14	0.1800
3-oxoglutaric acid	1.00±0.29	2.50±0.91	0.1650	1.60±0.48	0.7860	1.37±0.27	0.9330
Glyceric acid	1.00±0.07	1.02±0.11	0.9980	0.93±0.12	0.9330	0.75±0.07	0.1870
Iminodiacetic acid	1.00±0.17	1.17±0.15	0.7310	1.31±0.07	0.3110	2.27±0.15	**0.0010**
Lactic acid	1.00±0.13	1.01±0.19	1.0000	1.10±0.21	0.9410	0.93±0.07	0.9820
Nicotinic acid	1.00±0.07	1.15±0.15	0.6820	1.09±0.11	0.9040	1.02±0.12	0.9990
6-hydroxynicotinic acid	1.00±0.11	1.09±0.15	0.8850	1.01±0.08	1.0000	1.05±0.09	0.9830
Phosphoric acid	1.00±0.14	1.30±0.34	0.7280	1.10±0.31	0.9830	0.83±0.11	0.9220
Ribonic acid	1.00±0.13	1.16±0.13	0.6250	0.80±0.08	0.4700	0.85±0.11	0.6750
Shikimic acid	1.00±0.08	1.02±0.11	0.9940	0.94±0.07	0.9050	0.92±0.07	0.8420
Cis-sinapic acid	1.00±0.10	1.27±0.23	0.5220	1.06±0.16	0.9890	1.03±0.12	0.9980
Threonic acid	1.00±0.11	1.11±0.13	0.7470	0.94±0.06	0.9540	0.90±0.07	0.7940
Uric acid	1.00±0.11	1.05±0.09	0.9580	1.00±0.09	1.0000	1.08±0.08	0.8840
1-pyrroline-2-carboxylate	1.00±0.36	0.69±0.10	0.7120	0.93±0.29	0.9950	0.85±0.15	0.9520

Amino acids							
3-iodotyrosine	1.00±0.09	0.81±0.05	0.1400	0.85±0.06	0.2750	0.89±0.06	0.5190
4-aminobutanoic acid	1.00±0.44	2.16±0.32	**0.0483**	2.44±0.08	**0.0130**	4.90±0.33	**0.0010**
Alanine	1.00±0.15	1.30±0.15	0.3538	1.80±0.12	**0.0027**	2.41±0.16	**0.0010**
Arginine [-NH3]	1.00±0.12	0.75±0.11	0.2070	0.81±0.08	0.4020	0.81±0.08	0.4090
Asparagine	1.00±0.14	1.05±0.19	0.9840	1.00±0.09	1.0000	1.07±0.10	0.9710
Aspartic acid	1.00±0.11	1.07±0.17	0.9630	0.94±0.11	0.9720	0.95±0.07	0.9780
Beta- alanine	1.00±0.07	1.37±0.25	0.2140	1.37±0.14	0.2220	1.18±0.05	0.7130
DL-2-aminobutyric acid	1.00±0.07	1.44±0.34	0.2570	0.98±0.10	1.0000	0.95±0.09	0.9960
DL-glutamine	1.00±0.11	0.98±0.10	0.9990	0.91±0.08	0.8370	1.00±0.09	1.0000
Glutamic acid	1.00±0.10	1.07±0.15	0.9290	0.97±0.08	0.9920	0.99±0.07	1.0000
Glycine	1.00±0.21	0.99±0.19	1.0000	1.31±0.22	0.5540	0.88±0.15	0.9480
Glycylglycylglycine	1.00±0.07	0.81±0.07	0.2080	0.83±0.07	0.2710	0.94±0.09	0.8800
Homoserine	1.00±0.09	0.73±0.11	0.0820	0.74±0.07	0.1081	0.59±0.07	0.0079
Isoleucine	1.00±0.15	0.84±0.09	0.9270	1.20±0.37	0.8730	1.05±0.19	0.9980
Leucine	1.00±0.15	0.80±0.14	0.6730	1.12±0.21	0.8990	0.92±0.07	0.9660
Methionine	1.00±0.09	1.00±0.12	1.0000	0.96±0.06	0.9740	0.90±0.07	0.7660
O-acetylserine	1.00±0.14	1.44±0.15	**0.0478**	1.32±0.06	0.1756	2.06±0.11	**0.0010**
Ornithine	1.00±0.18	0.96±0.17	0.9970	0.70±0.10	0.3870	0.72±0.14	0.4410
Ornithine-1,5-lactam	1.00±0.10	0.77±0.15	0.3040	0.73±0.06	0.2100	0.77±0.10	0.3330
Phenylalanine	1.00±0.10	0.90±0.11	0.7610	0.89±0.07	0.7140	0.91±0.08	0.8440
Proline	1.00±0.13	0.96±0.11	0.9980	1.32±0.26	0.5640	1.38±0.26	0.4370

Pyroglutamic acid	1.00±0.14	0.87±0.12	0.7490	0.98±0.08	0.9990	0.93±0.11	0.9530
Serine	1.00±0.08	1.13±0.15	0.7630	1.07±0.13	0.9500	1.01±0.08	1.0000
Threonine	1.00±0.06	0.97±0.09	0.9910	1.07±0.12	0.8980	0.97±0.05	0.9880
Trans-4-hydroxyproline	1.00±0.10	1.02±0.14	0.9990	0.99±0.07	0.9990	0.98±0.09	0.9990
Tryptophan	1.00±0.19	1.17±0.32	0.9290	1.12±0.19	0.9680	0.89±0.24	0.9750
Valine	1.00±0.19	1.14±0.18	0.9210	1.25±0.23	0.6990	1.23±0.18	0.7420
TCA cycle intermediates							
Cis-aconitic acid	1.00±0.15	0.98±0.14	0.9990	0.85±0.15	0.7860	0.87±0.10	0.8310
Citric acid	1.00±0.06	0.87±0.07	0.4060	0.92±0.09	0.7090	0.86±0.04	0.3280
Fumaric acid	1.00±0.08	1.38±0.08	**0.0021**	1.05±0.07	0.9296	0.98±0.04	0.9964
2-oxoglutaric acid	1.00±0.13	0.85±0.12	0.6530	0.69±0.08	0.1340	0.71±0.09	0.1720
Malic acid	1.00±0.08	0.92±0.04	0.7920	0.97±0.11	0.9850	0.90±0.05	0.6860
Pyruvic acid	1.00±0.14	0.98±0.13	0.9980	1.02±0.16	1.0000	0.83±0.07	0.6630
Succinic acid	1.00±0.16	1.36±0.21	0.2410	1.00±0.11	1.0000	1.09±0.07	0.9470
2-methylmalic acid	1.00±0.09	1.11±0.10	0.6790	0.94±0.09	0.9400	0.90±0.06	0.7460
2,3-dimethylsuccinic acid	1.00±0.10	1.17±0.10	0.3350	0.99±0.06	1.0000	0.99±0.05	1.0000
Phosphate intermediates							
Fructose-6-phosphate	1.00±0.14	0.86±0.11	0.7890	1.05±0.15	0.9860	0.93±0.12	0.9650
Glucose-6-phosphate	1.00±0.12	1.34±0.21	0.1793	1.01±0.08	0.9997	1.40±0.07	0.0997
2-amino-2-deoxyglucose-6-phosphate	1.00±0.16	1.28±0.12	0.2230	1.08±0.08	0.9350	1.26±0.08	0.2650
Glycerol-3-phosphate	1.00±0.12	1.24±0.19	0.4150	0.97±0.09	0.9980	1.02±0.08	0.9980
Miscellaneous							

5-methylthioadenosine	1.00±0.06	1.11±0.10	0.6230	1.05±0.07	0.9290	1.08±0.06	0.7800
Butylamine	1.00±0.06	1.32±0.34	0.5140	1.01±0.14	1.0000	0.95±0.08	0.9950
Putrescine	1.00±0.07	0.96±0.12	0.9730	0.93±0.07	0.8620	0.88±0.04	0.5840
2,3-dihydroxypyridine	1.00±0.09	1.36±0.20	0.1700	1.00±0.14	1.0000	0.91±0.06	0.9310
Spermidine	1.00±0.06	1.07±0.17	0.9500	0.99±0.10	1.0000	0.92±0.07	0.9150
Sphingosine	1.00±0.08	1.02±0.10	0.9980	0.97±0.10	0.9860	0.90±0.06	0.7210
Ethanolamine	1.00±0.14	0.69±0.14	0.3300	0.94±0.15	0.9800	1.00±0.15	1.0000
1,2,4-triolbenzene	1.00±0.13	1.32±0.30	0.5080	1.03±0.12	0.9990	1.04±0.15	0.9980
Nicotinamide	1.00±0.08	1.10±0.11	0.7560	0.98±0.09	0.9980	0.99±0.08	0.9990
Uracil	1.00±0.14	1.35±0.35	0.5360	0.96±0.15	0.9990	0.92±0.14	0.9880
Urea	1.00±0.16	1.46±0.28	0.2170	0.79±0.07	0.7680	1.04±0.19	0.9980
3-indoleacetonitrile	1.00±0.09	1.01±0.13	0.9990	0.98±0.07	0.9980	1.02±0.07	0.9960

Supplemental Table S2 Fold changes in metabolite profiles in tomato fruits of the wild type and NTRC-RNAi lines. Tomato fruits were harvested at 35 and 65 days-after-flowering (DAF). Mean values and standard errors derived from 6 biological replicates. The statistical analyses were performed by using ANOVA and the Dunnett's test (*$P<0.05$, in comparison to the wild type).

Stage	Green tomato (35 DAF)									
Genotype	WT	RNAi-2			RNAi-26			RNAi-33		
Metabolite	Fold change	Fold change	p-value (t-test)	p-value (ANOVA)	Fold change	p-value (t-test)	p-value (ANOVA)	Fold change	p-value (t-test)	p-value (ANOVA)
Soluble sugars										
Arabinose	1.00 ± 0.10	1.29 ± 0.07	**0.0332**	0.0697	1.24 ± 0.06	0.0619	0.1644	1.30 ± 0.11	0.0780	0.0663
D-Cellobiose	1.00 ± 0.23	1.84 ± 0.19	**0.0189**	**0.0074**	1.28 ± 0.13	0.3153	0.5361	0.99 ± 0.11	0.9573	0.9999
Erythrose	1.00 ± 0.06	1.95 ± 0.49	0.0849	0.0658	1.79 ± 0.17	**0.0015**	0.1442	1.07 ± 0.19	0.7370	0.9961
Fructose	1.00 ± 0.08	0.67 ± 0.03	**0.0025**	**0.0010**	0.69 ± 0.04	**0.0055**	**0.0016**	0.87 ± 0.05	0.1700	0.2117
Gentiobiose	1.00 ± 0.12	0.87 ± 0.18	0.5603	0.8870	0.93 ± 0.15	0.7100	0.9760	1.02 ± 0.18	0.9440	1.0000
Glucose	1.00 ± 0.10	0.55 ± 0.06	**0.0023**	**0.0010**	0.60 ± 0.06	**0.0061**	**0.0012**	0.80 ± 0.04	0.0825	0.1141
1,6-anhydro-beta-Glucose	1.00 ± 0.07	1.67 ± 0.14	**0.0019**	**0.0010**	1.55 ± 0.11	**0.0017**	**0.0059**	1.03 ± 0.11	0.7998	0.9930
Isomaltose	1.00 ± 0.05	1.58 ± 0.14	**0.0028**	**0.0105**	1.13 ± 0.08	0.1903	0.8132	1.24 ± 0.19	0.2600	0.4320
Maltose	1.00 ± 0.20	0.97 ± 0.12	0.9154	0.9990	0.72 ± 0.08	0.2314	0.5580	1.31 ± 0.25	0.3587	0.4720
Melibiose	1.00 ± 0.12	1.48 ± 0.19	0.0615	0.0707	1.08 ± 0.15	0.6660	0.9540	0.75 ± 0.09	0.1245	0.4720
Palatinose	1.00 ± 0.13	1.46 ± 0.16	**0.0479**	0.1070	1.15 ± 0.08	0.3475	0.8220	1.26 ± 0.20	0.3059	0.4830
Raffinose	1.00 ± 0.18	0.79 ± 0.09	0.3093	0.7380	0.77 ± 0.21	0.4280	0.7010	0.53 ± 0.21	0.1144	0.1790
Ribose	1.00 ± 0.07	1.02 ± 0.10	0.8683	0.9970	0.77 ± 0.05	**0.0268**	0.2150	0.96 ± 0.13	0.8136	0.9860
Sucrose	1.00 ± 0.27	0.44 ± 0.07	0.0706	**0.0374**	0.40 ± 0.05	0.0522	**0.0246**	0.56 ± 0.09	0.1462	0.1122

Threose	1.00 ± 0.15	1.27 ± 0.06	0.1161	0.4160	1.12 ± 0.12	0.5365	0.8760	0.83 ± 0.20	0.5016	0.7230
alpha,alpha'-D-Trehalose	1.00 ± 0.14	0.33 ± 0.05	**0.0012**	**0.0010**	0.61 ± 0.12	0.0554	**0.0371**	0.54 ± 0.09	**0.0193**	**0.0147**
D-Xylobiose	1.00 ± 0.18	2.67 ± 0.35	**0.0018**	**0.0010**	1.99 ± 0.36	**0.0330**	**0.0456**	0.91 ± 0.11	0.6722	0.9897
Xylose	1.00 ± 0.21	0.79 ± 0.04	0.3402	0.5300	0.81 ± 0.10	0.4353	0.6260	0.87 ± 0.12	0.6074	0.8340
Sugar alcohols										
Erythritol	1.00 ± 0.17	1.63 ± 0.11	**0.0110**	**0.0371**	1.18 ± 0.20	0.5197	0.7990	0.96 ± 0.18	0.8867	0.9974
Galactinol	1.00 ± 0.13	0.77 ± 0.08	0.1673	0.8260	1.60 ± 0.34	0.1291	0.1870	1.54 ± 0.27	0.1032	0.2610
Glycerol	1.00 ± 0.11	1.24 ± 0.15	0.2324	0.3190	0.83 ± 0.09	0.2502	0.5820	0.94 ± 0.08	0.6476	0.9560
myo-Inositol	1.00 ± 0.08	0.74 ± 0.09	0.0585	0.0727	0.58 ± 0.08	**0.0053**	**0.0034**	0.53 ± 0.05	**0.0008**	**0.0013**
Maltitol	1.00 ± 0.10	1.28 ± 0.19	0.2204	0.3690	1.06 ± 0.16	0.7519	0.9800	1.30 ± 0.08	**0.0402**	0.3230
Xylitol	1.00 ± 0.09	1.82 ± 0.17	**0.0017**	**0.0010**	1.68 ± 0.11	**0.0008**	**0.0039**	1.08 ± 0.13	0.6139	0.9426
Organic acids										
1-Pyrroline-2-carboxylate	1.00 ± 0.18	0.82 ± 0.24	0.5647	0.8630	0.98 ± 0.20	0.9382	1.0000	0.85 ± 0.17	0.5661	0.9140
2-Imidazolidone-4-carboxylic acid	1.00 ± 0.22	2.31 ± 0.82	0.1531	0.2170	1.96 ± 0.48	0.1003	0.4450	1.21 ± 0.39	0.6486	0.9840
2-Piperidinecarboxylic acid	1.00 ± 0.15	0.53 ± 0.16	0.0595	0.2010	0.93 ± 0.21	0.7902	0.9870	0.69 ± 0.21	0.2584	0.5110
trans-Aconitic acid	1.00 ± 0.27	2.48 ± 0.41	**0.0127**	**0.0043**	1.70 ± 0.26	0.0901	0.2263	1.25 ± 0.14	0.4276	0.8696
Arabinonic acid	1.00 ± 0.10	1.68 ± 0.12	**0.0017**	**0.0021**	1.58 ± 0.14	**0.0082**	**0.0084**	1.07 ± 0.12	0.6585	0.9548
2-amino-Butanoic acid	1.00 ± 0.16	1.50 ± 0.38	0.2591	0.4450	1.47 ± 0.26	0.1519	0.4840	0.91 ± 0.24	0.7531	0.9900
2-oxo-Butanoic acid	1.00 ± 0.14	0.92 ± 0.10	0.6479	0.9590	0.77 ± 0.12	0.2551	0.5650	1.07 ± 0.20	0.7653	0.9680
4-amino-Butanoic acid	1.00 ± 0.08	0.53 ± 0.14	**0.0158**	0.0653	0.76 ± 0.15	0.1765	0.4647	0.51 ± 0.16	**0.0233**	0.0532
trans-Caffeic acid	1.00 ± 0.18	2.96 ± 0.87	0.0527	**0.0349**	2.47 ± 0.38	**0.0057**	0.1350	1.90 ± 0.32	**0.0336**	0.4708
Erythronic acid	1.00 ± 0.14	1.33 ± 0.20	0.1996	0.4750	1.16 ± 0.21	0.5458	0.8830	1.00 ± 0.20	0.9864	1.0000

Galactaric acid	1.00 ± 0.09	1.55 ± 0.13	**0.0070**	**0.0083**	1.06 ± 0.14	0.7283	0.9675	0.75 ± 0.09	0.0829	0.3170
Galacturonic acid	1.00 ± 0.21	1.02 ± 0.27	0.9552	1.0000	0.88 ± 0.12	0.6393	0.9530	0.86 ± 0.17	0.6104	0.9200
Glucaric acid-1,4-lactone	1.00 ± 0.09	1.00 ± 0.09	0.9888	1.0000	0.97 ± 0.08	0.8040	0.9850	0.87 ± 0.05	0.2538	0.5550
Glucoheptonic acid-1,4-lactone	1.00 ± 0.26	1.53 ± 0.09	0.0779	0.0655	1.11 ± 0.11	0.7124	0.9319	1.26 ± 0.11	0.3746	0.5230
Glucuronic acid	1.00 ± 0.12	1.19 ± 0.11	0.2662	0.4360	0.92 ± 0.09	0.6354	0.9210	1.15 ± 0.09	0.3311	0.6050
Glyceric acid	1.00 ± 0.30	2.20 ± 0.37	**0.0311**	0.2030	0.75 ± 0.12	0.4619	0.9660	1.74 ± 0.80	0.4101	0.5630
Glycolic acid	1.00 ± 0.07	1.26 ± 0.06	**0.0185**	0.1510	1.16 ± 0.14	0.3244	0.4950	1.01 ± 0.09	0.9021	0.9990
Gulonic acid	1.00 ± 0.08	0.60 ± 0.06	**0.0034**	**0.0028**	0.52 ± 0.08	**0.0018**	**0.0010**	0.60 ± 0.07	**0.0045**	**0.0029**
2-ethyl-Hexanoic acid	1.00 ± 0.08	1.35 ± 0.13	0.0505	0.3030	1.22 ± 0.25	0.4196	0.6420	1.00 ± 0.12	0.9982	1.0000
3-amino-Isobutanoic acid	1.00 ± 0.05	1.41 ± 0.28	0.1848	0.3700	1.33 ± 0.23	0.1892	0.5330	0.52 ± 0.17	**0.0257**	0.2550
Oxalic acid	1.00 ± 0.15	1.85 ± 0.25	**0.0151**	**0.0167**	1.64 ± 0.21	**0.0306**	0.0788	0.91 ± 0.16	0.6916	0.9771
Phosphoric acid	1.00 ± 0.11	1.22 ± 0.17	0.2899	0.4370	0.87 ± 0.10	0.4246	0.8040	0.92 ± 0.09	0.5712	0.9280
Picolinic acid	1.00 ± 0.14	1.32 ± 0.19	0.2004	0.4230	1.19 ± 0.16	0.3946	0.7850	1.01 ± 0.19	0.9752	1.0000
Quinic acid	1.00 ± 0.16	3.21 ± 0.49	**0.0017**	**0.0001**	1.43 ± 0.30	0.2355	0.6349	1.41 ± 0.12	0.0665	0.6644
3-caffeoyl-cis-Quinic acid	1.00 ± 0.14	1.30 ± 0.19	0.2350	0.7712	1.79 ± 0.43	0.1088	0.1221	1.91 ± 0.22	**0.0055**	0.0654
3-caffeoyl-trans-Quinic acid	1.00 ± 0.29	1.47 ± 0.24	0.2337	0.5214	1.64 ± 0.33	0.1774	0.2973	2.12 ± 0.28	**0.0203**	**0.0321**
Ribonic acid	1.00 ± 0.10	1.65 ± 0.11	**0.0012**	**0.0005**	1.16 ± 0.11	0.2983	0.5540	1.17 ± 0.09	0.2484	0.5231
Amino acids										
Alanine	1.00 ± 0.18	1.11 ± 0.23	0.7170	0.9600	0.87 ± 0.13	0.5771	0.9400	1.08 ± 0.23	0.7989	0.9860
3-cyano-Alanine	1.00 ± 0.10	2.29 ± 0.64	0.0767	0.1540	2.27 ± 0.40	**0.0116**	0.1630	1.42 ± 0.53	0.4582	0.8630
beta-Alanine	1.00 ± 0.09	0.62 ± 0.06	**0.0051**	0.1110	0.98 ± 0.19	0.9322	0.9992	0.38 ± 0.12	**0.0021**	**0.0061**
Asparagine	1.00 ± 0.35	2.80 ± 0.83	0.0745	**0.0477**	1.72 ± 0.33	0.1643	0.6153	1.06 ± 0.25	0.8898	0.9995

Aspartic acid	1.00 ± 0.13	1.62 ± 0.20	**0.0282**	**0.0268**	1.25 ± 0.16	0.2612	0.5422	1.10 ± 0.10	0.5768	0.9459
Cysteine	1.00 ± 0.25	0.86 ± 0.25	0.6920	0.9780	1.24 ± 0.45	0.6505	0.9120	1.28 ± 0.29	0.4823	0.8730
S-methyl-DL-Cysteine	1.00 ± 0.12	1.06 ± 0.16	0.7795	0.9880	1.30 ± 0.20	0.2295	0.4180	0.75 ± 0.14	0.2199	0.5690
Glutamic acid	1.00 ± 0.17	1.31 ± 0.27	0.3605	0.5910	1.25 ± 0.18	0.3335	0.7170	0.92 ± 0.18	0.7634	0.9860
Glutamine	1.00 ± 0.41	1.60 ± 0.51	0.3839	0.5460	1.18 ± 0.31	0.7317	0.9730	0.75 ± 0.18	0.5917	0.9340
Glycine	1.00 ± 0.11	1.25 ± 0.32	0.4865	0.7310	1.16 ± 0.20	0.4889	0.9000	0.47 ± 0.12	**0.0089**	0.1990
Histidine	1.00 ± 0.55	1.43 ± 0.65	0.6204	0.8860	1.26 ± 0.52	0.7431	0.9720	0.69 ± 0.32	0.6395	0.9540
Homoserine	1.00 ± 0.10	1.64 ± 0.36	0.1189	0.1330	1.51 ± 0.14	**0.0157**	0.2710	1.42 ± 0.19	0.0767	0.4060
Isoleucine	1.00 ± 0.13	0.99 ± 0.07	0.9499	1.0000	0.99 ± 0.17	0.9766	1.0000	1.01 ± 0.27	0.9699	1.0000
Leucine	1.00 ± 0.14	0.76 ± 0.08	0.1699	0.6430	1.09 ± 0.19	0.7095	0.9660	0.79 ± 0.24	0.4761	0.7320
Lysine	1.00 ± 0.16	0.82 ± 0.16	0.4532	0.7207	1.04 ± 0.09	0.8438	0.9955	0.52 ± 0.15	0.0522	0.0699
Methionine	1.00 ± 0.06	1.39 ± 0.24	0.1495	0.3550	1.47 ± 0.17	**0.0278**	0.2230	0.90 ± 0.23	0.6969	0.9710
Ornithine	1.00 ± 0.13	1.67 ± 0.72	0.3786	0.5200	1.60 ± 0.27	0.0703	0.6000	0.64 ± 0.23	0.2063	0.8660
Phenylalanine	1.00 ± 0.15	0.89 ± 0.09	0.5409	0.9500	1.24 ± 0.19	0.3436	0.6780	1.02 ± 0.26	0.9514	1.0000
Proline	1.00 ± 0.06	0.58 ± 0.12	**0.0120**	0.0528	0.76 ± 0.13	0.1280	0.3776	0.53 ± 0.15	**0.0141**	**0.0284**
Serine	1.00 ± 0.07	0.96 ± 0.20	0.8598	0.9970	1.17 ± 0.19	0.3999	0.8240	0.79 ± 0.21	0.3666	0.7440
O-acetyl-Serine	1.00 ± 0.10	1.59 ± 0.29	0.0838	0.1080	1.21 ± 0.09	0.1606	0.7870	0.92 ± 0.22	0.7398	0.9820
Threonic acid	1.00 ± 0.11	1.90 ± 0.15	**0.0007**	**0.0010**	1.13 ± 0.17	0.5456	0.8430	1.12 ± 0.08	0.4036	0.8670
Threonine	1.00 ± 0.14	1.00 ± 0.20	0.9992	1.0000	1.40 ± 0.26	0.2094	0.4600	0.95 ± 0.27	0.8623	0.9960
Tryptophan	1.00 ± 0.15	1.58 ± 0.15	**0.0223**	0.2443	2.17 ± 0.32	**0.0079**	**0.0072**	1.15 ± 0.29	0.6640	0.9501
Tyrosine	1.00 ± 0.08	0.93 ± 0.11	0.6074	0.9760	1.50 ± 0.15	**0.0138**	0.0780	1.12 ± 0.23	0.6218	0.8910
Valine	1.00 ± 0.12	0.98 ± 0.25	0.9558	1.0000	1.16 ± 0.19	0.5010	0.9180	0.94 ± 0.27	0.8478	0.9950

TCA cycle intermediates										
Citric acid	1.00 ± 0.17	2.39 ± 0.25	**0.0010**	**0.0010**	1.48 ± 0.18	0.0826	0.1760	1.45 ± 0.09	**0.0463**	0.2250
Fumaric acid	1.00 ± 0.14	1.90 ± 0.12	**0.0006**	**0.0010**	1.07 ± 0.10	0.7125	0.9730	1.18 ± 0.17	0.4325	0.6630
2-oxo-Glutaric acid	1.00 ± 0.07	1.84 ± 0.27	**0.0137**	0.0550	1.71 ± 0.32	0.0536	0.1150	1.52 ± 0.21	**0.0431**	0.3110
Malic acid	1.00 ± 0.06	1.55 ± 0.12	**0.0019**	**0.0011**	1.05 ± 0.11	0.7003	0.9631	0.96 ± 0.06	0.6741	0.9835
2-methyl-Malic acid	1.00 ± 0.13	2.00 ± 0.15	**0.0005**	**0.0000**	1.04 ± 0.12	0.8056	0.9900	0.94 ± 0.11	0.7220	0.9740
Pyruvic acid	1.00 ± 0.08	1.83 ± 0.17	**0.0012**	**0.0010**	1.39 ± 0.16	0.0531	0.1150	1.36 ± 0.09	**0.0108**	0.1460
Succinic acid	1.00 ± 0.13	0.84 ± 0.05	0.2811	0.6070	0.93 ± 0.12	0.7119	0.9450	0.86 ± 0.11	0.4196	0.6790
2,3-dimethyl-Succinic acid	1.00 ± 0.17	0.93 ± 0.13	0.7437	0.9730	0.95 ± 0.18	0.8397	0.9890	1.03 ± 0.09	0.8654	0.9970
Phosphate intermediates										
Fructose-6-phosphate	1.00 ± 0.07	1.39 ± 0.10	**0.0107**	**0.0289**	1.24 ± 0.12	0.1067	0.2267	0.95 ± 0.10	0.6691	0.9612
Galactose-6-phosphate	1.00 ± 0.07	1.38 ± 0.17	0.0681	0.0759	1.17 ± 0.10	0.2046	0.5883	0.90 ± 0.09	0.4029	0.8677
Glucose-6-phosphate	1.00 ± 0.09	1.35 ± 0.18	0.1153	0.1770	1.15 ± 0.12	0.3276	0.7430	0.92 ± 0.12	0.5957	0.9460
2-amino-2-deoxy-Glucose-6-phosphate	1.00 ± 0.17	1.23 ± 0.40	0.6068	0.8630	1.17 ± 0.19	0.5082	0.9330	1.01 ± 0.20	0.9773	1.0000
Glycerol-3-phosphate	1.00 ± 0.12	1.70 ± 0.34	0.0845	0.0756	1.45 ± 0.17	0.0538	0.3220	1.07 ± 0.13	0.6836	0.9894
Mannose-6-phosphate	1.00 ± 0.17	1.28 ± 0.28	0.4044	0.6170	1.22 ± 0.20	0.4136	0.7590	0.89 ± 0.09	0.5566	0.9530
myo-Inositol-1-phosphate	1.00 ± 0.09	3.70 ± 0.96	**0.0193**	**0.0102**	2.01 ± 0.63	0.1454	0.4845	1.02 ± 0.10	0.9045	1.0000
2-deoxy-Ribose-5-phosphate	1.00 ± 0.10	1.48 ± 0.28	0.1340	0.1240	1.15 ± 0.06	0.2153	0.8490	1.01 ± 0.13	0.9401	1.0000
Ribulose-5-phosphate	1.00 ± 0.17	1.38 ± 0.14	0.1115	0.0966	1.12 ± 0.07	0.5341	0.8368	0.80 ± 0.08	0.3055	0.5249
Sorbitol-6-phosphate	1.00 ± 0.19	1.42 ± 0.24	0.2090	0.2180	1.05 ± 0.10	0.8299	0.9940	0.84 ± 0.07	0.4628	0.8440
Miscellaneous										
Adenosine	1.00 ± 0.21	1.50 ± 0.11	0.0651	0.0617	1.31 ± 0.14	0.2492	0.3233	1.06 ± 0.08	0.8131	0.9860

Butyro-1,4-lactam	1.00 ± 0.08	0.53 ± 0.09	**0.0035**	**0.0139**	0.71 ± 0.12	0.0662	0.1536	0.48 ± 0.12	**0.0053**	**0.0062**
Ethanolamine	1.00 ± 0.27	1.28 ± 0.17	0.3940	0.7270	1.55 ± 0.27	0.1797	0.2510	1.13 ± 0.20	0.7132	0.9630
Guanosine	1.00 ± 0.14	0.46 ± 0.08	**0.0076**	**0.0170**	0.65 ± 0.09	0.0595	0.1520	0.78 ± 0.17	0.3469	0.4870
Hydroquinone	1.00 ± 0.07	1.57 ± 0.12	**0.0021**	**0.0183**	1.71 ± 0.21	**0.0093**	**0.0032**	1.31 ± 0.09	**0.0233**	0.2793
Hydroxyurea	1.00 ± 0.13	1.87 ± 0.49	0.1177	0.0770	1.02 ± 0.13	0.9301	1.0000	1.01 ± 0.07	0.9449	1.0000
N-acetyl-Mannosamine	1.00 ± 0.11	1.39 ± 0.14	0.0602	0.0589	1.00 ± 0.12	0.9829	1.0000	0.79 ± 0.05	0.1141	0.4235
Nicotinamide	1.00 ± 0.09	1.81 ± 0.32	**0.0343**	**0.0222**	1.26 ± 0.10	0.0732	0.6680	1.22 ± 0.18	0.2934	0.7546
Ornithine-1,5-lactam	1.00 ± 0.17	0.87 ± 0.28	0.6957	0.9570	1.17 ± 0.25	0.5927	0.9170	0.52 ± 0.20	0.1006	0.3500
Phosphoric acid monomethyl ester	1.00 ± 0.08	0.80 ± 0.16	0.2914	0.5610	0.88 ± 0.16	0.5103	0.8300	0.78 ± 0.08	0.0892	0.4860
Putrescine	1.00 ± 0.05	0.92 ± 0.17	0.6800	0.9600	0.72 ± 0.06	**0.0044**	0.3690	0.79 ± 0.20	0.3378	0.5850
Uracil	1.00 ± 0.23	2.01 ± 0.24	**0.0124**	**0.0100**	1.90 ± 0.18	**0.0122**	**0.0219**	1.34 ± 0.21	0.3085	0.5689
Urea	1.00 ± 0.08	1.48 ± 0.37	0.2348	0.2910	1.22 ± 0.11	0.1466	0.8100	0.81 ± 0.16	0.3165	0.8630

Stages	Red tomato (65 DAF)									
Genotype	WT	RNAi-2			RNAi-26			RNAi-33		
Metabolite	Fold change	Fold change	p-value (t-test)	p-value (ANOVA)	Fold change	p-value (t-test)	p-value (ANOVA)	Fold change	p-value (t-test)	p-value (ANOVA)
Soluble sugars										
Arabinose	1.00 ± 0.09	0.76 ± 0.04	**0.0383**	0.0992	0.91 ± 0.09	0.5179	0.7748	0.82 ± 0.08	0.1635	0.2644
D-Cellobiose	1.00 ± 0.14	0.83 ± 0.09	0.3319	0.5680	0.80 ± 0.05	0.1936	0.4280	0.82 ± 0.13	0.3550	0.5040
Erythrose	1.00 ± 0.16	1.38 ± 0.20	0.1764	0.3210	0.89 ± 0.07	0.5309	0.9380	1.15 ± 0.22	0.5969	0.8750
Fructose	1.00 ± 0.03	0.81 ± 0.04	**0.0026**	**0.0123**	0.87 ± 0.03	**0.0125**	0.1126	0.92 ± 0.06	0.3099	0.4538
Gentiobiose	1.00 ± 0.18	0.22 ± 0.04	**0.0018**	**0.0010**	0.39 ± 0.07	**0.0110**	**0.0010**	0.28 ± 0.02	**0.0030**	**0.0010**
Glucose	1.00 ± 0.07	0.63 ± 0.09	**0.0083**	**0.0078**	0.72 ± 0.06	**0.0172**	**0.0494**	0.70 ± 0.08	**0.0232**	**0.0318**
1,6-anhydro-beta-Glucose	1.00 ± 0.07	1.69 ± 0.18	**0.0062**	**0.0164**	1.38 ± 0.15	**0.0474**	0.2359	1.35 ± 0.19	0.1212	0.2983
Isomaltose	1.00 ± 0.17	0.53 ± 0.06	**0.0298**	**0.0261**	0.61 ± 0.12	0.0987	0.0700	0.54 ± 0.07	**0.0328**	**0.0276**
Maltose	1.00 ± 0.21	0.42 ± 0.04	**0.0210**	**0.0058**	0.50 ± 0.03	**0.0382**	**0.0167**	0.57 ± 0.09	0.0883	**0.0441**
Melibiose	1.00 ± 0.13	0.78 ± 0.04	0.1446	0.2813	0.68 ± 0.07	0.0612	0.0785	0.67 ± 0.11	0.0905	0.0690
Palatinose	1.00 ± 0.12	0.76 ± 0.06	0.1011	0.1540	0.79 ± 0.06	0.1586	0.2430	0.76 ± 0.09	0.1536	0.1670
Raffinose	1.00 ± 0.22	1.05 ± 0.09	0.8341	0.9920	0.94 ± 0.13	0.8230	0.9880	1.05 ± 0.18	0.8650	0.9930
Ribose	1.00 ± 0.14	0.39 ± 0.05	**0.0024**	**0.0010**	0.49 ± 0.05	**0.0074**	**0.0007**	0.44 ± 0.03	**0.0033**	**0.0003**
Sucrose	1.00 ± 0.07	0.71 ± 0.10	**0.0396**	0.1672	0.77 ± 0.11	0.1209	0.3339	0.66 ± 0.13	**0.0466**	0.0903
Threose	1.00 ± 0.05	1.13 ± 0.10	0.2783	0.6620	1.24 ± 0.07	**0.0188**	0.1950	1.18 ± 0.13	0.2350	0.4130
alpha,alpha'-D-Trehalose	1.00 ± 0.12	0.57 ± 0.07	**0.0108**	**0.0110**	0.72 ± 0.08	0.0788	0.1120	0.79 ± 0.10	0.1961	0.2720

D-Xylobiose	1.00 ± 0.22	1.20 ± 0.23	0.5364	0.8570	1.13 ± 0.21	0.6732	0.9540	1.05 ± 0.24	0.8897	0.9980
Xylose	1.00 ± 0.08	1.09 ± 0.06	0.3803	0.9490	1.21 ± 0.26	0.4582	0.6290	0.96 ± 0.10	0.7455	0.9940
Sugar alcohols										
Erythritol	1.00 ± 0.09	1.10 ± 0.12	0.5128	0.9150	1.15 ± 0.18	0.4538	0.7760	1.12 ± 0.15	0.5199	0.8780
Galactinol	1.00 ± 0.31	0.65 ± 0.07	0.3037	0.4010	0.83 ± 0.11	0.6100	0.8320	0.94 ± 0.11	0.8587	0.9900
Glycerol	1.00 ± 0.10	1.14 ± 0.09	0.3354	0.6500	1.05 ± 0.10	0.7270	0.9670	0.97 ± 0.10	0.8459	0.9940
myo-Inositol	1.00 ± 0.14	0.77 ± 0.13	0.2556	0.3678	0.64 ± 0.11	0.0756	0.1029	0.53 ± 0.07	**0.0139**	**0.0236**
Maltitol	1.00 ± 0.09	0.82 ± 0.09	0.1872	0.4900	0.94 ± 0.13	0.7218	0.9600	1.02 ± 0.10	0.8897	0.9980
Xylitol	1.00 ± 0.10	1.84 ± 0.22	**0.0056**	**0.0084**	1.50 ± 0.16	**0.0297**	0.1492	1.44 ± 0.20	0.0804	0.2167
Organic acids										
1-Pyrroline-2-carboxylate	1.00 ± 0.18	0.41 ± 0.05	**0.0095**	**0.0125**	0.33 ± 0.05	**0.0046**	**0.0044**	0.52 ± 0.18	0.0847	**0.0442**
2-Imidazolidone-4-carboxylic acid	1.00 ± 0.32	3.03 ± 0.86	0.0511	0.0849	1.61 ± 0.39	0.2575	0.8374	2.02 ± 0.77	0.2509	0.5363
2-Piperidinecarboxylic acid	1.00 ± 0.35	0.98 ± 0.23	0.9554	1.0000	0.96 ± 0.25	0.9331	0.9990	0.67 ± 0.19	0.4208	0.6990
trans-Aconitic acid	1.00 ± 0.21	1.50 ± 0.19	0.1101	0.7210	2.01 ± 0.51	0.0954	0.2150	1.90 ± 0.56	0.1622	0.2940
Arabinonic acid	1.00 ± 0.10	1.18 ± 0.17	0.3813	0.6510	0.38 ± 0.08	**0.0008**	**0.0110**	0.72 ± 0.16	0.1654	0.3350
2-amino-Butanoic acid	1.00 ± 0.24	1.80 ± 0.22	**0.0342**	0.0906	1.70 ± 0.28	0.0906	0.1587	1.21 ± 0.26	0.5761	0.8887
2-oxo-Butanoic acid	1.00 ± 0.21	1.30 ± 0.20	0.3359	0.5530	1.16 ± 0.19	0.5801	0.8740	0.72 ± 0.14	0.3082	0.6110
4-amino-Butanoic acid	1.00 ± 0.37	1.37 ± 0.39	0.5037	0.7020	0.44 ± 0.15	0.1882	0.4070	0.55 ± 0.19	0.3019	0.5710
trans-Caffeic acid	1.00 ± 0.15	1.58 ± 0.17	**0.0276**	0.0673	1.31 ± 0.17	0.2017	0.4540	1.36 ± 0.20	0.1811	0.3399
Erythronic acid	1.00 ± 0.07	1.13 ± 0.11	0.3211	0.7260	1.16 ± 0.14	0.3234	0.6020	1.01 ± 0.11	0.9477	1.0000
Galactaric acid	1.00 ± 0.12	1.23 ± 0.16	0.2740	0.8780	1.29 ± 0.42	0.5208	0.7830	1.16 ± 0.26	0.5878	0.9500
Galacturonic acid	1.00 ± 0.07	0.89 ± 0.04	0.1860	0.7923	0.67 ± 0.16	0.0909	0.0983	0.69 ± 0.11	**0.0386**	0.1253

Glucaric acid-1,4-lactone	1.00 ± 0.13	0.83 ± 0.07	0.2725	0.5280	0.74 ± 0.10	0.1441	0.2230	0.83 ± 0.11	0.3194	0.5100
Glucoheptonic acid-1,4-lactone	1.00 ± 0.07	1.49 ± 0.13	**0.0083**	**0.0294**	1.58 ± 0.12	**0.0018**	**0.0104**	1.51 ± 0.16	**0.0138**	**0.0225**
Glucuronic acid	1.00 ± 0.10	0.95 ± 0.07	0.7203	0.9500	1.01 ± 0.06	0.9190	0.9990	0.86 ± 0.06	0.2398	0.4100
Glyceric acid	1.00 ± 0.14	1.01 ± 0.13	0.9650	1.0000	1.20 ± 0.12	0.2902	0.5470	1.04 ± 0.12	0.8311	0.9920
Glycolic acid	1.00 ± 0.15	0.92 ± 0.11	0.6920	0.9410	0.88 ± 0.11	0.5127	0.7990	0.90 ± 0.10	0.5728	0.8680
Gulonic acid	1.00 ± 0.10	0.77 ± 0.09	0.1112	0.1251	0.72 ± 0.08	0.0509	0.0534	0.72 ± 0.03	**0.0215**	**0.0486**
2-ethyl-Hexanoic acid	1.00 ± 0.18	1.09 ± 0.16	0.7266	0.9660	1.08 ± 0.18	0.7558	0.9720	0.93 ± 0.14	0.7779	0.9850
3-amino-Isobutanoic acid	1.00 ± 0.34	1.98 ± 0.42	0.1000	0.1340	0.77 ± 0.20	0.5835	0.9360	1.45 ± 0.36	0.3848	0.6740
Oxalic acid	1.00 ± 0.31	1.33 ± 0.50	0.5840	0.8410	1.40 ± 0.36	0.4244	0.7640	0.52 ± 0.13	0.1875	0.6520
Phosphoric acid	1.00 ± 0.09	1.10 ± 0.07	0.3921	0.8450	0.91 ± 0.14	0.6016	0.8910	0.88 ± 0.12	0.4564	0.7830
Picolinic acid	1.00 ± 0.19	1.13 ± 0.16	0.6008	0.8970	1.17 ± 0.17	0.5284	0.8260	1.03 ± 0.16	0.9047	0.9980
Quinic acid	1.00 ± 0.11	1.62 ± 0.07	**0.0006**	**0.0021**	1.38 ± 0.15	0.0692	0.0664	1.43 ± 0.10	**0.0135**	**0.0305**
3-caffeoyl-cis-Quinic acid	1.00 ± 0.12	0.51 ± 0.07	**0.0056**	**0.0093**	0.63 ± 0.11	**0.0491**	0.0527	0.70 ± 0.10	0.0866	0.1315
3-caffeoyl-trans-Quinic acid	1.00 ± 0.45	0.86 ± 0.20	0.7800	0.9910	0.68 ± 0.20	0.5263	0.9110	1.59 ± 0.68	0.4881	0.6570
Ribonic acid	1.00 ± 0.06	1.45 ± 0.09	**0.0026**	**0.0316**	1.26 ± 0.14	0.1216	0.2727	1.31 ± 0.14	0.0713	0.1747
Amino acids										
Alanine	1.00 ± 0.22	1.29 ± 0.21	0.3622	0.5940	1.16 ± 0.18	0.5839	0.8870	0.71 ± 0.16	0.3032	0.5790
3-cyano-Alanine	1.00 ± 0.22	3.59 ± 1.40	0.0968	0.1280	2.06 ± 0.60	0.1308	0.7390	2.27 ± 0.89	0.1979	0.6280
beta-Alanine	1.00 ± 0.31	1.61 ± 0.31	0.1900	0.2660	0.68 ± 0.12	0.3556	0.7300	0.98 ± 0.28	0.9609	1.0000
Asparagine	1.00 ± 0.21	2.34 ± 0.65	0.0795	0.1690	1.75 ± 0.39	0.1211	0.5910	2.04 ± 0.61	0.1373	0.3420
Aspartic acid	1.00 ± 0.21	1.10 ± 0.17	0.7310	0.9810	1.03 ± 0.26	0.9392	1.0000	1.20 ± 0.25	0.5487	0.8590
Cysteine	1.00 ± 0.20	1.17 ± 0.24	0.5927	0.9110	1.22 ± 0.28	0.5389	0.8460	0.85 ± 0.20	0.6127	0.9440

S-methyl-DL-Cysteine	1.00 ± 0.12	1.55 ± 0.25	0.0756	0.2491	1.77 ± 0.30	**0.0394**	0.0749	1.18 ± 0.22	0.4913	0.9043
Glutamic acid	1.00 ± 0.23	1.19 ± 0.17	0.5253	0.8720	0.84 ± 0.20	0.6221	0.9220	0.89 ± 0.26	0.7631	0.9710
Glutamine	1.00 ± 0.32	2.07 ± 0.75	0.2191	0.3620	1.25 ± 0.33	0.5953	0.9740	1.64 ± 0.58	0.3527	0.7270
Glycine	1.00 ± 0.33	1.02 ± 0.15	0.9660	1.0000	0.91 ± 0.14	0.8057	0.9780	0.49 ± 0.11	0.1728	0.2040
Histidine	1.00 ± 0.39	1.64 ± 0.73	0.4564	0.7430	1.92 ± 0.63	0.2438	0.5030	0.89 ± 0.32	0.8279	0.9980
Homoserine	1.00 ± 0.22	2.84 ± 0.22	**0.0001**	**0.0010**	1.95 ± 0.13	**0.0045**	0.0658	2.35 ± 0.44	**0.0212**	**0.0072**
Isoleucine	1.00 ± 0.22	0.87 ± 0.17	0.6463	0.8870	0.72 ± 0.11	0.2870	0.4910	0.57 ± 0.11	0.1125	0.1680
Leucine	1.00 ± 0.24	0.89 ± 0.12	0.6849	0.9320	0.80 ± 0.12	0.4835	0.7460	0.65 ± 0.16	0.2515	0.3420
Lysine	1.00 ± 0.29	1.12 ± 0.13	0.7114	0.9640	0.73 ± 0.21	0.4743	0.7450	0.80 ± 0.24	0.6022	0.8580
Methionine	1.00 ± 0.16	1.57 ± 0.15	**0.0266**	0.1180	1.36 ± 0.14	0.1193	0.4140	1.34 ± 0.28	0.3151	0.4600
Ornithine	1.00 ± 0.42	1.34 ± 0.33	0.5402	0.8250	0.70 ± 0.22	0.5505	0.8760	0.94 ± 0.37	0.9198	0.9990
Phenylalanine	1.00 ± 0.28	1.25 ± 0.29	0.5541	0.8180	0.99 ± 0.14	0.9857	1.0000	0.85 ± 0.24	0.6877	0.9460
Proline	1.00 ± 0.31	1.28 ± 0.32	0.5447	0.7640	0.53 ± 0.13	0.1884	0.4120	0.61 ± 0.17	0.3036	0.5690
Serine	1.00 ± 0.27	1.45 ± 0.29	0.2743	0.3900	0.89 ± 0.13	0.7174	0.9740	0.77 ± 0.21	0.5177	0.8290
O-acetyl-Serine	1.00 ± 0.20	2.14 ± 0.34	**0.0159**	**0.0399**	2.00 ± 0.31	**0.0210**	0.0768	1.55 ± 0.35	0.1990	0.4494
Threonic acid	1.00 ± 0.13	1.51 ± 0.14	**0.0233**	0.2230	1.60 ± 0.31	0.1049	0.1310	1.45 ± 0.20	0.0894	0.3190
Threonine	1.00 ± 0.27	1.58 ± 0.32	0.1936	0.3290	0.99 ± 0.18	0.9875	1.0000	1.02 ± 0.30	0.9641	1.0000
Tryptophan	1.00 ± 0.27	1.28 ± 0.27	0.4798	0.7510	1.23 ± 0.17	0.4801	0.8300	0.97 ± 0.23	0.9282	0.9990
Tyrosine	1.00 ± 0.20	1.13 ± 0.18	0.6336	0.9530	1.22 ± 0.32	0.5740	0.8230	0.82 ± 0.14	0.4626	0.8850
Valine	1.00 ± 0.21	1.47 ± 0.26	0.1952	0.3330	1.10 ± 0.14	0.7070	0.9790	0.98 ± 0.25	0.9425	1.0000
TCA cycle intermediates										
Citric acid	1.00 ± 0.07	2.49 ± 0.32	**0.0011**	**0.0010**	1.56 ± 0.23	**0.0429**	0.2078	1.77 ± 0.19	**0.0032**	0.0614

Fumaric acid	1.00 ± 0.12	1.20 ± 0.13	0.2880	0.5920	1.26 ± 0.07	0.0916	0.3800	1.09 ± 0.18	0.7058	0.9400
2-oxo-Glutaric acid	1.00 ± 0.17	1.37 ± 0.10	0.0943	0.5639	1.90 ± 0.21	**0.0082**	**0.0383**	1.76 ± 0.38	0.0974	0.0903
Malic acid	1.00 ± 0.13	1.43 ± 0.15	0.0559	0.0965	1.02 ± 0.10	0.9005	0.9991	1.10 ± 0.16	0.6571	0.9270
2-methyl-Malic acid	1.00 ± 0.06	1.21 ± 0.15	0.2240	0.6620	1.33 ± 0.13	**0.0462**	0.3390	1.35 ± 0.24	0.1839	0.3050
Pyruvic acid	1.00 ± 0.14	0.97 ± 0.04	0.8539	0.9950	1.04 ± 0.05	0.8067	0.9870	1.07 ± 0.12	0.7037	0.9150
Succinic acid	1.00 ± 0.13	0.93 ± 0.15	0.7304	0.9540	0.90 ± 0.09	0.5476	0.8880	0.88 ± 0.10	0.4793	0.8310
2,3-dimethyl-Succinic acid	1.00 ± 0.32	1.07 ± 0.23	0.8697	0.9920	0.83 ± 0.10	0.6209	0.8920	0.77 ± 0.09	0.5021	0.7780
Phosphate intermediates										
Fructose-6-phosphate	1.00 ± 0.14	1.90 ± 0.26	**0.0124**	0.0511	1.52 ± 0.27	0.1163	0.3476	1.59 ± 0.31	0.1070	0.2510
Galactose-6-phosphate	1.00 ± 0.12	2.01 ± 0.24	**0.0037**	**0.0427**	1.57 ± 0.31	0.1171	0.3399	1.75 ± 0.36	0.0773	0.1612
Glucose-6-phosphate	1.00 ± 0.14	1.82 ± 0.26	**0.0196**	**0.0445**	1.45 ± 0.24	0.1329	0.3694	1.49 ± 0.23	0.1001	0.3032
2-amino-2-deoxy-Glucose-6-phosphate	1.00 ± 0.18	1.05 ± 0.20	0.8462	0.9940	0.96 ± 0.15	0.8832	0.9980	0.89 ± 0.20	0.6891	0.9500
Glycerol-3-phosphate	1.00 ± 0.21	2.13 ± 0.32	**0.0139**	**0.0128**	1.14 ± 0.14	0.5976	0.9625	1.41 ± 0.30	0.2869	0.5369
Mannose-6-phosphate	1.00 ± 0.19	2.09 ± 0.47	0.0553	0.2900	2.08 ± 0.73	0.1829	0.2940	1.75 ± 0.39	0.1170	0.5720
myo-Inositol-1-phosphate	1.00 ± 0.14	2.58 ± 0.50	**0.0119**	**0.0475**	1.94 ± 0.57	0.1404	0.3198	1.42 ± 0.41	0.3634	0.8398
2-deoxy-Ribose-5-phosphate	1.00 ± 0.14	1.27 ± 0.12	0.1873	0.4920	1.08 ± 0.21	0.7512	0.9660	1.02 ± 0.14	0.9119	0.9990
Ribulose-5-phosphate	1.00 ± 0.09	1.29 ± 0.07	**0.0249**	**0.0339**	1.02 ± 0.05	0.8227	0.9925	1.02 ± 0.09	0.9004	0.9977
Sorbitol-6-phosphate	1.00 ± 0.08	1.42 ± 0.14	**0.0294**	0.1740	1.20 ± 0.19	0.3637	0.7070	1.07 ± 0.19	0.7533	0.9820
Miscellaneous										
Adenosine	1.00 ± 0.07	1.02 ± 0.15	0.9255	1.0000	0.95 ± 0.12	0.7109	0.9850	1.16 ± 0.16	0.3758	0.7040
Butyro-1,4-lactam	1.00 ± 0.30	1.31 ± 0.27	0.4688	0.6820	0.59 ± 0.13	0.2406	0.4750	0.67 ± 0.19	0.3718	0.6310
Ethanolamine	1.00 ± 0.20	0.89 ± 0.09	0.6408	0.9030	0.87 ± 0.10	0.5759	0.8380	0.80 ± 0.13	0.4302	0.6200

Guanosine	1.00 ± 0.19	1.53 ± 0.28	0.1499	0.2480	1.25 ± 0.21	0.4041	0.7730	1.30 ± 0.20	0.3025	0.6680
Hydroquinone	1.00 ± 0.22	1.00 ± 0.07	0.9944	1.0000	0.96 ± 0.09	0.8614	0.9920	0.91 ± 0.11	0.7351	0.9440
Hydroxyurea	1.00 ± 0.08	1.21 ± 0.12	0.1738	0.5010	1.23 ± 0.16	0.2164	0.4240	1.14 ± 0.13	0.3876	0.7850
N-acetyl-Mannosamine	1.00 ± 0.04	1.03 ± 0.08	0.7713	0.9900	0.87 ± 0.08	0.1855	0.4700	0.82 ± 0.09	0.0885	0.2260
Nicotinamide	1.00 ± 0.10	1.87 ± 0.17	**0.0014**	**0.0045**	1.54 ± 0.21	**0.0451**	0.0937	1.40 ± 0.17	0.0746	0.2579
Ornithine-1,5-lactam	1.00 ± 0.51	1.07 ± 0.31	0.9139	0.9980	0.47 ± 0.14	0.3439	0.5720	0.69 ± 0.30	0.6139	0.8590
Phosphoric acid monomethyl ester	1.00 ± 0.13	0.96 ± 0.06	0.7631	0.9900	1.08 ± 0.12	0.6568	0.9450	1.08 ± 0.18	0.7281	0.9490
Putrescine	1.00 ± 0.30	1.35 ± 0.22	0.3724	0.6240	0.94 ± 0.14	0.8517	0.9950	0.86 ± 0.28	0.7452	0.9590
Uracil	1.00 ± 0.27	1.17 ± 0.15	0.5884	0.9110	1.25 ± 0.22	0.4895	0.7850	1.12 ± 0.26	0.7603	0.9690
Urea	1.00 ± 0.14	0.86 ± 0.23	0.6051	0.8960	1.17 ± 0.15	0.4074	0.8280	1.18 ± 0.18	0.4398	0.8040

6   Reference

Arsova B, Hoja U, Wimmelbacher M, Greiner E, Ustün S, Melzer M, Petersen K, Lein W, Börnke F (2010) Plastidial thioredoxin z interacts with two fructokinase-like proteins in a thiol-dependent manner: evidence for an essential role in chloroplast development in *Arabidopsis* and *Nicotiana benthamiana*. Plant Cell **22**: 1498–515

Backhausen JE, Kitzmann C, Horton P, Scheibe R (2000) Electron acceptors in isolated intact spinach chloroplasts act hierarchically to prevent over-reduction and competition for electrons. Photosynth Res **64**: 1–13

Ballicora MA, Frueauf JB, Fu Y, Schurmann P, Preiss J (2000) activation of the potato tuber ADP-glucose pyrophosphorylase by thioredoxin. J Biol Chem **275**: 1315–1320

Bashandy T, Taconnat L, Renou JP, Meyer Y, Reichheld JP (2009) Accumulation of flavonoids in an ntra ntrb mutant leads to tolerance to UV-C. Mol Plant **2**: 249–258

Benitez-Alfonso Y, Cilia M, San Roman A, Thomas C, Maule A, Hearn S, Jackson D (2009) Control of Arabidopsis meristem development by thioredoxin-dependent regulation of intercellular transport. Proc Natl Acad Sci U S A **106**: 3615–3620

Berger F, Ramírez-Hernández MH, Ziegler M (2004) The new life of a centenarian: Signalling functions of NAD(P). Trends Biochem Sci **29**: 111–118

Bohrer AS, Massot V, Innocenti G, Reichheld JP, Issakidis-Bourguet E, Vanacker H (2012) New insights into the reduction systems of plastidial thioredoxins point out the unique properties of thioredoxin z from Arabidopsis. J Exp Bot **63**: 6315–6323

Buchanan B, Gruissem W, Jones R (2015) Biochemistry and molecular biology of plants, 2nd ed. doi: 10.1201/b11003-3

Cabrillac D, Cock JM, Dumas C, Gaude T (2001) The S-locus receptor kinase is inhibited by thioredoxins and activated by pollen coat proteins. Nature **410**: 220–223

Calderón A, Ortiz-Espín A, Iglesias-Fernández R, Carbonero P, Pallardó FV, Sevilla F, Jiménez A (2017) Thioredoxin (Trx o 1) interacts with proliferating cell nuclear antigen (PCNA) and its overexpression affects the growth of tobacco cell culture. Redox Biol **11**: 688–700

Calderón A, Sánchez-Guerrero A, Ortiz-Espín A, Martínez-Alcalá I, Camejo D, Jiménez A, Sevilla F (2018) Lack of mitochondrial thioredoxin o1 is compensated by antioxidant components under salinity in *Arabidopsis thaliana* plants. Physiol Plant **164**: 251–267

La Camera S, L'Haridon F, Astier J, Zander M, Abou-Mansour E, Page G, Thurow C, Wendehenne D, Gatz C, Métraux JP, et al (2011) The glutaredoxin ATGRXS13 is required to facilitate Botrytis cinerea infection of Arabidopsis thaliana plants. Plant J

68: 507–519

Carrari F, Fernie AR (2006) Metabolic regulation underlying tomato fruit development. J Exp Bot **57**: 1883–1897

Carrillo LR, Froehlich JE, Cruz JA, Savage LJ, Kramer DM (2016) Multi-level regulation of the chloroplast ATP synthase: The chloroplast NADPH thioredoxin reductase C (NTRC) is required for redox modulation specifically under low irradiance. Plant J **87**: 654–663

Cejudo FJ, Ferrández J, Cano B, Puerto-Galán L, Guinea M (2012) The function of the NADPH thioredoxin reductase C-2-Cys peroxiredoxin system in plastid redox regulation and signalling. FEBS Lett **586**: 2974–2980

Centeno DC, Osorio S, Nunes-Nesi A, Bertolo ALF, Carneiro RT, Araújo WL, Steinhauser M-C, Michalska J, Rohrmann J, Geigenberger P, et al (2011) Malate plays a crucial role in starch metabolism, ripening, and soluble solid content of tomato fruit and affects postharvest softening. Plant Cell **23**: 162–84

Cha JY, Kim JY, Jung IJ, Kim MR, Melencion A, Alam SS, Yun DJ, Lee SY, Kim MG, Kim WY (2014) NADPH-dependent thioredoxin reductase A (NTRA) confers elevated tolerance to oxidative stress and drought. Plant Physiol Biochem **80**: 184–191

Cheng NH, Liu JZ, Brock A, Nelson RS, Hirschi KD (2006) AtGRXcp, an Arabidopsis chloroplastic glutaredoxin, is critical for protection against protein oxidative damage. J Biol Chem **281**: 26280–26288

Cheng NH, Liu JZ, Liu X, Wu Q, Thompson SM, Lin J, Chang J, Whitham SA, Park S, Cohen JD, et al (2011) Arabidopsis monothiol glutaredoxin, AtGRXS17, is critical for temperature-dependent postembryonic growth and development via modulating auxin response. J Biol Chem **286**: 20398–20406

Cho MJ, Wong JH, Marx C, Jiang W, Lemaux PG, Buchanan BB (1999) Overexpression of thioredoxin h leads to enhanced activity of starch debranching enzyme (pullulanase) in barley grain. Proc Natl Acad Sci U S A **96**: 14641–14646

Clough SJ, Bent AF (1998) Floral dip: A simplified method for Agrobacterium-mediated transformation of Arabidopsis thaliana. Plant J **16**: 735–743

Courteille A, Vesa S, Sanz-Barrio R, Cazalé AC, Becuwe-Linka N, Farran I, Havaux M, Rey P, Rumeau D (2013) Thioredoxin m4 controls photosynthetic alternative electron pathways in Arabidopsis. Plant Physiol **161**: 508–520

Couturier J, Jacquot JP, Rouhier N (2009) Evolution and diversity of glutaredoxins in photosynthetic organisms. Cell Mol Life Sci **66**: 2539–2557

Da Q, Wang P, Wang M, Sun T, Jin H, Liu B, Wang J, Grimm B, Wang H-B (2017) Thioredoxin and NADPH-dependent thioredoxin reductase C regulation of Tetrapyrrole Biosynthesis. Plant Physiol **175**: 652–666

Daloso DM, Müller K, Obata T, Florian A, Tohge T, Bottcher A, Riondet C, Bariat L, Carrari F, Nunes-Nesi A, et al (2015) Thioredoxin , a master regulator of the tricarboxylic acid cycle in plant mitochondria. Proc Natl Acad Sci U S A **112**: 1392–1400

Davies JN, Hobson GE (1981) The constituents of tomato--the influence of environment, nutrition, and genotype. Rev Food Sci Nutr **15**: 205–280

Doyle JJ, Doyle JL (1987) A rapid DNA isolation procedure for small quantities of fresh leaf tissue. Phytochem Bull **19**: 11–15

Draculic T, Dawes IW, Grant CM (2000) A single glutaredoxin or thioredoxin gene is essential for viability in the yeast Saccharomyces cerevisiae. Mol Microbiol **36**: 1167–1174

Erban A, Schauer N, Fernie AR, Kopka J (2007) Nonsupervised construction and application of mass spectral and retention time index libraries from time-of-flight gas chromatography-mass spectrometry metabolite profiles. Metabolomics Methods Mol Biol **358**: 19–38

Fait A, Fromm H, Walter D, Galili G, Fernie AR (2008) Highway or byway: the metabolic role of the GABA shunt in plants. Trends Plant Sci **13**: 14–19

Faix B, Radchuk V, Nerlich A, Hümmer C, Radchuk R, Emery RJN, Keller H, Götz KP, Weschke W, Geigenberger P, et al (2012) Barley grains, deficient in cytosolic small subunit of ADP-glucose pyrophosphorylase, reveal coordinate adjustment of C:N metabolism mediated by an overlapping metabolic-hormonal control. Plant J **69**: 1077–1093

Farré EM, Tiessen A, Roessner U, Geigenberger P, Trethewey RN (2001) Analysis of the compartmentation of glycolytic intermediates, nucleotides, sugars, organic acids, amino acids, and sugar alcohols in potato tubers using a nonaqueous fractionation method. Plant Physiol **127**: 685–700

Fernie AR, Tiessen A, Stitt M, Willmitzer L, Geigenberger P (2003) Altered metabolic fluxes result from shifts in metabolite levels in sucrose phosphorylase-expressing potato tubers. Plant, Cell Environ **25**: 1219–1232

Florez-Sarasa I, Obata T, Del-Saz NF, Reichheld J-P, Meyer EH, Rodriguez-Concepcion M, Ribas-Carbo M, Fernie AR (2019) The lack of mitochondrial thioredoxin TRXo1 affects in vivo alternative oxidase activity and

carbon metabolism under different light conditions. Plant Cell Physiol **1**: 2369–2381

Florian A, Araújo WL, Fernie AR (2013) New insights into photorespiration obtained from metabolomics. Plant Biol **15**: 656–666

da Fonseca-Pereira P, Souza PVL, Hou L-Y, Schwab S, Geigenberger P, Nunes-Nesi A, Timm S, Fernie AR, Thormählen I, Araújo WL, et al (2020) Thioredoxin h2 contributes to the redox regulation of mitochondrial photorespiratory metabolism. Plant Cell Environ **43**: 188–208

Frommer WB, Mielchen C, Martin T (1994) Metabolic control of patatin promoters from potato in transgenic tobacco and tomato plants. Plant Physiol (Life Sci Adv) **13**: 329–334

Gardeström P, Igamberdiev AU, Raghavendra AS (2002) Mitochondrial functions in the light and significance to carbon-nitrogen interactions. *In* CH Foyer, G Noctor, eds, Adv. Photosynth. Respir. Photosynth. Nitrogen Assim. Assoc. Carbon Metab. Kluwer Academic Publishers, p pp.151-172

Geigenberger P, Fernie AR (2014) Metabolic control of redox and redox control of metabolism in plants. Antioxid Redox Signal **21**: 1389–421

Geigenberger P, Stitt M, Fernie AR (2004) Metabolic control analysis and regulation of the conversion of sucrose to starch in growing potato tubers. Plant, Cell Environ **27**: 655–673

Geigenberger P, Thormählen I, Daloso DM, Fernie AR (2017) The unprecedented versatility of the plant thioredoxin system. Trends Plant Sci **22**: 249–262

Gelhaye E, Rouhier N, Jacquot JP (2004) The thioredoxin h system of higher plants. Plant Physiol Biochem **42**: 265–271

Gierson D, Kader AA (1986) Fruit ripening and quality. *In* JG Atherton, J Rudich, eds, Tomato Crop. pp 241–280

Giovannoni JJ (2004) Genetic regulation of fruit development and ripening. Plant Cell **16**: S170–S180

Haink G, Deussen A (2003) Liquid chromatography method for the analysis of adenosine compounds. J Chromatogr B **784**: 189–193

Hatzfeld WD, Stitt M (1990) A study of the rate of recycling of triose phosphates in heterotrophic Chenopodium rubrum cells, potato tubers, and maize endosperm. Planta **180**: 198–204

Häusler RE, Fischer KL, Flügge UI (2000) Determination of low-abundant metabolites in plant extracts by NAD(P)H fluorescence with a microtiter plate reader. Anal Biochem **281**: 1–8

He T, Song B, Liu J, Chen X, Ou Y, Lin Y, Zhang H, Xie C (2012) A new isoform of thioredoxin h group in potato, SbTRXh1, regulates cold-induced sweetening of potato tubers by adjusting sucrose content. Plant Cell Rep **31**: 1463–1471

Helenius M, Jalkanen S, Yegutkin GG (2012) Enzyme-coupled assays for simultaneous detection of nanomolar ATP, ADP, AMP, adenosine, inosine and pyrophosphate concentrations in extracellular fluids. Biochim Biophys Acta - Mol Cell Res **1823**: 1967–1975

Hendriks JHM, Anna K, Yves G, Stitt M, Geigenberger P (2003) ADP-Glucose pyrophosphorylase is activated by posttranslational redox-modification in response to light and to sugars in leaves of arabidopsis and other plant species. Plant Physiol **133**: 838–849

Hoefnagel MHN, Atkin OK, Wiskich JT (1998) Interdependence between chloroplasts and mitochondria in the light and the dark. Biochim Biophys Acta - Bioenerg **1366**: 235–255

Igamberdiev AU, Bykova N V., Lea PJ, Gardeström P (2001) The role of photorespiration in redox and energy balance of photosynthetic plant cells: A study with a barley mutant deficient in glycine decarboxylase. Physiol Plant **111**: 427–438

Igamberdiev AU, Hurry V, Krömer S, Gardeström P (1998) The role of mitochondrial electron transport during photosynthetic induction. A study with barley (Hordeum vulgare) protoplasts incubated with rotenone and oligomycin. Physiol Plant **104**: 431–439

Jelitto T, Sonnewald U, Willmitzer L, Hajirezeai M, Stitt M (1992) Inorganic pyrophosphate content and metabolites in potato and tobacco plants expressing E. coli pyrophosphatase in their cytosol. Planta **188**: 238–244

Johnson TC, Wada K, Buchanan BB, Holmgren A (1987) Reduction of purothionin by the wheat seed thioredoxin system. Plant Physiol **85**: 446–451

Kanayama Y (2017) Sugar metabolism and fruit development in the tomato. Hortic J **86**: 417–425

Kaul S, Koo HL, Jenkins J, Rizzo M, Rooney T, Tallon LJ, Feldblyum T, Nierman W, Benito MI, Lin X, et al (2000) Analysis of the genome sequence of the flowering plant Arabidopsis thaliana. Nature **408**: 796–815

Kim YS, Kim JJ, Park SI, Diamond S, Boyd JS, Taton A, Kim IS, Golden JW, Yoon HS (2018) Expression of osTPX gene improves cellular redox homeostasis and photosynthesis efficiency in synechococcus elongatus PCC 7942. Front Plant Sci **871**: 1–15

Kim YS, Schumaker KS, Zhu JK (2006) EMS mutagenesis of Arabidopsis. Methods Mol Biol **323**: 101–103

Kirchsteiger K, Ferrandez J, Pascual MB, Gonzalez M, Cejudo FJ (2012) NADPH thioredoxin reductase C is localized in plastids of photosynthetic and nonphotosynthetic tissues and is involved in lateral root formation in Arabidopsis. Plant Cell **24**: 1534–1548

Kirchsteiger K, Pulido P, Gonzálezlez M, Cejudo FJ (2009) NADPH thioredoxin reductase C controls the redox status of chloroplast 2-Cys peroxiredoxins in arabidopsis thaliana. Mol Plant **2**: 298–307

Kobrehel K, Wong JH, Balogh Á, Kiss F, Yee BC, Buchanan BB (1992) Specific reduction of wheat storage proteins by thioredoxin h. Plant Physiol **99**: 919–924

Kolbe A, Tiessen A, Schluepmann H, Paul M, Ulrich S, Geigenberger P (2005) Trehalose 6-phosphate regulates starch synthesis via posttranslational redox activation of ADP-glucose pyrophosphorylase. Proc Natl Acad Sci **102**: 11118–23

Kulichikhin K, Mukherjee S, Ayele BT (2016) Extraction and assays of ADP-glucose pyrophosphorylase, soluble starch synthase and granule bound starch synthase from wheat. Bio Protoc **6**: e1929

Laemmli UK (1970) Cleavage of structural proteins during the assembly of the head of bacteriophage T4. Nature **227**: 680–685

Laloi C, Mestres-Ortega D, Marco Y, Meyer Y, Reichheld JP (2004) The Arabidopsis cytosolic thioredoxin h5 gene induction by oxidative stress and its W-box-mediated response to pathogen elicitor. Plant Physiol **134**: 1006–1016

Laloi C, Rayapuram N, Chartier Y, Grienenberger JM, Bonnard G, Meyer Y (2001) Identification and characterization of a mitochondrial thioredoxin system in plants. Proc Natl Acad Sci U S A **98**: 14144–14149

Lamkemeyer P, Laxa M, Collin V, Li W, Finkemeier I, Schöttler MA, Holtkamp V, Tognetti VB, Issakidis-Bourguet E, Kandlbinder A, et al (2006) Peroxiredoxin Q of *Arabidopsis thaliana* is attached to the thylakoids and functions in context of photosynthesis. Plant J **45**: 968–981

Laporte D, Olate E, Salinas P, Salazar M, Jordana X, Holuigue L (2012) Glutaredoxin GRXS13 plays a key role in protection against photooxidative stress in Arabidopsis. J Exp Bot **63**: 503–515

Lepisto A, Kangasjarvi S, Luomala E-M, Brader G, Sipari N, Keranen M, Keinanen M, Rintamaki E (2009) Chloroplast NADPH-thioredoxin reductase interacts with photoperiodic development in Arabidopsis. Plant Physiol **149**: 1261–1276

Lepistö A, Pakula E, Toivola J, Krieger-Liszkay A, Vignols F, Rintamäki E (2013) Deletion of chloroplast NADPH-dependent thioredoxin reductase results in inability to regulate starch synthesis and causes stunted growth under short-day photoperiods. J Exp Bot **64**: 3843–3854

Li S, Lauri A, Ziemann M, Busch A, Bhave M, Zachgo S (2009a) Nuclear activity of ROXY1, a glutaredoxin interacting with TGA factors, is required for petal development in arabidopsis thaliana. Plant Cell **21**: 429–441

Li YC, Ren JP, Cho MJ, Zhou SM, Kim YB, Guo HX, Wong JH, Niu H Bin, Kim HK, Morigasaki S, et al (2009b) The level of expression of thioredoxin is linked to fundamental properties and applications of wheat seeds. Mol Plant **2**: 430–441

Lintala M, Schuck N, Thormählen I, Jungfer A, Weber KL, Weber APM, Geigenberger P, Soll J, Bölter B, Mulo P (2014) Arabidopsis tic62 trol mutant lacking thylakoid-bound ferredoxin-NADP+ oxidoredutase shows distinct metabolic phenotype. Mol Plant **7**: 45–57

Lisec J, Schauer N, Kopka J, Willmitzer L, Fernie AR (2006) Gas chromatography mass spectrometry-based metabolite profiling in plants. Nat Protoc **1**: 387–396

Luedemann A, Strassburg K, Erban A, Kopka J (2008) TagFinder for the quantitative analysis of gas chromatography - Mass spectrometry (GC-MS)-based metabolite profiling experiments. Bioinformatics **24**: 732–737

Lunn JE, Feil R, Hendriks JHM, Gibon Y, Morcuende R, Osuna D, Scheible W-R, Carillo P, Hajirezaei M-R, Stitt M (2006) Sugar-induced increases in trehalose 6-phosphate are correlated with redox activation of ADPglucose pyrophosphorylase and higher rates of starch synthesis in Arabidopsis thaliana . Biochem J **397**: 139–148

Luo T, Fan T, Liu Y, Rothbart M, Yu J, Zhou S, Grimm B, Luo M (2012) Thioredoxin redox regulates ATPase activity of magnesium chelatase CHLI subunit and modulates redox-mediated signaling in tetrapyrrole biosynthesis and homeostasis of reactive oxygen species in pea plant. Plant Physiol **159**: 118–130

Lytovchenko A, Eickmeier I, Pons C, Osorio S, Szecowka M, Lehmberg K, Arrivault S, Tohge T, Pineda B, Anton MT, et al (2011) Tomato fruit photosynthesis is seemingly unimportant in primary metabolism and ripening but plays a considerable role in seed development. Plant Physiol **157**: 1650–1663

Ma X, Balazadeh S, Mueller-Roeber B (2019) Tomato fruit ripening factor NOR controls leaf senescence. J Exp Bot **70**: 2727–2740

Martí MC, Olmos E, Calvete JJ, Díaz I, Barranco-Medina S, Whelan J, Lázaro JJ, Sevilla F, Jiménez A (2009) Mitochondrial and nuclear localization of a novel pea

thioredoxin: identification of its mitochondrial target proteins. Plant Physiol **150**: 646–657

Marx C, Wong JH, Buchanan BB (2003) Thioredoxin and germinating barley: Targets and protein redox changes. Planta **216**: 454–460

Maurino VG, Engqvist MKM (2015) 2-Hydroxy Acids in Plant Metabolism. Arab B **13**: e0182

Meng L, Wong JH, Feldman LJ, Lemaux PG, Buchanan BB (2010) A membrane-associated thioredoxin required for plant growth moves from cell to cell, suggestive of a role in intercellular communication. Proc Natl Acad Sci U S A **107**: 3900–3905

Meyer Y, Belin C, Delorme-Hinoux V, Reichheld J-P, Riondet C (2012) Thioredoxin and glutaredoxin systems in plants: Molecular mechanisms, crosstalks, and functional significance. Antioxid Redox Signal **17**: 1124–1160

Meyer Y, Reichheld JP, Vignols F (2005) Thioredoxins in Arabidopsis and other plants. Photosynth Res **86**: 419–433

Meyer Y, Riondet C, Constans L, Abdelgawwad MR, Reichheld JP, Vignols F (2006) Evolution of redoxin genes in the green lineage. Photosynth Res **89**: 179–192

Meyer Y, Siala W, Bashandy T, Riondet C, Vignols F, Reichheld JP (2008) Glutaredoxins and thioredoxins in plants. Biochim Biophys Acta - Mol Cell Res **1783**: 589–600

Michaeli S, Fromm H (2015) Closing the loop on the GABA shunt in plants: Are GABA metabolism and signaling entwined? Front Plant Sci **6**: 1–7

Michalska J, Zauber H, Buchanan BB, Cejudo FJ, Geigenberger P (2009) NTRC links built-in thioredoxin to light and sucrose in regulating starch synthesis in chloroplasts and amyloplasts. Proc Natl Acad Sci **106**: 9908–9913

Michelet L, Lemaire SD, Marchand CH, Fermani S, Sparla F, Morisse S, Pérez-Pérez ME, Trost P, Zaffagnini M, Danon A, et al (2013) Redox regulation of the Calvin–Benson cycle: something old, something new. Front Plant Sci **4**: 1–21

Miller GL (1959) Use of dinitrosalicylic acid reagent for determination of reducing sugar. Anal Chem **31**: 426–428

Müller P, Li XP, Niyogi KK (2001) Non-photochemical quenching. A response to excess light energy. Plant Physiol **125**: 1558–1566

Murmu J, Bush MJ, de Long C, Li S, Xu M, Khan M, Malcolmson C, Fobert PR, Zachgo S, Hepworth SR (2010) Arabidopsis basic leucine-zipper transcription factors TGA9 and TGA10 interact with floral glutaredoxins ROXY1 and ROXY2 and

are redundantly required for anther development. Plant Physiol **154**: 1492–1504

Naranjo B, Diaz-Espejo A, Lindahl M, Cejudo FJ (2016a) Type-f thioredoxins have a role in the short-term activation of carbon metabolism and their loss affects growth under short-day conditions in Arabidopsis thaliana. J Exp Bot **67**: 1951–1964

Naranjo B, Mignée C, Krieger-Liszkay A, Hornero-Méndez D, Gallardo-Guerrero L, Cejudo FJ, Lindahl M (2016b) The chloroplast NADPH thioredoxin reductase C, NTRC, controls non-photochemical quenching of light energy and photosynthetic electron transport in Arabidopsis. Plant, Cell Environ **39**: 804–822

Navrot N, Collin V, Gualberto J, Gelhaye E, Hirasawa M, Rey P, Knaff DB, Issakidis E, Jacquot JP, Rouhier N (2006) Plant glutathione peroxidases are functional peroxiredoxins distributed in several subcellular compartments and regulated during biotic and abiotic stresses. Plant Physiol **142**: 1364–1379

Ndamukong I, Abdallat A Al, Thurow C, Fode B, Zander M, Weigel R, Gatz C (2007) SA-inducible Arabidopsis glutaredoxin interacts with TGA factors and suppresses JA-responsive PDF1.2 transcription. Plant J **50**: 128–139

Neuhaus HE, Stitt M (2006) Control analysis of photosynthate partitioning. Planta **182**: 445–454

Nikkanen L, Toivola J, Rintamäki E (2016) Crosstalk between chloroplast thioredoxin systems in regulation of photosynthesis. Plant, Cell Environ **39**: 1691–1705

Niyogi KK (1999) Photoprotection revisited: genetic and molecular approaches. Annu Rev Plant Physiol Plant Mol Biol **50**: 333–359

Niyogi KK (2000) Safety valves for photosynthesis. Curr Opin Plant Biol **3**: 455–460

Noctor G, Foyer CH (2000) Homeostasis of adenylate status during photosynthesis in a fluctuating environment. J Exp Bot **51**: 347–356

Noctor G, Foyer CH (1998) A re-evaluation of the ATP:NADPH budget during C3 photosynthesis: A contribution from nitrate assimilation and its associated respiratory activity? J Exp Bot **49**: 1895–1908

Obiadalla-Ali H, Fernie AR, Kossmann J, Lloyd JR (2004) Developmental analysis of carbohydrate metabolism in tomato (Lycopersicon esculentum cv. Micro-Tom) fruits. Physiol Plant **120**: 196–204

Ocheretina O, Haferkamp I, Tellioglu H, Scheibe R (2000) Light-modulated NADP-malate dehydrogenases from mossfern and green algae: Insights into evolution of the enzyme's regulation. Gene **258**: 147–154

Okegawa Y, Motohashi K (2015) Chloroplastic thioredoxin m functions as a major regulator of Calvin cycle enzymes during photosynthesis in vivo. Plant J **84**: 900–913

Ortiz-Espín A, Iglesias-Fernández R, Calderón A, Carbonero P, Sevilla F, Jiménez A (2017) Mitochondrial AtTrxo1 is transcriptionally regulated by AtbZIP9 and AtAZF2 and affects seed germination under saline conditions. J Exp Bot **68**: 1025–1038

Osmond B, Badger M, Maxwell K, Björkman O, Leegood R (1997) Too many photon: photorespiration, photoinhibition and photooxidation. Trends Plant Sci **2**: 119–121

Osorio S, Fernie AR (2014) Fruit ripening: primary metabolism. *In* P Nath, M Bouzayen, AK Mattoo, JC Pech, eds, Fruit Ripening Physiol. Signal. Genomics. pp 15–27

Padmasree K, Padmavathi L, Raghavendra AS (2002) Essentiality of mitochondrial oxidative metabolism for photosynthesis: optimization of carbon assimilation and protection against photoinhibition. Crit Rev Biochem Mol Biol. doi: 10.1080/10409230290771465

Padmasree K, Raghavendra AS (2001) Consequence of restricted mitochondrial oxidative metabolism on photosynthetic carbon assimilation in mesophyll protoplasts: Decrease in light activation of four chloroplastic enzymes. Physiol Plant **112**: 582–588

Park SC, Kim IR, Kim JY, Lee Y, Yoo SH, Jung JH, Cheong GW, Lee SY, Jang MK, Lee JR (2019) Functional characterization of a rice thioredoxin protein ostrxm and its cysteine mutant variant with antifungal activity. Antioxidants. doi: 10.3390/antiox8120598

Park SK, Jung YJ, Lee JR, Lee YM, Jang HH, Lee SS, Park JH, Kim SY, Moon JC, Lee SY, et al (2009) Heat-shock and redox-dependent functional switching of an h-type Arabidopsis thioredoxin from a disulfide reductase to a molecular chaperone. Plant Physiol **150**: 552–561

Pérez-Ruiz JM, Cejudo FJ (2009) A proposed reaction mechanism for rice NADPH thioredoxin reductase C, an enzyme with protein disulfide reductase activity. FEBS Lett **583**: 1399–1402

Pérez-Ruiz JM, Guinea M, Puerto-Galán L, Cejudo FJ (2014) NADPH thioredoxin reductase C is involved in redox regulation of the Mg-Chelatase I subunit in arabidopsis thaliana chloroplasts. Mol Plant **7**: 1252–1255

Pérez-Ruiz JM, Naranjo B, Ojeda V, Guinea M, Cejudo FJ (2017) NTRC-dependent redox balance of 2-Cys peroxiredoxins is needed for optimal function of the photosynthetic apparatus. Proc Natl Acad Sci **114**: 12069–12074

Pérez-Ruiz JM, Spínola MC, Kirchsteiger K, Moreno J, Sahrawy M, Cejudo FJ (2006) Rice NTRC is a high-efficiency redox system for chloroplast protection against oxidative damage. Plant Cell **18**: 2356–2368

Petreikov M, Yeselson L, Shen S, Levin I, Schaffer AA, Dagan B, Efrati A, Bar M, Co GS (2009) Carbohydrate balance and accumulation during development of near-isogenic tomato lines differing in the AGPase-L1 allele. J Am Soc Hortic Sci **134**: 134–140

Plaxton WC (1996) The organization and regulation of plant glycolysis. Annu Rev Plant Physiol Plant Mol Biol **47**: 185–214

Porra RJ, Thompson WA, Kriedemann PE (1989) Determination of accurate extinction coefficients and simultaneous equations for assaying chlorophylls a and b extracted with four different solvents: verification of the concentration of chlorophyll standards by atomic absorption spectroscopy. Biochim Biophys Acta **975**: 384–394

Raghavendra AS, Padmasree K (2003) Beneficial interactions of mitochondrial metabolism with photosynthetic carbon assimilation. Trends Plant Sci **8**: 546–553

Reichheld J-P, Khafif M, Riondet C, Droux M, Bonnard G, Meyer Y (2007) Inactivation of thioredoxin reductases reveals a complex interplay between thioredoxin and glutathione pathways in Arabidopsis development. Plant Cell **19**: 1851–1865

Reichheld JP, Mestres-Ortega D, Laloi C, Meyer Y (2002) The multigenic family of thioredoxin h in Arabidopsis thaliana: Specific expression and stress response. Plant Physiol Biochem **40**: 685–690

Reichheld JP, Meyer E, Khafif M, Bonnard G, Meyer Y (2005) AtNTRB is the major mitochondrial thioredoxin reductase in Arabidopsis thaliana. FEBS Lett **579**: 337–342

Reinholdt O, Bauwe H, Hagemann M, Timm S (2019a) Redox-regulation of mitochondrial metabolism through thioredoxin o1 facilitates light induction of photosynthesis. Plant Signal Behav. doi: 10.1080/15592324.2019.1674607

Reinholdt O, Schwab S, Zhang Y, Reichheld JP, Fernie AR, Hagemann M, Timm S (2019b) Redox-regulation of photorespiration through mitochondrial thioredoxin o1. Plant Physiol **181**: 442–457

Richter AS, Peter E, Rothbart M, Schlicke H, Toivola J, Rintamäki E, Grimm B (2013) Posttranslational influence of NADPH-dependent thioredoxin reductase C on enzymes in tetrapyrrole synthesis. Plant Physiol **162**: 63–73

Riondet C, Desouris JP, Montoya JG, Chartier Y, Meyer Y, Reichheld JP (2012) A dicotyledon-specific glutaredoxin GRXC1 family with dimer-dependent redox regulation is functionally redundant with GRXC2. Plant, Cell Environ **35**: 360–373

Rocha-Sosa M, Sonnewald U, Frommer W, Stratmann M, Schell J, Willmitzer L (1989) Both developmental and metabolic signals activate the promoter of a class I

patatin gene. EMBO J **8**: 23–29

Roessner-Tunali U, Hegemann B, Lytovchenko A, Carrari F, Bruedigam C, Granot D, Fernie AR (2003) Metabolic profiling of transgenic tomato plants overexpressing hexokinase reveals that the influence of hexose phosphorylation diminishes during fruit development. Plant Physiol **133**: 84–99

Roessner U, Luedemann A, Brust D, Fiehn O, Linke T, Willmitzer L, Fernie AR (2001) Metabolic profiling allows comprehensive phenotyping of genetically or environmentally modified plant systems. Plant Cell **13**: 11–29

Sanz-Barrio R, Corral-Martinez P, Ancin M, Segui-Simarro JM, Farran I (2013) Overexpression of plastidial thioredoxin f leads to enhanced starch accumulation in tobacco leaves. Plant Biotechnol J **11**: 618–627

Saroussi S, Karns DAJ, Thomas DC, Bloszies C, Fiehn O, Posewitz MC, Grossman AR (2019) Alternative outlets for sustaining photosynthetic electron transport during dark-to-light transitions. Proc Natl Acad Sci U S A **166**: 11518–11527

Schaffer AA, Levin I, Oguz I, Petreikov M, Cincarevsky F, Yeselson Y, Shen S, Gilboa N, Bar M (2000) ADPglucose pyrophosphorylase activity and starch accumulation in immature tomato fruit: The effect of a Lycopersicon hirsutum-derived introgression encoding for the large subunit. Plant Sci **152**: 135–144

Scheibe R (1991) Redox-modulation of chloroplast enzymes: A common principle for individual control. Plant Physiol **96**: 1–3

Scheibe R (1987) NADP+ -malate dehydrogenase in C3-plants: regulation and role of a light-activated enzyme. Physiol Plant **71**: 393–400

Schmittgen TD, Zakrajsek BA, Mills AG, Gorn V, Singer MJ, Reed MW (2000) Quantitative reverse transcription-polymerase chain reaction to study mRNA decay: Comparison of endpoint and real-time methods. Anal Biochem **285**: 194–204

Schwarzländer M, Fuchs P (2019) Keeping mitochondrial alternative oxidase reduced and active in vivo does not require thioredoxin o1. Plant Cell Physiol **1**: 2357–2359

Serrato AJ, Cejudo FJ (2003) Type-h thioredoxins accumulate in the nucleus of developing wheat seed tissues suffering oxidative stress. Planta **217**: 392–399

Serrato AJ, Pérez-Ruiz JM, Spínola MC, Cejudo FJ (2004) A novel NADPH thioredoxin reductase, localized in the chloroplast, which deficiency causes hypersensitivity to abiotic stress in *Arabidopsis thaliana*. J Biol Chem **279**: 43821–43827

Shelp BJ, Bozzo GG, Trobacher CP, Zarei A, Deyman KL, Brikis CJ (2012) Hypothesis/review: contribution of putrescine to 4-aminobutyrate (GABA) production

in response to abiotic stress. Plant Sci **193–194**: 130–135

Shirokane Y, Ichikawa K, Suzuki M (2000) A novel enzymic determination of maltose. Carbohydr Res **329**: 699–702

Skryhan K, Cuesta-Seijo JA, Nielsen MM, Marri L, Mellor SB, Glaring MA, Jensen PE, Palcic MM, Blennow A (2015) The role of cysteine residues in redox regulation and protein stability of *Arabidopsis thaliana* starch synthase 1. PLoS One **10**: 1–23

Skryhan K, Gurrieri L, Sparla F, Trost P, Blennow A (2018) Redox Regulation of Starch Metabolism. Front Plant Sci **9**: 1–8

Spínola MC, Pérez-Ruiz JM, Pulido P, Kirchsteiger K, Guinea M, González M, Cejudo FJ (2008) NTRC new ways of using NADPH in the chloroplast. Physiol Plant **133**: 516–524

Sweat TA, Wolpert TJ (2007) Thioredoxin h5 is required for victorin sensitivity mediated by a CC-NBS-LRR gene in Arabidopsis. Plant Cell **19**: 673–687

Sweetlove LJ, Lytovchenko A, Morgan M, Nunes-nesi A, Taylor NL, Baxter CJ, Eickmeier I, Fernie AR (2006) Mitochondrial uncoupling protein is required for efficient photosynthesis. **103**: 3–8

Tauberger E, Fernie AR, Emmermann M, Renz A, Kossmann J, Willmitzer L, Trethewey RN (2000) Antisense inhibition of plastidial phosphoglucomutase provides compelling evidence that potato tuber amyloplasts import carbon from the cytosol in the form of glucose-6-phosphate. Plant J **23**: 43–53

Thormählen I, Meitzel T, Groysman J, Öchsner AB, von Roepenack-Lahaye E, Naranjo B, Cejudo FJ, Geigenberger P (2015) Thioredoxin f1 and NADPH-dependent thioredoxin reductase C have overlapping functions in regulating photosynthetic metabolism and plant growth in response to varying light conditions. Plant Physiol **169**: pp.01122.2015

Thormählen I, Ruber J, Von Roepenack-Lahaye E, Ehrlich SM, Massot V, Hümmer C, Tezycka J, Issakidis-Bourguet E, Geigenberger P (2013) Inactivation of thioredoxin f1 leads to decreased light activation of ADP-glucose pyrophosphorylase and altered diurnal starch turnover in leaves of Arabidopsis plants. Plant, Cell Environ **36**: 16–29

Thormählen I, Zupok A, Rescher J, Leger J, Weissenberger S, Groysman J, Orwat A, Chatel-Innocenti G, Issakidis-Bourguet E, Armbruster U, et al (2017) Thioredoxins Play a Crucial Role in Dynamic Acclimation of Photosynthesis in Fluctuating Light. Mol Plant **10**: 168–182

Tiessen A, Hendriks JHM, Stitt M, Branscheid A, Gibon Y, Farré EM, Geigenberger

P (2002) Starch synthesis in potato tubers is regulated by post-translational redox modification of ADP-glucose pyrophosphorylase. Plant Cell **14**: 2191–2213

Tiessen A, Nerlich A, Faix B, Hümmer C, Fox S, Trafford K, Weber H, Weschke W, Geigenberger P (2012) Subcellular analysis of starch metabolism in developing barley seeds using a non-aqueous fractionation method. J Exp Bot **63**: 2071–2087

Timm S, Bauwe H (2013) The variety of photorespiratory phenotypes - employing the current status for future research directions on photorespiration. Plant Biol **15**: 737–747

Toledano MB, Kumar C, Le Moan N, Spector D, Tacnet F (2007) The system biology of thiol redox system in Escherichia coli and yeast: differential functions in oxidative stress, iron metabolism and DNA synthesis. FEBS Lett **581**: 3598–3607

Traverso JA, Micalella C, Martinez A, Brown SC, Satiat-Jeunemaître B, Meinnel T, Giglione C (2013) Roles of N-terminal fatty acid acylations in membrane compartment partitioning: Arabidopsis h-type thioredoxins as a case study. Plant Cell **25**: 1056–1077

Trethewey RN, Geigenberger P, Riedel K, Hajirezaei MR, Sonnewald U, Stitt M, Riesmeier JW, Willmitzer L (1998) Combined expression of glucokinase and invertase in potato tubers leads to a dramatic reduction in starch accumulation and a stimulation of glycolysis. Plant J **15**: 109–118

Trotter EW, Grant CM (2005) Overlapping roles of the cytoplasmic and mitochondrial redox regulatory systems in the yeast Saccharomyces cerevisiae. Eukaryot Cell **4**: 392–400

Trotter EW, Grant CM (2002) Thioredoxins are required for protection against a reductive stress in the yeast Saccharomyces cerevisiae. Mol Microbiol **46**: 869–878

Trotter EW, Grant CM (2003) Non-reciprocal regulation of the redox state of the glutathione-glutaredoxin and thioredoxin systems. EMBO Rep **4**: 184–188

Vernoux T, Wilson RC, Seeley KA, Reichheld JP, Muroy S, Brown S, Maughan SC, Cobbett CS, Van Montagu M, Inzé D, et al (2000) The ROOT MERISTEMLESS1/CADMIUM SENSITIVE2 gene defines a glutathione-dependent pathway involved in initiation and maintenance of cell division during postembryonic root development. Plant Cell **12**: 97–109

Vigeolas H, Möhlmann T, Martini N, Neuhaus HE, Geigenberger P (2004) Embryo-specific reduction of ADP-Glc pyrophosphorylase leads to an inhibition of starch synthesis and a delay in oil accumulation in developing seeds of oilseed rape. Plant Physiol **136**: 2676–2686

Whippo CW, Khurana P, Davis PA, Deblasio SL, Desloover D, Staiger CJ, Hangarter RP (2011) THRUMIN1 is a light-regulated actin-bundling protein involved in chloroplast motility. Curr Biol **21**: 59–64

Winer J, Jung CKS, Shackel I, Williams PM (1999) Development and validation of real-time quantitative reverse transcriptase-polymerase chain reaction for monitoring gene expression in cardiac myocytes in vitro. Anal Biochem **270**: 41–49

Wong JH, Kim YB, Ren PH, Cai N, Cho MJ, Hedden P, Lemaux PG, Buchanan BB (2002) Transgenic barley grain overexpressing thioredoxin shows evidence that the starchy endosperm communicates with the embryo and the aleurone. Proc Natl Acad Sci U S A **99**: 16325–16330

Xing S, Rosso MG, Zachgo S (2005) ROXY1, a member of the plant glutaredoxin family, is required for petal development in Arabidopsis thaliana. Development **132**: 1555–1565

Yang L, Hu G, Li N, Habib S, Huang W, Li Z (2017) Functional characterization of SlSAHH2 in tomato fruit ripening. Front Plant Sci **8**: 1–12

Yano H (2014) Ongoing applicative studies of plant thioredoxins. Mol Plant **7**: 4–13

Yoshida K, Hara S, Hisabori T (2015) Thioredoxin selectivity for thiol-based redox regulation of target Proteins in Chloroplasts. J Biol Chem **290**: 14278–14288

Yoshida K, Hisabori T (2016) Two distinct redox cascades cooperatively regulate chloroplast functions and sustain plant viability. Proc Natl Acad Sci **113**: E3967–E3976

Zeeman SC, Northrop F, Smith AM, Rees T (1998) A starch-accumulating mutant of Arabidopsis thaliana deficient in a chloroplastic starch-hydrolysing enzyme. Plant J **15**: 357–365

Zhang C-J, Zhao B-C, Ge W-N, Zhang Y-F, Song Y, Sun D-Y, Guo Y (2011) An Apoplastic H-type thioredoxin is involved in stress response through regulation of the apoplastic reactive oxygen species in rice. Plant Physiol **157**: 1884–1899

Acknowledgements

Eidesstattliche Erklärung

Ich versichere hiermit an Eides statt, dass die vorgelegte Dissertation von mir selbständig und ohne unerlaubte Hilfe angefertigt ist. Der Autor hat zuvor nicht versucht, anderweitig eine Dissertation einzureichen oder sich einer Doktorprüfung zu unterziehen. Die Dissertation wurde keiner weiteren Prüfungskommission weder in Teilen noch als Ganzes vorgelegt.

München, den 27.03.2020

Liang-Yu Hou